AN ABSTRACT OF THE THESIS OF

Hong Gao for the degree of Doctor of Philosophy in Forest Products presented on August 22, 1994. Title: Dynamic Mechanical Analysis of Wood and Wood-based Composites.

Abstract approved: Redacted for privacy

James B. Wilson

Wood and wood-based composites are being used in either new or more demanding applications. A means is needed to successfully analyze new materials and to predict their long-term performance. Two techniques, dynamic mechanical analysis (DMA) and time-temperature superposition (TTS) offer a means to accomplish this objective. The outcome of this study is an analysis method that could be used to evaluate the structural characteristics of wood, resin, and wood-based composites as affected by temperature, frequency, and humidity, and the possibility of using this information to define changes in the production process or product.

Dynamic mechanical analysis characterizes a material's properties in terms of the deformation response to periodic forces. To accomplish this analysis, small samples of material were subjected to sinusoidal loads in the center point while the temperature was varied in a controlled manner. The dynamic mechanical properties such as storage modulus, loss modulus, and internal friction were determined,

in addition to the glass transition temperature, all as a function of temperature, frequency and moisture content.

The applicability of dynamic mechanical analysis (DMA) and time-temperature superposition (TTS) was investigated. The time-temperature superposition principle provides a much broader effective range of frequency by making measurements of the dynamic properties at different temperatures and by shifting the data to construct a master curve. Verification studies confirmed the applicability of DMA/TTS.

Dynamic properties of wood and its components of earlywood and latewood were measured. The data was used to successfully predict the properties of wood. The properties of particulate wood-based composites indicate that adhesives play an important role in the temperature dependence of the dynamic properties of wood-based composites. The relationship between dynamic internal friction and static internal bond strength was also investigated. The internal friction measurement is suggested as a potential bonding characterization of wood-based composites.

Dynamic Mechanical Analysis of Wood and Wood-based Composites

by

Hong Gao

A THESIS

submitted to

Oregon State University

in partial fulfillment of
the requirements for the
degree of

Doctor of Philosophy

Completed August 22, 1994
Commencement June 1995

Doctor of Philosophy thesis of Hong Gao presented on August 22, 1994

APPROVED:

Redacted for privacy

Major Professor, representing Forest Products

Redacted for privacy

Head of Department of Forest Products

Redacted for privacy

Dean of Graduate School

I understand that my thesis will become part of the permanent collection of Oregon State University libraries. My signature below authorizes release of my thesis to any reader upon request.

Redacted for privacy

Hong Gao, Author

ACKNOWLEDGMENTS

I would like to acknowledge and express my thanks to several persons who provided considerable support and assistance during the research and writing of the dissertation. My sincere gratitude is go to my advisor, Dr. James B. Wilson, for his continual guidance and his valuable advice throughout my studies at Oregon State University. I thank my committee members for their participating in the dissertation committee. I thank Milo Clauson for his persistent help in my experiments and for his friendship and kindness.

I am forever grateful to my parents who always encouraged me to do my best. I dedicate this dissertation to my lovely daughter, Arlene, for her after-work entertainment which washed away my tiredness and recharged my energy to do more work the next day. Last but not the least, my love and appreciation are for my husband, Shen, for his understanding and supporting me to pursue this degree.

TABLE OF CONTENTS

TABLE OF CONTENTS (Continued)

TABLE OF CONTENTS (Continued)

LIST OF FIGURES

LIST OF FIGURES (Continued)

LIST OF FIGURES (Continued)

LIST OF TABLES

LIST OF TABLES (Continued)

Dynamic Mechanical Analysis of Wood and Wood-based Composites

OVERVIEW

Dynamic mechanical properties characterize a material's deformation response to periodic force. Analysis of these responses, called dynamic mechanical analysis (DMA), can be used to define a material's microstructure or used to study the effect of environmental conditions upon its properties.

Dynamic mechanical analysis is widely used in research on materials such as polymers and metals, but of limited application to date in research on wood and wood-based composites. This study investigates the dynamic mechanical properties of wood and wood-based composites when subjected to a wide range of temperatures and frequencies. The results should contribute to a better understanding of performance of solid wood and wood-based composites.

This dissertation consists of three manuscripts given as three chapters. Chapter 1, **Temperature, humidity, and frequency effects on the dynamic properties of Douglas-fir,** covers the investigation of dynamic mechanical properties of solid wood as influenced by environmental variables. Chapter 2, **Application of time-temperature superposition technique to predict time-dependent property of solid wood,** uses the dynamic mechanical properties of wood as measured at different temperatures to obtain wider range of time behavior

by shifting the storage moduli using a prescribed methodology. Chapter 3, **Thermal and dynamic properties of wood-based composites**, presents the viscoelastic properties of wood-based particulate composites bonded with three different types of resin. These composites are investigated in terms of those characteristics of their components, wood and resin, as well as the bonded composite. The applicability of time-temperature superposition is investigated for these materials. Finally, the summary is drawn from all three chapters.

CHAPTER 1
TEMPERATURE, HUMIDITY, AND FREQUENCY EFFECTS ON THE DYNAMIC PROPERTIES OF DOUGLAS-FIR

Introduction

Dynamic mechanical properties are the mechanical properties of materials as they deform under periodic forces. An analysis of these properties, called dynamic mechanical analysis (DMA), provides insight into various aspects of material structure, especially in response to variations in temperature, humidity, and oscillating loads. Even though the principles of dynamic mechanical analysis are well established, large discrepancies exist in the literature because data was obtained by researchers using different analysis methods. Information about dynamic mechanical properties of wood is limited, incomplete, and significantly complicated by the nature of wood, which greatly varies among species. Wood even has large variations in mechanical properties within individual trees. Therefore the experiments performed here are not only to describe the dynamic properties of the wood, but also to relate these properties to their anatomical characteristics. The objective of this study is to apply dynamic mechanical analysis technology to study the temperature, humidity, and frequency dependence of Douglas-fir (*Pseudotsuga menziesii* (Mirb.) Franco) in terms of storage modulus (E'), internal

friction (tanδ). The glass transition temperatures (T_g) of dry wood are also identified.

Completed this study will provide a greater understanding of the viscoelastic behavior of wood. More specifically the study shows the contributions made by the individual growth rings in terms of percentage of earlywood and latewood to the overall properties of solid wood.

Literature Review

Dynamic mechanical analysis (DMA) is a means to investigate mechanical response to vibrational forces induced by mechanical load or deformation. This part of the paper reviews the principle of dynamic mechanical analysis and how dynamic properties of wood vary with moisture content, temperature, and frequency of loading.

Principle of Dynamic Mechanical Analysis

Dynamic mechanical analysis measures the force when a specimen is subjected to alternating displacements. For linear viscoelastic materials, the relationship between stress and strain is given by (Ferry, 1980):

$$\begin{aligned} \textit{strain}\ \gamma &= \gamma_0 \sin\omega t, \\ \textit{stress}\ \sigma &= \sigma_0 \sin(\omega t+\delta). \end{aligned} \qquad \textbf{(1.1)}$$

where:

ω = angular frequency,

δ = phase lag.

Expanding this expression, the stress can be considered to consist of two components: (1) its magnitude in phase with the strain and (2) its magnitude 90^{o} out of phase with the strain:

$$\sigma = \gamma_0 E' \sin\omega t + \gamma_0 E'' \cos\omega t$$

$$E' = \frac{\sigma_0}{\gamma_0}\cos\delta \qquad (1.2)$$

$$E'' = \frac{\sigma_0}{\gamma_0}\sin\delta$$

The real part of the modulus (E') is called the storage modulus which defines the energy stored in the specimen during the test. The imaginary part (E") is called the loss modulus which describes the dissipation of energy. The ratio between the loss modulus and the storage modulus is called internal friction (tanδ), which is given by:

$$\tan\delta = E''/E' \qquad (1.3)$$

There are several different types of dynamic tests, such as free vibration, forced vibration, sonic wave transmission, and torsion pendulum (Back and Didriksson, 1969; Ferry, 1980; Blankenhorn *et al.*, 1973).

Dynamic Mechanical Properties of Solid Wood

Reports on the dynamic behavior of solid wood are limited in the literature. Winter and Mjöberg (1985; 1986) tested dynamic properties of Norway spruce by superimposing small sinusoidal strain oscillations on a compression strain.

With increasing temperature, the wood became softer. The similar findings were reported by Murakami and Matsuda (1989), Kelley *et al.* (1987) and Sellevold *et al.* (1975).

Temperature, however, is not the only factor affecting the viscoelastic properties of wood. These properties also depend on the rate of loading of mechanical strain, i.e. the frequency, and on its moisture content. Winter and Mjöberg (1985; 1986) showed that an increased frequency reduces the total amount of fiber damage measured as a reduction in viscosity. In general, wood becomes stiffer with increasing frequency (Goldsmith and Grossman, 1967; Moslemi, 1967; Sadoh, 1981; Murakami and Matsuda, 1989; Nakano *et al.*, 1990a; 1990b).

As moisture content increases, the storage modulus of wood decreases (Moslemi, 1967). Blankenhorn (1972) established that when the moisture content decreased, the internal friction curve tended to broaden and shift. Goldsmith (1967) found no interaction between the frequency effect and the effects of temperature and moisture content.

Although the majority of research results agree in terms of effects of temperature and moisture content on the dynamic properties of wood, discrepancies are often observed among data obtained from different test instruments, different analysis methods, or even different laboratories using identical instruments.

Analysis of thermal dynamic properties of wood have several applications in forest products (Fujimura *et al.* 1990; Murakami and Matsuda, 1989; Kelley *et al.*, 1987; Sadoh, 1981). For example, the temperature and frequency effects on stiffness of wood are important in chip refining for paper pulp (Höglund *et al.*, 1976; Becker *et al.*, 1977). Unlike numerous applications of DMA in polymer science, the use of DMA in forest products are still limited.

Glass Transition Temperature of Wood and Wood Components

Most materials are hard or rigid below a certain temperature, known as the glass transition temperature (T_g). Above that temperature, the material becomes soft, and flexible; and is either an elastomer or a very viscous liquid. Mechanical properties show profound changes in the region of the glass transition. For example, the storage modulus will decrease enormously within the transition region, thus greatly affecting its performance characteristic. Therefore, T_g can be considered a very important material characteristic since many uses of wood and its components depend on such parameters (Ferry, 1980; Murayama, 1978).

Transitions in material properties also occur for internal friction ($\tan\delta$) versus temperature where several inflection points can be noted. Each transition corresponds

to specific molecular motions related to structure and property relationships of the material. Three transitions are commonly documented for polymers. They are labelled the alpha, beta, and gamma transitions. The alpha transition is associated with crystalline relaxation, whereas the beta transition relates to the motion of the amorphous region side-chain that branch from the main backbone. The intensity of the beta transition varies with the degree of branching. Gamma transition is caused by the rotation of short main chain segments and can influence low temperature impact resistance of materials.

The position and intensity of thermally-induced transitions of common synthetic polymers are comparatively well known (Ferry, 1980). But it has been more difficult to identify them in natural materials, such as wood. Kelley *et al.* (1987) found two separate glass transitions corresponding to the amorphous lignin and hemicellulose matrix in the wood, they were 90°C and 60°C respectively. They noted that the plasticizing effect of water was to lower the glass transition temperature. Irvine (1984) found that the transition of *in situ* lignin in water-saturated wood samples occurs within about 60-90°C. The glass transition temperature of cellulose was found to be at 230°C (Back and Didriksson, 1969) by sonic pulse technique. There were also four secondary transitions: -20°, 40°, 130°, and 200°C. Klason and Kubát (1976) determined the thermal transitions in

dry cellulose by using torsion pendulum, dilatometry, and dielectric methods. The results showed that the main dispersion phenomenon, apart from a glass transition temperature at 237°C, occurred at -73°C for 1 Hz in cellulose. Table 1.1 shows glass transition temperature and the secondary transitions of wood and wood components observed by various researchers using different methods.

Macro-structure of Wood and its Effect on Dynamic Mechanical Properties

Wood has unique anatomical characteristics which influence its use in engineering. Different tree species living in temperate regions have growth increments greatly varying in width, cell composition, and density. Typically, the layered arrangement called the annual growth ring consists of two distinct parts. The wood formed early in the growing season, called earlywood, is light weight with large cell cavities and thin walls. The portion of the growth ring that occurs late in the growing season which is dense, dark in color, and has small cell cavities with thick walls is called latewood (Panshin and de Zeeuw, 1980). Because of the difference between earlywood and latewood, their respective physical and mechanical properties are expected to be different (Ifju *et al.*, 1965). Their results showed that the modulus of elasticity of earlywood of water-saturated

Douglas-fir is 0.22 x 10^6 psi (4.6 x 10^{10} dyne/cm^2) and latewood is 1.3 x 10^6 psi (9.0 x 10^{10} dyne/cm^2). The wood could be considered as a laminated composite of earlywood and latewood. According to the law of mixtures (Bodig and Jayne, 1982), E' of a composite system for orthotopic materials can be calculated as:

$$E' = \frac{1}{t} \sum_{i=1}^{n} (E'_i t_i) \qquad \textbf{(1.4)}$$

where:

E' = storage modulus of composite,

E'_i = storage modulus of each layer,

t = total thickness of composite,

t_i = thickness of each layer,

n = number of layers in composite.

Koponen *et al.* (1989, 1991) developed a model for estimating elastic properties of wood from its polymeric constituents and cell structure. The calculated elastic properties are in good agreement with test results.

Overall, only a few researchers have examined dynamic properties of wood and wood-based composites. The results have been quite diverse and often of limited value because the experiments were often confined to only one or two species of wood, environments, or a very narrow frequency range.

Methodology

Materials

The specie of samples has been chosen to be Douglas-fir (*Pseudotsuga menziesii* (Mirb.) Franco) in this study. Douglas-fir is widely used in building and construction in the form of lumber, timbers, structural plywood and others. It is one of the most popular structural softwoods in northwest America.

Samples were cut from two pieces of kiln dried lumber purchased from a local supplier in Corvallis, Oregon. One group of samples, Group-A, was quarter-sawn into 2mm X 12mm X 52mm. Each sample consisted of at least five complete growth rings. Another group, Group-B, was also quarter-sawn but each sample only had one complete growth-ring. The third group (Group-C) of samples were flat-sawn into 1.5mm X 12mm X 52mm and cut from the same piece of board as the Group-B. Each sample in Group-C had either latewood or earlywood only. All samples had been selected to have as straight grain as possible. Specimens were free from any defect on the scale of the annual ring. The latewood percentage of sample was determined using the NIH Image program (Rasband, 1992). Images of the sample's cross-section were captured through a video camera and sent to an Apple computer. Sixteen frames were averaged in order to reduce time-varying random noise.

The separation of earlywood and latewood was done by visualizing the different colors between them on the computer monitor. In the Group-A samples, the numbers of growth rings ranged from 5 to 12. The average percentage of latewood of the Group-A samples was 26.1% with a standard deviation of 5.3%. Group-B samples had wide-growth rings so the earlywood and latewood can be easily separated and cut into small pieces later. There was only one complete growth ring in each sample. The average of latewood percentages was 14.7% with a standard deviation of 1.9%. The complete measurement data are listed in Appendix 1B.

Equipment

A Rheometrics Solid Analyzer II, (RSA II, Rheometrics®), was used to determine dynamic properties. The testing machine (Appendix 1A) was equipped with a temperature controlled chamber that encased the DMA test sample. Temperature control was performed by a combination of liquid nitrogen cooling and electric heat. Advanced DMA software (RSA Owner's Manual, 1991) was used in the automatic system calibration. All tests were performed by three-point bending with a rectangular sample supported in a horizontal position with a center load. In order to maintain the sample in compression throughout the test, a static force (autotension) was applied on the sample. The amplitude of autotension

varied correspondingly to the changing of dynamic force. Autotension was held at 120% of dynamic force throughout the test. Such a setting provided the minimum static force required for the test.

Procedures

Temperature and Frequency Effects on Dry Wood

The objective of this test was to establish the relationship between temperature and frequency, and the dynamic properties of dry wood. Prior to measurement, the quarter-sawn samples were dried in a desiccator with drying agent of phosphorus pentoxide (P_2O_5) for not less than four hours.

A. The dynamic tests were done to obtain E', E", and tanδ values of each sample within the temperature range of from -100°C to 320°C, at three frequencies of 1 rad/sec, 10 rad/sec, and 100 rad/sec. There are three repetitions for each condition. Each test cycle consisted of holding the sample at dynamic strain of 5×10^{-5} and controlled frequency while increasing temperature at the rate of 5°C per step. The sample was allowed to thermally equilibrate for 60 seconds before DMA data was collected. The process was repeated until the final temperature was reached.

B. The frequency effect of the dynamic properties was evaluated by running the DMA logarithmic frequency sweep from 0.1 rad/sec to 100 rad/sec on each sample. Sampling rate was ten points per each decade of frequency. Successive measurements were taken at different frequencies while holding a constant strain and temperature. Test temperatures were: 10°, 20°, 30°, 40°, 50°, and 60°C for each sweep respectively. After each completed frequency sweep, the sample was put back into the P_2O_5 desiccator to redry. Frequency sweep was then repeated at a higher temperature than the former one for the same sample. A total of three samples were tested.

Humidity and Temperature Effects on the Solid Wood

Six sample sets, with six repetitions on each set, were analyzed by measuring storage modulus (E') at a fixed frequency (10 rad/sec) and temperatures (10°, 25°, 40°, 55°C). Each samples was conditioned to a specific equilibrium moisture content (EMC) and temperature.

EMC conditioning was done by storing six samples in different desiccators which contained different hydrated inorganic compounds. The equalized specimens had five desired equally spaced moisture contents (ovendry basis), about dry (0%), 4%, 8%, 12%, and 16% at room temperature. The sixth group of samples was submerged in water. Only the

water which absorbed within the cell walls would affect the viscoelastic properties of wood (Sadoh, 1981). The desired moisture content of these samples was 50% at T = 25°C. Table 1.2 gives the details of conditioning environments and actual moisture content of samples.

The formula for calculating moisture content on an ovendry basis is (Wood Handbook, 1987):

$$M.C.(\%) = \frac{W_w - W_{od}}{W_{od}} \times 100\% \qquad (1.5)$$

where:

W_w = weight of the sample

W_{od} = oven dry weight.

After tests were finished, the samples were placed in an oven at 103° C to allow drying for two hours to obtain ovendry weight of each sample. Actual moisture content of each sample is listed in Appendix 1C.

Dynamic Mechanical Properties of Earlywood and Latewood

Six pieces of earlywood (Group-A), six pieces of latewood (Group-B), and six pieces of plain-sawn (Group-C) ovendry samples were used in this study.

A. The samples of Group-A and Group-B were subjected to three-point bending with load in the wood's radial direction.

The DMA tests were run by incrementing temperature 5°C per step starting from -120°C and ending at 300°C for each sample. There was a 60 seconds waiting period between each temperature step. The frequency of 10 rad/sec was held constant during the test. The strain levels were 0.005% and 0.003% for earlywood and latewood samples respectively. The average values of six samples were used to assess the difference between the storage modulus of earlywood and latewood samples.

B. The difference between storage modulus of dry earlywood and latewood along-the-grain orientation was investigated. A DMA single-data measurement was done at a fixed frequency (10 rad/sec) and temperature (25°C). The tests were completed by loading dynamic forces on the sample tangentially and radially. The E' averages of the two groups were compared to see whether they were statistically different. The results provided the information about how the orientation of test affect the dynamic properties of wood.

The model for storage modulus of wood is that of a laminate with two components (earlywood and latewood layers) as the laminae. By knowing the storage modulus of each layer, and the volume percentage of each layer, the law of mixtures was used to model the properties of bulk wood. Prediction ($E_{predict}$) was compared to the experimental data (E_{test}) to see how well they agreed. The applicability of

the law of mixtures in computing mechanical properties of wood using the growth increments was investigated.

Glass Transition Temperature of the Dry Wood

One indicator of the glass transition temperature in a polymer is a change in its internal friction (tanδ). In dynamic mechanical test, samples are heated at a steadily increasing rate. The tanδ was recorded as a function of temperature at a constant frequency. A glass transition appears in the DMA curve where tanδ reaches maximum. Such technique can observe the glass transition (α) and possibly secondary transitions (β or γ) of solid wood. The dynamic testing data have been smoothed in order to eliminate some unwanted noise.

Results and Discussion

Effects on the Dynamic Properties of Wood

The dynamic properties of wood are affected by temperature, frequency, and moisture content. It was observed that either temperature increase or frequency decrease would result in storage modulus decrease.

Figure 1.1 shows the temperature dependence of the dynamic mechanical properties of dry Douglas-fir sample over a temperature range from -120° to 300°C. There were considerable differences in storage moduli for different samples as a result of morphological variations, such as, specific gravity and relative amounts of earlywood and latewood. For example, three samples tested at a frequency of 10 rad/sec had specific gravity variation of about 10% which resulted in a variation of storage modulus of about 25% at a temperature of -100°C. This appeared also to be true for the earlywood and latewood samples.

Viscoelastic material became stiffer with increasing frequency within the linear range (Ferry, 1980). The overall trend was a rise of storage modulus with frequency (Fig.1.2). For example, at a temperature of 30°C, the difference between storage moduli observed at 0.1 rad/sec and 100 rad/sec respectively was as high as 16%. The experimental results were in general agreement with the observations of

other investigators (Höglund *et al.*, 1976; Fujimura *et al.*, 1990). The result confirmed that dynamic properties of solid wood are time-dependent.

The statistical analysis has been done on the storage modulus in samples at four different humidities. The average values of storage moduli and error mean square (s^2) are shown in Table 1.3. The maximum average storage modulus was 3.4 x 10^{10} dyne/cm^2 when samples had 1.47% moisture content at 9.6°C. Comparisons revealed the samples became less stiff when they either had a higher moisture content (63.2% MC) or were at a higher temperature (51.5°C).

The water saturated wood sample was at an average moisture content of 63.2%. The storage modulus was 2.146 x 10^{10} dyne/cm^2 at 9.6°C. E' decreased with increasing temperature. At 51.5°C, the storage modulus equalled 1.156 x 10^{10} dyne/cm^2 which was about 54% of E' at 9.61°C. At all temperatures, the storage moduli decreased with increase of moisture content. The storage modulus of dry wood was 3.403 x 10^{10} dyne/cm^2 at 9.61°C which was about 159% of the values for water saturated samples at the same temperature.

Table 1.4 gave results of analysis of variance of average storage modulus. The analysis subdivided into the following components:

Moisture content

Temperature (within moisture content)

Pooled error.

The F-value for the moisture content effect was 20.06 which was well beyond the 5% level. This showed that either temperature or moisture contents has significant effect on the storage modulus in the samples.

Difference between Properties of Earlywood and Latewood

Figure 1.3 displays dynamic properties of earlywood and latewood samples. The storage modulus in latewood was higher than earlywood's E' as expected since the average specific gravity of latewood was 3.4 times higher than that of earlywood in this study. At a temperature of 25°C, the storage moduli were 1.6×10^{11} dyne/cm^2 and 3.1×10^{10} dyne/cm^2 for latewood and earlywood respectively.

Knowing the storage modulus of earlywood and latewood and the percentage of each in the material, the law of mixtures (Equ.1.4) was used to predict the storage modulus of wood. Figure 1.4 illustrates the results of predicting storage modulus from information on the earlywood and latewood. The predicted storage modulus was lower than tested. For example, the predicted value of storage modulus was 27% lower than the actual value at 25°C. The experimental error was most likely due to the method used to determine the latewood percentage and cut of earlywood and latewood samples. A better prediction may have been achieved if intermediate density layers were included in the

simplified model to account for the transition regions between the earlywood and latewood. Wood in these regions has a lower density than latewood but higher than earlywood.

Glass Transition Temperature of Dry Wood

Wood is a complex composite of lignin, hemicellulose, and cellulose. Lignin and hemicellulose are amorphous and essentially thermoplastic whereas cellulose is semicrystalline. These three components have different glass transition temperatures. Lignin has the lowest and cellulose the highest (Table 1.1).

The dry wood glass transition temperature varies because of differences in the chemical and physical properties of different wood species. Even in the same wood species, different glass transition temperatures were observed from earlywood and latewood samples. The tanδ response revealed temperature transition at temperature 288° and 273°C for earlywood and latewood respectively (Table 1.5). The explanation of such phenomenon might be the differences in the degree of polymerization, higher packing density, molecular weight, and degree of crystallinity in earlywood and latewood (Back and Salmén, 1982).

For the dry solid wood, the transition temperature shifts to lower temperature as the frequency decreases (Table 1.6). At a frequency of 100 rad/sec, glass transition

temperature equals 294°C. When the frequency equals 1 rad/sec, T_g is only 261°C. The relationship between T_g and frequency can be used to optimize refining in the paper pulping process.

In this study, the glass transition temperatures are higher than published data. Four possible factors were acknowledged. First, the glass transition temperature of wood is a function of frequency and moisture content. For an average viscoelastic material, an increase of 10 times in frequency corresponds to an increase in temperature of 7° - 10°C (Ferry, 1980). Influence of water is to lower the glass transition temperature (Back and Salmén, 1982; Kelley *et al.*, 1987). The second is the thermal histories of samples. The transition of the dry material decreased in strength and shifted to higher temperatures from run to run (Young, 1978; Wang and Cheng, 1988). The third is the variation among samples from different species or from different pieces of wood. The glass transition temperature of dry solid wood occured within the interval of 299.0°C and 290.6°C even through samples were cut from the same piece of board and tested under the same conditions in this study. Since different wood samples were used by different researchers, a big disparity was expected. The fourth is that the variation might be due to the different definitions of transition temperature.

Conclusions

The results obtained from this investigation confirm the viscoelastic nature of solid wood by applying dynamic mechanical analysis. The study made clear that either increase of temperature, decrease of frequency or increase of moisture content resulted in a decrease of storage modulus.

Concerning the influence of temperature, measurements of internal friction of dry Douglas-fir samples showed the glass transition in the vicinity of 280°C. The average glass transition temperatures of earlywood is 288°C, and latewood's is about 15°C lower.

When modelled as a layered composite, the dynamic properties of solid wood could be reasonably predicted based on the properties of earlywood, latewood, and their percentages. Simplifying assumptions made in the modeling process and the possibility of not accurately difining the zones of earlywood and latewood in the sample, may account for the slight undervaluation of the predicted values.

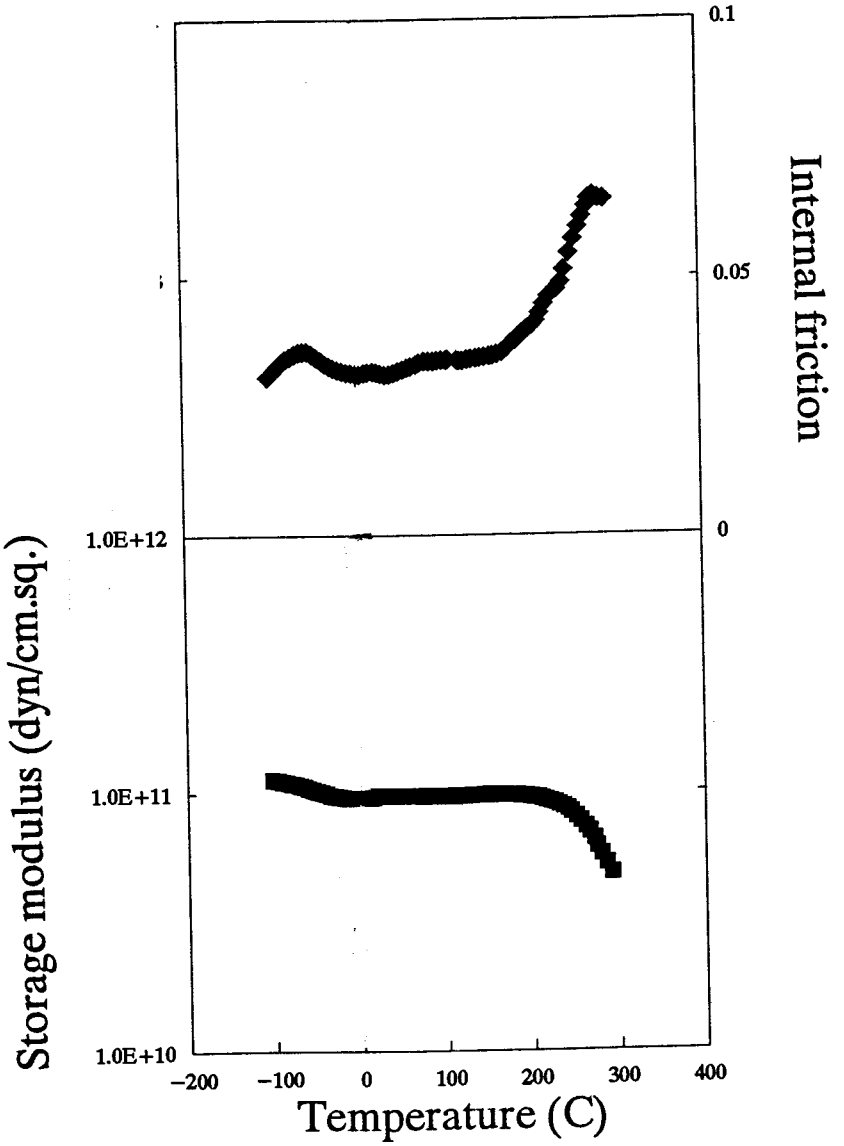

Figure 1.1 Temperature effect on storage modulus (E') and internal friction (tanδ) (frequency = 10 rad/sec).

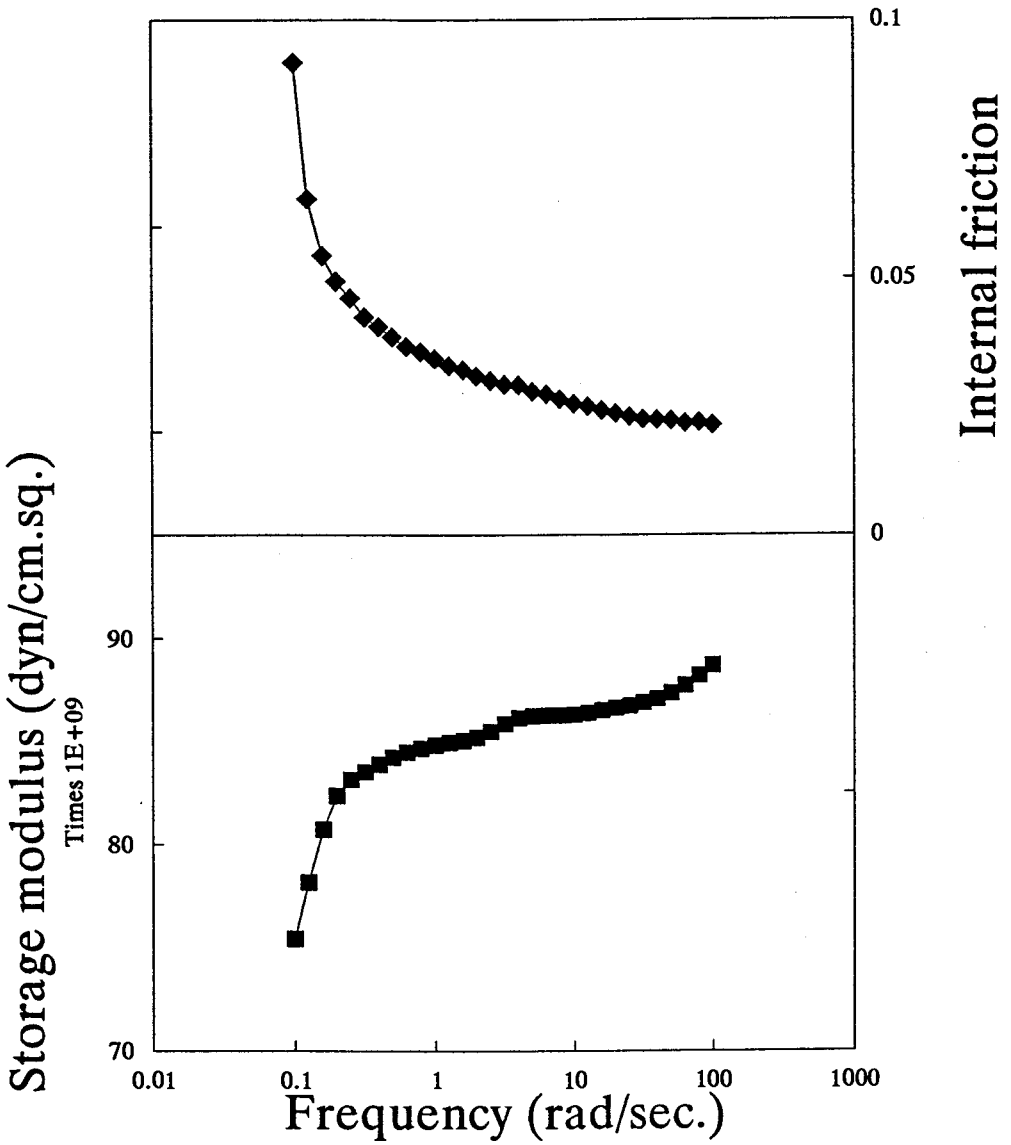

Figure 1.2 Effect of frequency on dynamic properties (temperature = 30°C).

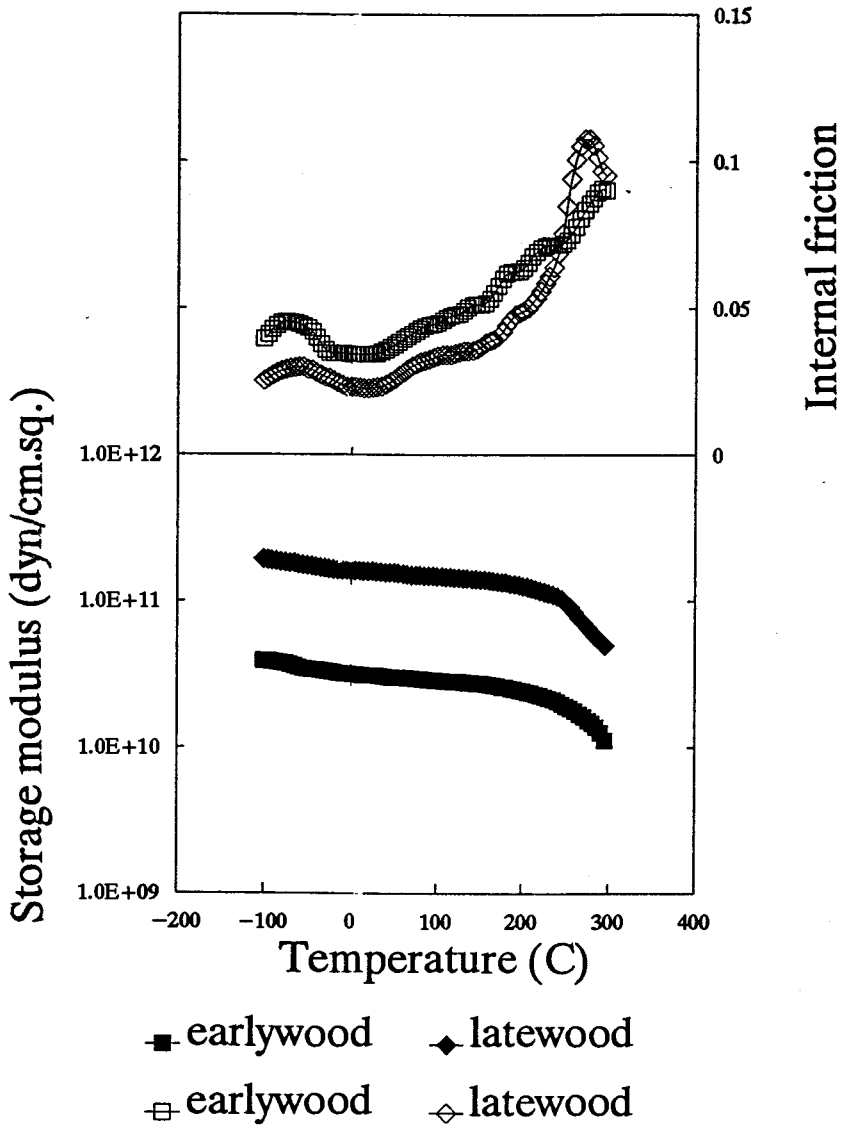

Figure 1.3 Dynamic properties of earlywood and latewood.

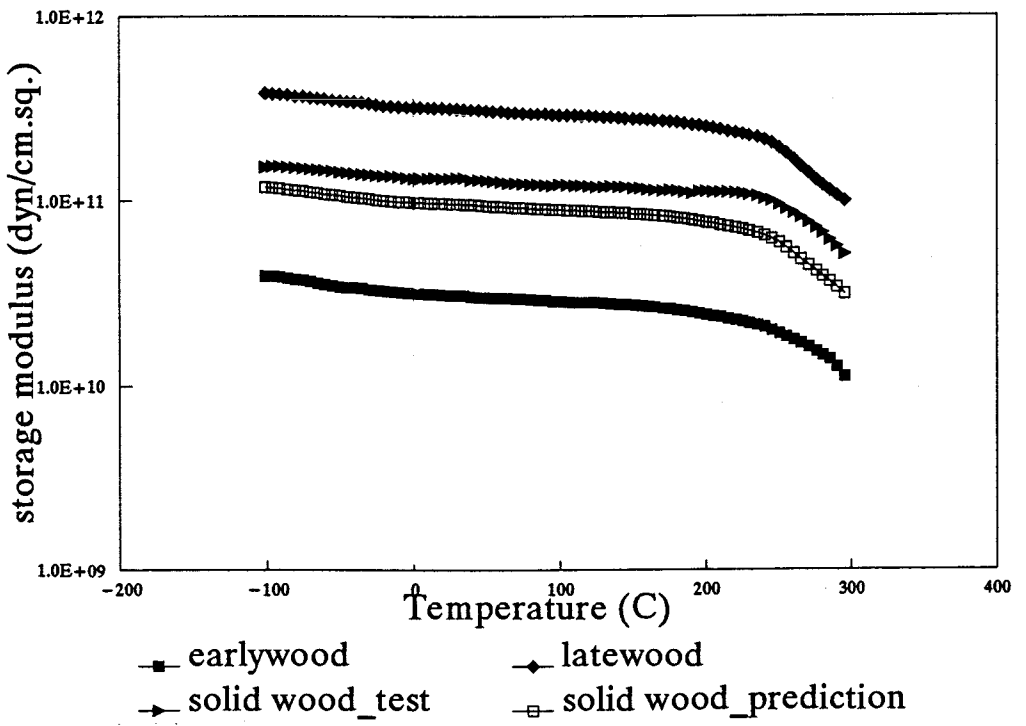

Figure 1.4 Comparison of observed and predicted storage modulus.

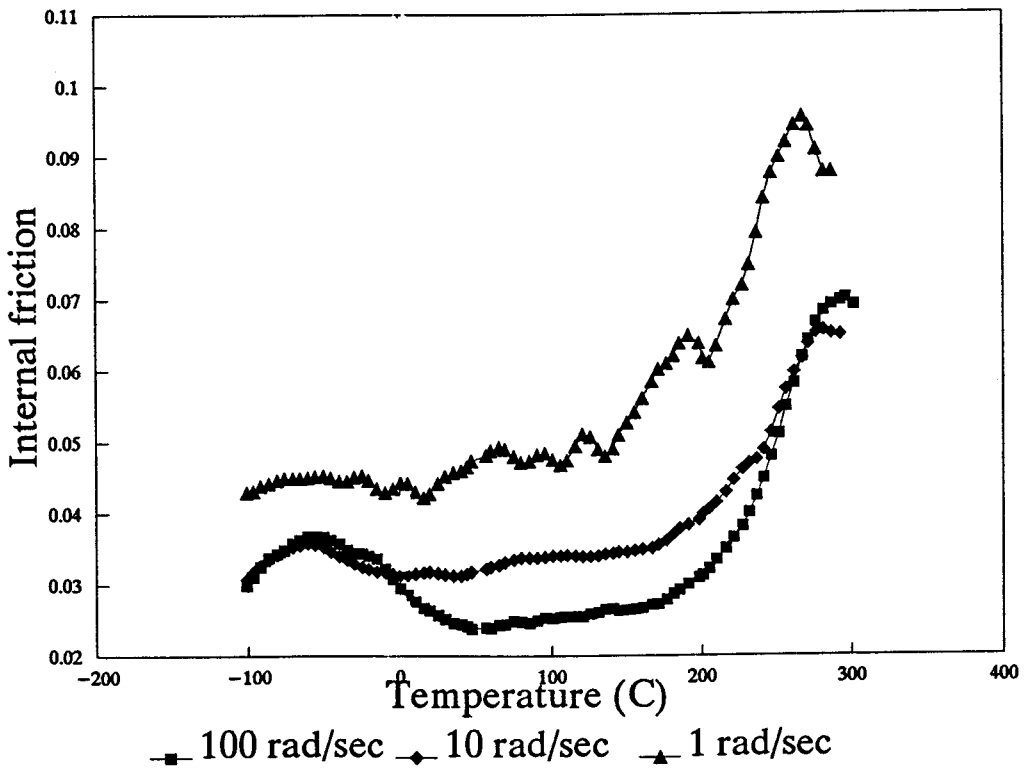

Figure 1.5 The tanδ response of Douglas-fir with different frequencies.

Table 1.1 Glass transition temperature of wood and wood components from literatures.

Reference	T_g (α)	2nd trans	Materials	Temperature range (°C)	Methods
Back & Didriksson	230°C	-20° 40° 130° 200°C	dry cotton linters /bleached pine kraft papers	-70 -- 375	sonic pulse technique
Irvine	120°C 80°C 110°C 120°C		Hemicellulose milled wood lignin solid wood milled wood	40 -- 105	Differential thermal analysis
Kelley *et al.*	90°C 60°C	-110°C	*in situ* lignin *in situ* hm.cellulose	-140 -- 150	dynamic mechanical thermal analysis
Klason & Kubat		-73 °C -33 °C	cellulose (pulp)	-153 -- 147	torsion pendulum dielectric method dilatometry
Nakano *et al.*		-60°C	solid wood	-120 -- 230	damped oscillation
Rials & Glasser	95°C		lignin	25 -- 175	differential scanning calorimetry
Sadoh	235°C		solid wood	30 -- 240	torsional pendulum
Salmén	100°C		*in situ* lignin/wet	20 -- 140	forced vibration
Sellevold *et al.*		-36°C	solid wood	-130 -- 20	resonance method
Wang & Cheng	215°C		*in situ* lignin	100 -- 300	torsional pendulum
Young	150°C		kraft paper	60 -- 230	torsional pendulum

Table 1.2 Details of humidity control environments. [1]

	Salt solution					
	P_2O_5	LiCl	K_2CO_3	$NaNO_2$	$(NH_4)_2SO_4$	Water[3]
Desired RH(%)	1	15	43	66	80	N/A
Desired EMC(%)	O.D.[2]	4	8	12	16	50

1: at a temperature of 20°C (Handbook of Chemistry and Physics, 1983)
2: Oven dry, on weight basis.
3: Wood samples were soaked in water at the same temperature as test temperature.

Table 1.3 Effect of temperature and moisture content on the average storage modulus.

Temperature (C)	storage modulus 10^{10} dyne/cm^2 Average moisture content of each group			
	1.47%	7.45%	14.31%	63.21%
9.61	3.403	2.451	2.560	2.146
23.74	2.660	2.775	2.075	1.288
37.27	3.077	2.342	1.849	1.268
51.51	3.010	2.104	1.798	1.156
s^2	0.625	0.528	0.436	0.480
d.f.	20	20	20	20

Table 1.4 Analysis of Variance of storage modulus.

Source of variation	Sum of Squares	d.f.	Mean square	F-ratio
M.C.	31.139014	3	10.379671	20.064
Temp. (within M.C.)	9.027897	12	0.752325	1.454
RESIDUAL	41.386511	80	.5173314	
TOTAL (CORRECTED)	81.553422	95		

All F-ratios are based on the residual mean square error.

Table 1.5 Glass transition temperatures of earlywood and latewood.

Earlywood		Latewood	
Sample #	T_g (°C)	Sample #	T_g (°C)
1–a–1	299.68	1–b–1	269.07
1–a–2	294.99	1–b–2	281.05
1–a–3	286.56	1–b–3	275.98
1–a–4	289.89	1–b–4	270.09
1–a–5	266.26	1–b–5	270.25
1–a–6	290.45	1–b–6	269.30
AVG	287.97	AVG	272.62
STD	10.56	STD	4.43

AVG: Average
STD: Standard deviation

Table 1.6 Glass transition temperatures of dry Douglas-fir samples.

Sample #	Frequency (rad/sec)	T_g (°C)
1–2	100	290.56
1–4	100	299.00
1–12	100	292.46
Average		294
1–11	10	279.60
1–10	10	276.40
1–5	10	*
Average		278
1–8	1	*
1–6	1	265.72
1–9	1	256.03
Average		261

*: can not be identified

References

Back, E. L., and E. I. Didriksson. 1969. Four secondary and the glass transition temperature of cellulose, evaluated by sonic pulse technique. Svensk Papperstidning, 72(21):687-694.

Back, E. L., and N. L. Salmén. 1982. Glass transitions of wood components hold implications for molding and pulping processes. Tappi, 65(7):107-110.

Becker, H., H. Höglund, and G. Tistad. 1977. Frequency and temperature in chip refining. Paperi ja Puu, 59(3):123-130.

Blankenhorn, P. R. 1972. Dynamic mechanical behavior of black cherry. Ph.D. thesis. The Pennsylvania State University, University Park, Pa.

Blankenhorn, P. R., D. E. Kline, and F. C. Beall. 1973. Dynamic mechanical behavior of black cherry. Wood and Fiber Science, 4(4):298-308.

Bodig, J., and B. A. Jayne. 1982. Mechanics of Wood and Wood Composites. Van Nostrand Reinhold Co. New York.

Ferry, J. D. 1980. Viscoelastic Properties of Polymers. John Wiley & Sons, Inc., New York.

Fujimura, Taira, M. Inoue, and I. Uemura. 1990. Durability of wood with acyl-high-polymer II. Dimensional stability with crosslinked acyl copolymer in wood. Mokuzai Gakkaishi, Vol.36, No.10: 851-859.

Goldsmith, Valerie, and P. U. A. Grossman. 1967. The effect of frequency of vibration on the viscoelastic properties of wood. Journal Inst. Wood Sci., 18:44-53.

Handbook of Chemistry and Physics. 1983. Ed by Weast, Robert C, Melvin J. Astle, and Willian H. Beyer. CRC Press,Inc. Boca Raton, Florida.

Höglund, H., U. Sohlin, and G. Tistad. 1976. Physical properties of wood in relation to chip refining. Tappi, 59(6):144-147.

Ifju, G., R. W. Wellwood, and J. W. Wilson. 1965. Relationship between certain intra-increment physical measurements on Douglas Fir. Pulp Paper Mag. Can., 66: T475-T483.

Irvine, G. M. 1984. The glass transitions of lignin and hemicellulose and their measurement by differential thermal analysis. Tappi, 67(5):118-121.

Kelley, S. S., T. G. Rials, and W. G. Glasser. 1987. Relaxation behavior of the amorphous components of wood. Journal of Material Science, 22:616-624.

Klason, Carl, and Joesf Kubát. 1976. Thermal transitions in cellulose. Svensk Papperstidning, (15):494-500.

Koponen, S., T. Toratti, and P. Kanerva. 1989. Modeling longitudinal elastic and shrinkage properties of wood. Wood Science and Technology, 23:55-63.

Koponen, S., T. Toratti, and P. Kanerva. 1991. Modeling elastic and shrinkage properties of wood based on cell structure. Wood Science and Technology, 25:25-32.

Marsoem, S. N., P. Bordonne and T. Okuyama. 1987. Mechanical responses of wood to repeated loading II. Effect of wave form on tensile fatigue. Mokuzai Gakkaishi, Vol.33(5):354-360.

Moslemi, A. A. 1967. Dynamic viscoelasticity in hardboard. Forest Products Journal. Vol 17(1):25-33.

Murakami, Koichi, and Hideaki Matsuda. 1989. Oligoesterified wood based on anhydride and epoxide VII. Dynamic mechanical properties of oligoesterified wood. Mokuzai Gakkaishi, Vol.36(1):49-56.

Murayama, Takayuki. 1978. Dynamic Mechanical Analysis of Polymeric Material. Materials Science Monographs, Vol.1. Elsevier Scientific Publishing Co. New York.

Nakano, T., S. Honma, and A. Matsumoto. 1990a. Physical properties of chemically-modified wood containing metal I. Mokuzai Gakkaishi, 36(12):1063-1068.

Nakano, T., S. Honma, and A. Matsumoto. 1990b. Physical properties of chemically-modified wood containing metal II. Mokuzai Gakkaishi, 37(10):924-929.

Panshin, A. J., and C. de Zeeuw. 1980. Textbook of Wood Technology. McGraw-Hill Book Company, New York.

Rasband, Wayne. 1992. Menu of NIH *Image* 1.47.

Rheometrics Solids Analyzer, Owner's Manual. 1991. Rheometrics,Inc. Piscataway, NJ.

Rials, T. G., and W. G. Glasser. 1984. Characterizing wood components as network polymer dynamic mechanical analysis. Wood and Fiber Science, 16(4):537-542.

Rials, T. G., and W. G. Glasser. 1989. Multiphase materials with lignin.VI.effect of cellulose derivative structure on blend morphology with lignin. Wood and Fiber Science, 2(1):80-90.

Sadoh, T. 1981. Viscoelastic properties of wood in swelling systems. Wood Science and Technology, 15:57-66.

Salmén, L. 1984. Viscoelastic properties of *in situ* lignin under water-saturated conditions. Journal of Material Science, 19:3090-3096.

Sellevold, E. J., F. Radjy, P. Hoffmeyer, and L. Bach. 1975. Low temperature internal friction and dynamic modulus for beach wood. Wood and Fiber, 7(3):162-169.

Wang, Yage, and P. Cheng. 1988. With the dynamic method to examine the glass's transition of Populus lignin. Journal of Nanjing Forestry University, 2:81-85. (in Chinese).

Winter, R. 1986. Compression of wood with superimposed small sinusoidal oscillations. Part II: High temperature. Wood and Fiber Science, 18(1):11-22.

Winter, R., and P. J. Mjöberg. 1985. Compression of wood with superimposed small sinusoidal oscillations. Part I. Room temperature. Wood and Fiber Science, 17(4):444-463.

Wood Handbook. 1987. United States Department of Agriculture, U.S. Forest Products Lab. Agriculture Handbook No 72, U.S. Government Printing Office, Washington, D.C.

Young, R. A. 1978. Thermal transitions of wood polymers by torsional pendulum analysis. Wood Science, Vol.11(2):97-101.

CHAPTER 2
APPLICATION OF TIME-TEMPERATURE SUPERPOSITION TECHNIQUE TO PREDICT THE TIME-DEPENDENT PROPERTY OF WOOD

Introduction

Wood is a natural material consisting of cellulose, hemicellulose, lignin, and extractive. Wood, a relatively inexpensive, large volume structural material, tends to creep over time when subjected to load. The time-dependent deflection of beams and other wood members under loading is critical to their performance. The experimental methods, however, normally cover limited ranges of frequency or time. A very useful tool to the prediction of time-dependent property is time-temperature superposition (TTS) which can provide a much larger effective range of frequency by taking measurements of mechanical properties at different temperatures. Dynamic data with a wide range of frequency can be transformed to static data with a wide range of time.

Although the concept of time-temperature superposition is firmly grounded in polymer theory and is used in engineering plastics (Ferry, 1980), whether and under what conditions this principle applies to wood has not been fully investigated.

The objectives of this study were: (1) to test the validity of time-temperature superposition to wood by characterizing the properties of the relaxation spectra; (2)

to determine the temperature ranges where TTS would be valid; and (3) to predict the time-dependent property of dry wood using time-temperature superposition.

Literature Review

Rheological Characteristics of Wood

Wood responds differently to an imposed deformation or load depending on the time required to complete a given mechanical test. This rheological characteristic of wood is strongly influenced by environmental variables, such as temperature and humidity.

When wood is subjected to stress (load), the resulting strain (deformation) is the sum of instantaneous elastic strain, time-dependent strain, and permanent strain (Bodig and Jayne, 1982). One of the several experiments which can determine this time dependence of mechanical properties is called a creep test. One type of creep test for wood uses a fixed load on the specimen and measures the deflection as a function of time (McNatt and Hunt, 1982; Pearson, 1981; Smulski, 1989). The rate of increase in deflection is very rapid for a short initial period which is followed by a period of slight but steady increase in deflection (Yamada, *et al.*, 1961).

It has been known for a long time that temperature plays an important role in time-dependent mechanical properties of wood (Holzer *et al.*, 1989). Davidson (1962) studied the influence of temperature on creep in three wood species. An increase in temperature resulted in increasing the slope of

the creep curve. Bach and Pentoney (1968) examined longitudinal tension stress and found that creep parallel to grain was proportional to the square of the temperature. The influence of heat on the longitudinal creep of dry Douglas-fir was also investigated by Schaffer (1982).

Creep behavior of wood is sensitive to its moisture content (Salmén, 1984; Holzer, *et al.*, 1989; Gamalath, 1991). Breese and Bolton (1993) tested earlywood samples loaded in compression with moisture content varied from 0% to green. The results showed that increased moisture content resulted in increased creep. But there was no significant difference among the samples with moisture content less than 10%.

Prediction of Long-term Behavior of Wood

Long-term performance of wood is important for engineering design. Several methods have been proposed to predict long-term creep behavior, for example, rheological and mathematical models (Bodig and Jayne, 1982). Rheological modeling, also called a mechanical modeling, consists of spring and dashpot elements assembled in series and/or parallel. The model simulates the viscoelastic behavior of materials. The mechanical analogy model, however, is only valid over the time span for which the parameters are calculated, although some researches have extended the results outside of test time range (Holzer *et al.*, 1989).

Gamalath (1991) used finite-element modeling to predict long-term creep in wood but the numerical predictions did not agree with the experimental results.

One popular method used to describe creep behavior of wood is empirical curve fitting. This method requires that mathematical equations portray creep by a suitable statistical technique. The choice of appropriate model depends mostly on the researcher's preference, and the degree of accuracy required. The power law form was widely used to describe creep of wood (Schniewind and Barrett, 1972), using an equation:

$$D(t) = D_0 + mt^n \qquad \textbf{(2.1)}$$

where: D is creep compliance, m and n are constants, and t is time.

Dynamic Mechanical Analysis and Time-temperature Superposition

Dynamic mechanical analysis (DMA) measures the material's response to oscillation imposed by period deformation. DMA provides insight into various aspects of material structure (detailed in Chapter 1).

Time-temperature superposition (TTS) principle describes the equivalence of time and temperature of linear viscoelastic materials. TTS has been used since the 1940s in

a variety different areas, such as polymers and metals. The method was developed empirically prior to the theories which now support it. It is a means of displaying the interchangeability of frequency (or time) and temperature in dynamic or static processes.

According to the Rouse theory, simultaneous motions of all the segment junctions of polymers can be described through a transformation of coordinates as the sum of a series of cooperative modes. Each mode corresponds to a discrete contribution to the relaxation spectrum. Therefore, the storage modulus (E') can be expressed as (Ferry, 1980):

$$E'(\omega) = (cRT/M) \sum_{p=1}^{N} \omega^2\tau_p^2/(1+\omega^2\tau_p^2) \qquad \textbf{(2.2)}$$

where:

c = constant

M = molecular weight

R = gas constant

T = temperature

ω = frequency

τ = relaxation time.

In other words, a storage modulus measured at frequency ω and temperature T is equivalent to a storage modulus measured at temperature T_0 and frequency ω multiplied by a shift factor. The time-temperature dependence of dynamic properties acts differently in different temperature regions.

In the glass transition temperature region, the shift factor (a_T) can be described by the Williams-Landel-Ferry (WLF) equation (Williams *et al.*, 1955):

$$Log\ a_T = \frac{C_1(T-T_{ref})}{C_2+(T-T_{ref})} \qquad \textbf{(2.3)}$$

where a_T is the shift factor or degree of horizontal shift required to superimpose a given set of DMA data onto a reference set at a chosen reference temperature (T_{ref}), and C_1 and C_2 are constants. A master curve of dynamic modulus against logarithm of the frequency can be generated by shifting each curve horizontally.

For highly crystalline polymers and temperature below glass transition (T_g), the temperature dependence of a_T follows an Arrhenius form:

$$\log a_T = \frac{E_a}{R}\left(\frac{1}{T}-\frac{1}{T_{ref}}\right) \qquad \textbf{(2.4)}$$

where:

R = gas constant,

E_a = activation energy.

Dynamic modulus curves, obtained at different temperatures, can be superposed by horizontal shifts along a logarithmic frequency scale to give a single composite curve covering a larger frequency range.

If TTS is to be successfully applied to materials, several criteria must be met : (1) an exact match in the shapes of the adjacent curves, (2) the same set of a_T for all the viscoelastic functions (i.e. one set of a_T values should be used for both E' and E" shifting), (3) a temperature dependence of a_T must have a reasonable form consistent with experiments.

Salmén (1984) applied time-temperature superposition to the dynamic mechanical behavior of *in situ* lignin under water-saturated conditions. The reference temperature was set at 112.3°C while tests were conducted in the range of 20° to 140°C. The result showed that the shift factors follow the WLF equation when temperature was between 72°C and 130°C.

Time-temperature superposition was found applicable to spruce wood plasticized with non-aqueous diluents (Kelley *et al.*, 1987). The temperature range studied was from 30°C to 120°C, while the reference temperature was 60°C. The WLF equation was found to be valid for the temperature range of 30°C to 116°C.

Tissaoui *et al.* (1992) constructed a master curve from a number of short-term tensile and compressive tests. Temperature varied from 20°C to 60°C, and there were three different moisture contents (6%, 9%, 12%). The creep data was extrapolated from a five hours test to seventy-five days. The horizontal shift factors were found to follow the Arrhenius equation. The same conclusion was drawn in creep

and recovery modeling (Gamalath, 1991; Samarasinghe *et al.*, 1994). However, attention was only given to bringing multi-curves into coincidence with a reference curve in the research. Little demonstration to provide the validity of the procedure was made by those researchers.

Methodology

Materials and Equipment

The samples were cut from two pieces of kiln dried Douglas-fir (one had wide-growth ring, and another had narrow-growth ring) purchased from a local lumber retailer in Corvallis, Oregon. The boards were selected on the basis of straightness of grain and free of defects. The first group of samples was quarter-sawn 7.62mm X 50.8mm X 457.2mm for static long-term creep tests. The second group of samples was quarter-sawn 2mm X 12mm X 52mm and each sample consisted of at least three complete growth rings. The second group of samples were used for the dynamic mechanical analysis of TTS.

The equipment used for the dynamic mechanical analysis was Rheometrics Solid Analyzer, RSA II (detailed in Chapter 1).

Procedures

Long-term Creep Test of Solid Wood

The objective of this test was to investigate the long-term performance of solid wood in terms of relative creep under a constant load. The results would be used to evaluate dynamic TTS prediction data.

The static creep test was conducted in a conditioned room at 30°C and a relative humidity of 30% resulting in an average actual moisture content of 4.2%. The total of 14 samples were center loaded under constant weight (9,080 gram) for two months (60 days). The bending stress for this load was approximately 25% of the maximum bending strength as given by the Wood Handbook (1987). An ordinary dial gauge with an accuracy of one hundredth millimeter was used to obtain load-deflection data.

The general nature of the time-deflection curves was shown in Fig.2.1. On the average, beams increased their deflection to about 1.3 times the initial deflection after two months.

The data from the creep test were fitted to a power law (Equ.2.1) since it was widely used and the degree of accuracy was satisfied. The curve fitting is done by differentiating Equ.2.1 with respect to time by

$$\frac{dD(t)}{dt} = mnt^{n-1} \qquad \textbf{(2.5)}$$

The influence of initial deflection was eliminated by this mathematical procedure. The time derivation was calculated as:

$$\dot{D}(t_i) = \frac{D(t_{i+1}) - D(t_{i-1})}{t_{i+1} - t_{i-1}} \qquad (2.6)$$

i=2, 3, 4.....

Then, logarithms were taken

$$\ln(\dot{D}(t)) = \ln(m\ n) + (n-1)\ln\ t \qquad (2.7)$$

Equ.2.7 was used as the model for a least squares fit of the transformed data which yielded values of m, n, and D_0. These values then were averaged to the final value of the parameter.

Time-temperature Superposition of Solid Wood

(a) Dynamic mechanical tests

Twelve Douglas-fir specimens were dried in a desiccator with phosphorus pentoxide (P_2O_5) for not less than four hours. Dynamic mechanical analysis was performed in three-point bending. The sample was subjected to a sinusoidal alternating strain of 5 x 10^{-5}, which was well below the linear elastic limit of the wood. Each test sequence (frequency-temperature sweep) combined the frequency and temperature sweep to generate a group of curves. The temperature was incremented from 0°C through 200°C at 10 degrees per step and each step was approximately ten minutes.

While holding temperature constant, the frequency was increased from 0.1 to 100 rad/sec. Ten data points were measured at each decade of frequency. Figure 2.2 shows the dependence of viscoelastic properties on temperature and frequency.

(b) Generation of the relaxation spectra from the DMA data

Since one of the important criteria for the applicability of time-temperature superposition depends on the characteristic of the relaxation spectra, dynamic moduli were converted into isothermal relaxation spectra.

Relaxation spectrum (H) can be transformed from dynamic modulus, either E' or E" or both of them, as:

$$H(\tau=\frac{1}{\omega}) = \pm\frac{1}{\pi} Im\ E^*(\omega e^{\pm i\pi})$$

$$H(\tau=\frac{1}{\omega}) = \pm\frac{2}{\pi} Im\ E'(\omega e^{\pm i\pi/2}) \qquad \textbf{(2.8)}$$

$$H(\tau=\frac{1}{\omega}) = \frac{2}{\pi} Re\ E''(\omega e^{\pm i\pi/2})$$

where ω is frequency, Im and Re represent imaginary and real part of complex (Ferry, 1980). Relaxation spectra of dry Douglas-fir wood at different temperatures are shown in Figure 2.3.

(c) Application of TTS to dry Douglas-fir

Automatic TTS shift was done by using software and algorithm contained in RSA II (Rheometrics®). The reference temperature was 30°C in this study. The shifting was

fulfilled by minimizing the difference between the reference and shifting modulus. The most probable local residuals and best shift factors were calculated after shifting. TTS shift resulted in a composite curve which is called the master curve. The shift factors were fitted into Arrhenius equation since the temperature range in this study was well below the glass transition temperature. From test obtained shifting factor values, the activation energy of such material was calculated according to Equation 2.4. Figure 2.4 shows the results of shifting dry Douglas-fir at a reference temperature of 30°C.

Results and Discussion

Examine the Criterion for Applicability of TTS

Ferry (1980) suggested that the validity of the superposition should be verified before its use. A careful examination of relaxation spectra should assure applicability of time-temperature superposition. Figure 2.3 shows the plot of spectrum (H) with time. The differences between H values at different temperatures were calculated. The statistical analysis was done to see whether the shapes remain unaltered when the temperature changed. The results showed that the curve shape remained unchanged until temperature up to 90°C.

The results of TTS are shown in Table 2.1. Temperature was used as a sorting parameter in the TTS process, a_T is the horizontal shift factor, b_T is vertical shift factor and χ^2 gives the error in the shift as calculated by the weighted average over each variable used in the sum of the local residuals at each point where there is an overlap. The experimental criteria for the TTS prediction was that the composite master curves be smooth within experimental error. This was satisfied in this study (Fig.2.4) and χ^2 values were all reasonably small (less than 0.027).

Another criterion is that the shift factor should have a reasonable form consistent with past experience. The temperature dependence of the shift factors (a_T) obtained in

TTS procedures was a smooth function with no gross fluctuations (Fig. 2.5). The empirical values of a_T were then fit into the Arrhenius equation with an average of r=0.98 and 0.99 for the wide-growth-ring and narrow-growth-ring samples. From the empirical values of shifting factors, the apparent activation energy is calculated according to the Equ.2.4. The average apparent activation energy (E_a) is 141 kJ/mol and 169 kJ/mol for the two sample groups. By knowing the activation energy of a material, the shifting factors for such material can be calculated without actually testing such material. Therefore, the time-dependent property of such material can be predicted by using the information of the activation energy.

By completed DMA/TTS procedure, the dynamic test data was extended to four decades wider frequency range than test data. Using the dynamic modulus of master curves, the stress relaxation modulus E(t) was calculated. The stress relaxation modulus is defined as the stress to strain ratio at constant deformation. It can be written as:

$$E(t) = E_e + \int_{-\infty}^{\infty} He^{-t/\tau} d\ln\tau \qquad \textbf{(2.9)}$$

where:

E_e = constant,

H = relaxation spectrum,

τ = characteristic time.

The result is presented by dots in Fig.2.6. The result exhibited the time-dependent behavior of solid wood and provided the same patterns of relationship between the time and mechanical properties that is associated with long-term creep.

Evaluation of Prediction

The time-temperature superposition prediction was evaluated by comparing it to the results of long-term creep tests. In order to compare the results from two different tests, the average creep compliance obtained from static tests were converted to relaxation modulus.

The following criteria were applied in this comparison. First, average relaxation moduli of static test data and relaxation moduli converted from TTS/DMA data were compared (Fig.2.6). The difference between DMA predicting data to creep data is given in Table 2.2 (in term of "difference*"), with an average difference of 6%.

Second, the coefficient of determination (R^2_a) in regression using reference data (dynamic data measured at the reference temperature) only was calculated. This measure referred to how well the predicted values compared to actual values based on unshifted points only. The averaged R^2 was 0.72 and 0.67 for the two groups samples, respectively.

Third, the coefficient of determination (R^2_b) of the regression using all shifted data was calculated. This is a measure of the accuracy of predicting long-term performance from short-term data. The average was 0.88 for wide growth-ring samples group and 0.82 for narrow growth-ring samples.

Fourth, the number of over-predictions versus the number of under-predictions was investigated. Within the context of the limited data, there was a tendency for DMA predictions to give lower values than static creep values. The result is consist with the fact that creep samples had a higher moisture content. Since the DMA data was compared to the long-term creep test data, it is likely that the two tests were not conducted under identical conditions. The static creep test and DMA test were conducted in different environmental conditions. The loads in these two tests were different. Whereas the tests were in the linear region, the time-dependent property was associated with the stress of test samples. Also the differences in sample size might result in a difference in creep. Although there was no statistical data available, big samples have the potential for more defects which would contribute to more creep than for smaller samples. Further research is recommended to conduct matching sample tests under exactly identical conditions.

Conclusions

An examination of the detailed dynamic mechanical behavior of dry wood shows that time-temperature superposition is applicable to dry Douglas-fir. The temperature range, where all criteria for DMA/TTS were met, is from 30° to 80°C. The shifting factors were fitted into Arrhenius equation with an average r=0.98. The stress relaxation moduli converted from DMA/TTS data shows a good agreement with data obtained from static creep tests (R^2=0.8).

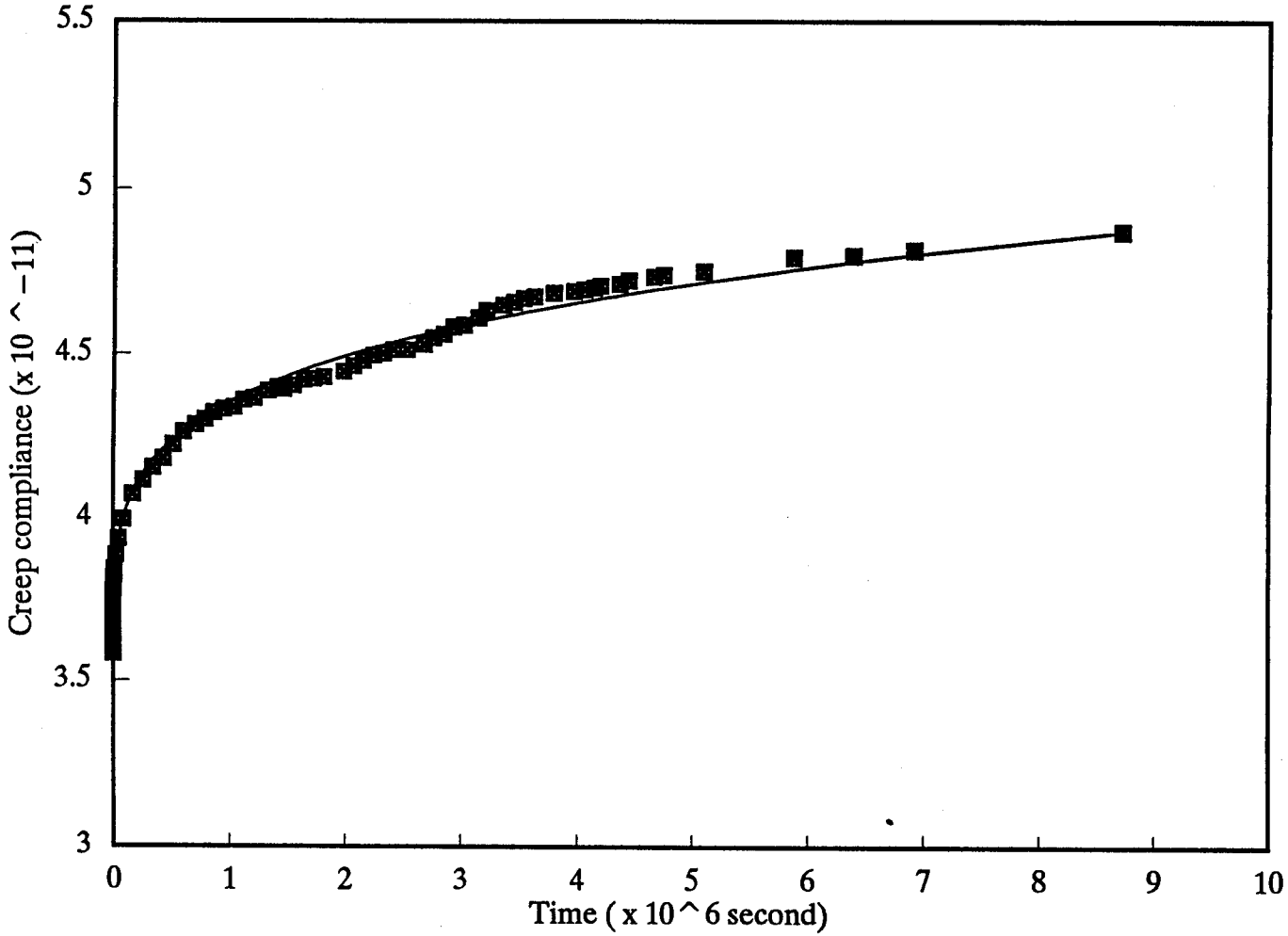

Figure 2.1 Creep of Douglas-fir in three-point bending with curve fitting (sample #10).

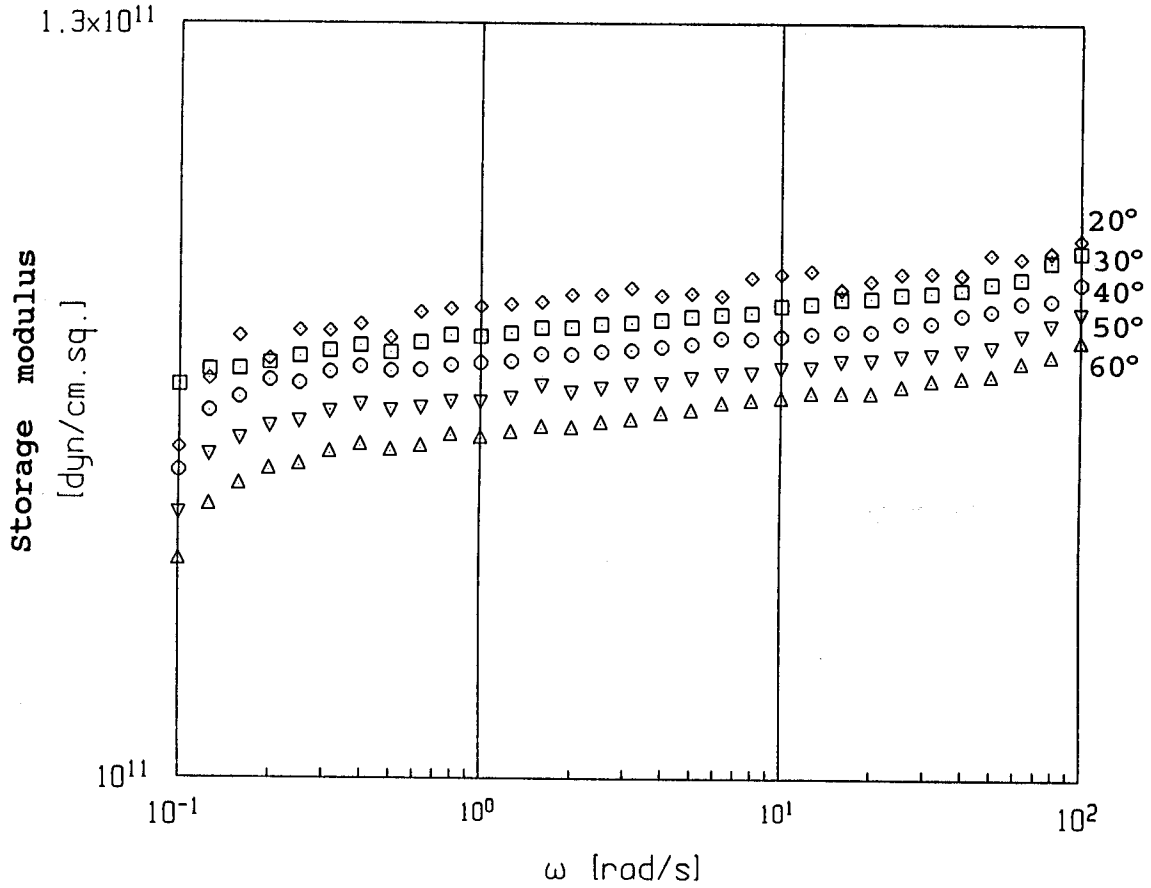

Figure 2.2 Storage modulus of Douglas-fir at different temperatures and frequencies.

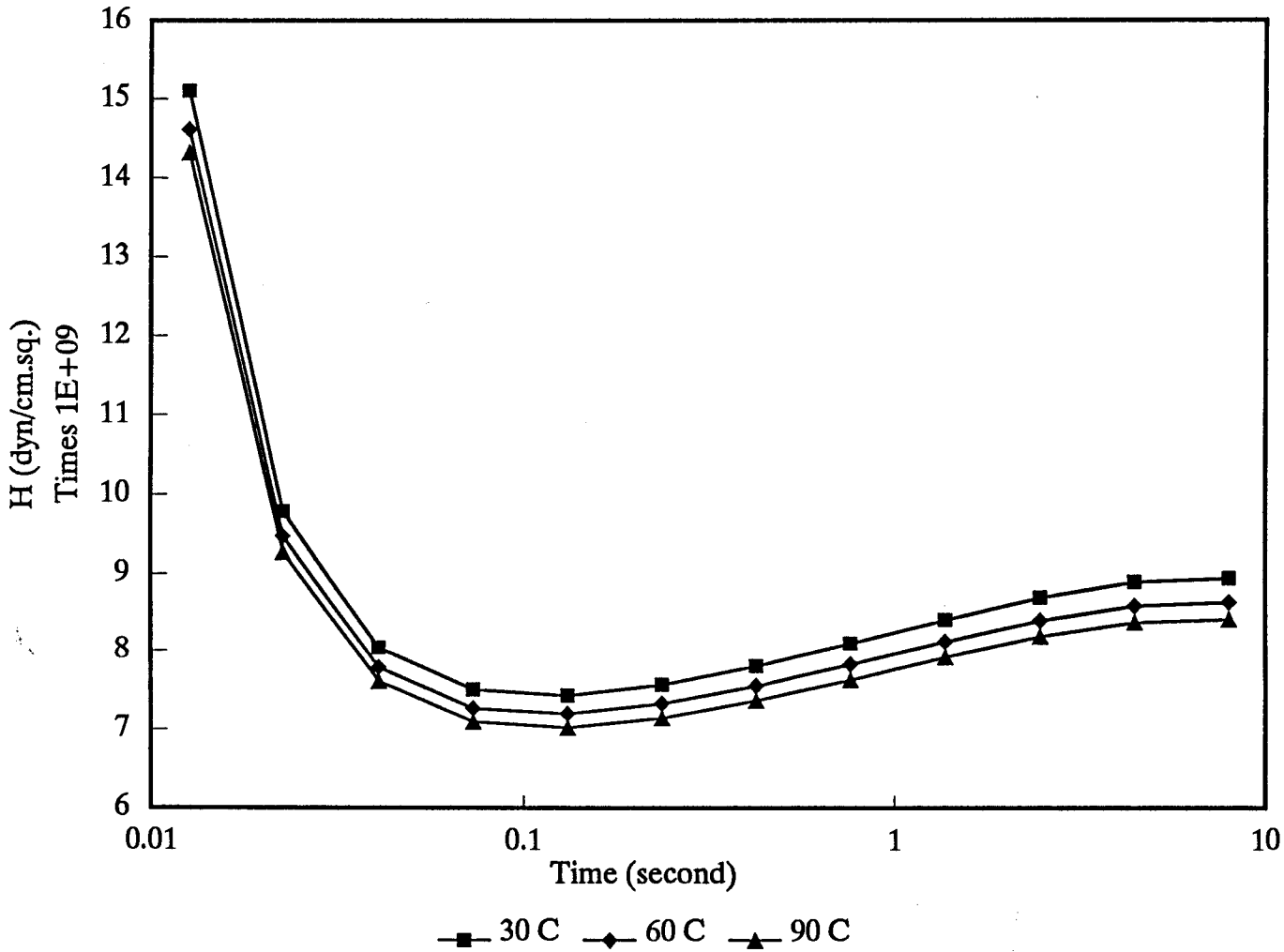

Figure 2.3 Relaxation spectra (H) of Douglas-fir in different temperatures as indicated.

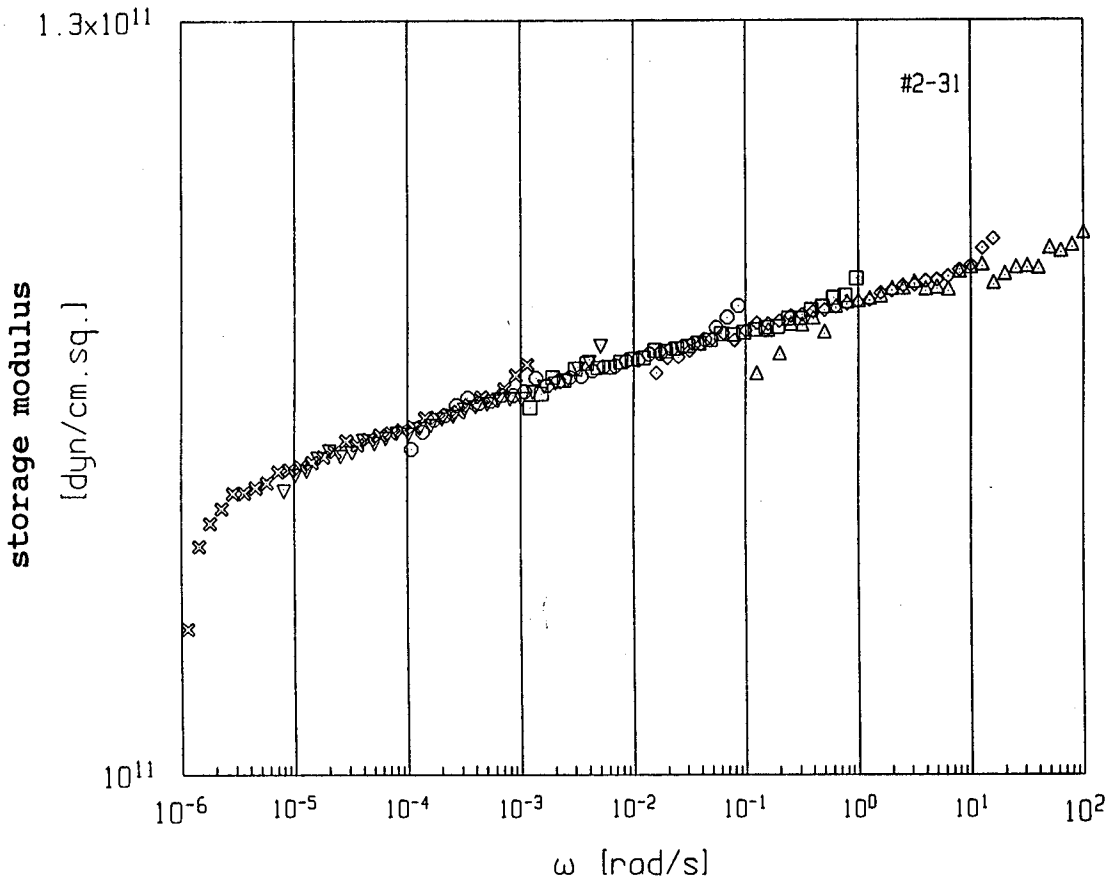

Figure 2.4 Master curve of storage modulus (E') obtained by composite of the data of Fig.2.2 (reference temperature=30°C).

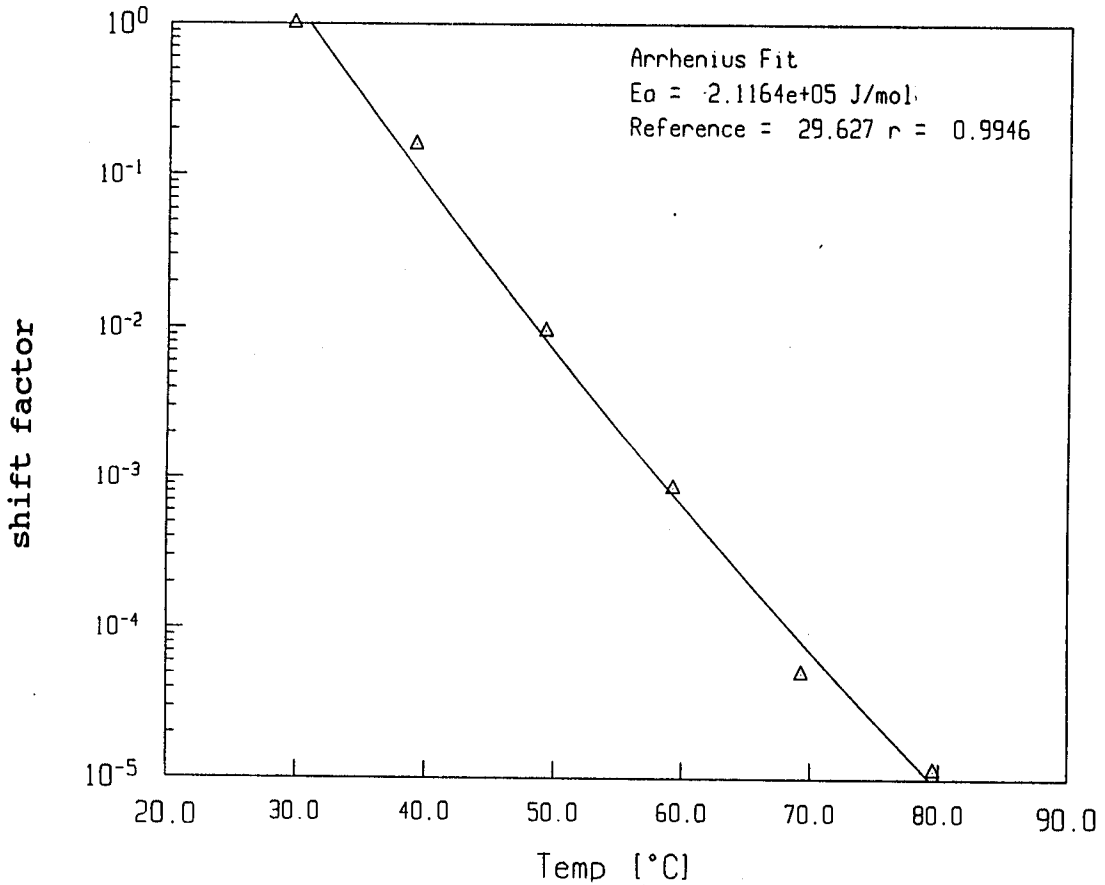

Figure 2.5 Temperature dependence of the shift factors a_T used in plotting Fig.2.4.

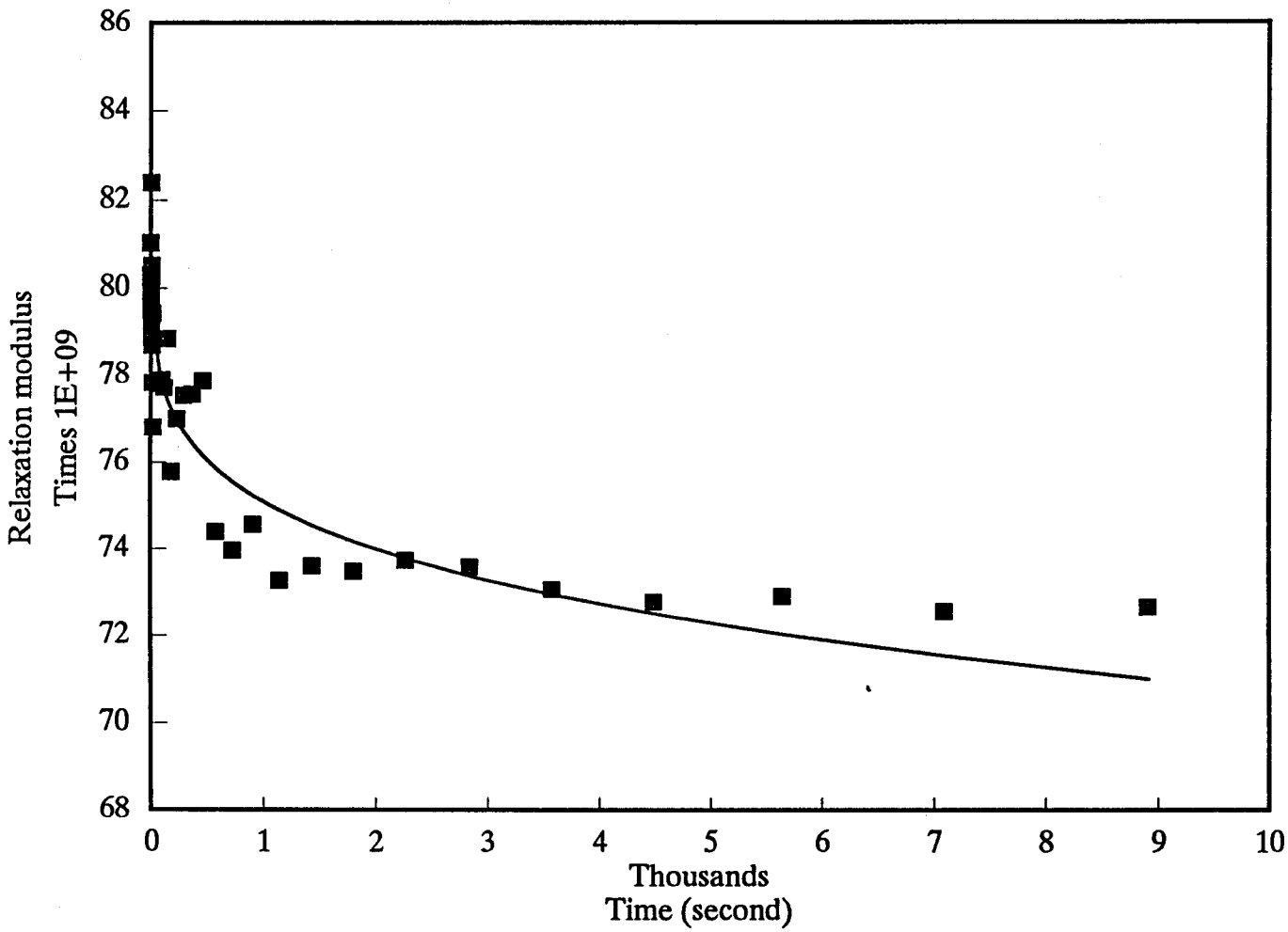

Figure 2.6 Comparison of relaxation modulus obtained from DMA (dots) (sample #2-17) and average creep data (solid line).

Table 2.1 Determination of a_T values for dry Douglas-fir.

Sample #	Temp(C)	a_T	b_T	χ^2	Arrhenius fit	
					Ea (J/mol)	r
#2-12	34.0	1.00E+00	1.000		1.424E+05	0.9985
	44.1	2.27E-01	1.033	0.004		
	54.3	3.41E-02	1.065	0.004		
	64.3	8.53E-03	1.096	0.003		
	74.5	1.66E-03	1.126	0.004		
	84.7	4.00E-04	1.165	0.012		
#2-13	29.6	1.00E+00	1.000		1.616E+05	0.9818
	39.2	4.59E-01	1.020	0.007		
	49.3	5.74E-02	1.066	0.015		
	59.3	5.46E-03	1.094	0.011		
	69.4	7.17E-04	1.131	0.013		
	79.6	2.18E-04	1.164	0.005		
#2-14	29.8	1.00E+00	1.000		1.285E+05	0.9916
	39.2	1.16E-01	1.024	0.009		
	49.3	4.88E-02	1.063	0.005		
	59.3	8.64E-03	1.098	0.005		
	69.4	2.00E-03	1.129	0.004		
	79.6	6.52E-04	1.164	0.004		
#2-15	29.0	1.00E+00	1.000		1.341E+05	0.9233
	39.0	5.15E-01	1.033	0.003		
	49.2	2.34E-01	1.067	0.005		
	59.2	5.00E-02	1.098	0.012		
	69.3	3.00E-03	1.124	0.020		
	79.5	5.90E-04	1.159	0.020		
#2-17	29.5	1.00E+00	1.000		1.389E+05	0.9943
	39.1	2.55E-01	1.013	0.010		
	49.3	6.52E-02	1.062	0.020		
	59.3	8.98E-03	1.098	0.016		
	69.4	2.02E-03	1.133	0.015		
	79.6	4.49E-04	1.167	0.003		
#2-20	29.6	1.00E+00	1.000		1.406E+05	0.9926
	39.1	3.45E-01	1.025	0.008		
	49.2	5.00E-02	1.060	0.014		
	59.2	6.72E-03	1.091	0.013		
	69.3	1.86E-03	1.130	0.026		
	79.5	5.30E-04	1.163	0.007		
Average					1.410E+05	0.980

Table 2.1 Determination of a_T values for dry Douglas-fir (Continued).

Sample #	Temp(C)	a_T	b_T	χ^2	Arrhenius fit	
					Ea (J/mol)	r
#2-16	29.7	1.00E+00	1.000		1.725E+05	0.9868
	39.1	3.50E-01	1.032	0.004		
	49.3	3.16E-02	1.065	0.001		
	59.3	2.28E-03	1.095	0.002		
	69.4	4.38E-04	1.131	0.002		
	79.6	1.15E-04	1.164	0.001		
#2-30	29.6	1.00E+00	1.000		1.767E+05	0.986
	39.2	1.85E-01	1.033	0.004		
	49.3	3.55E-02	1.065	0.002		
	59.3	1.49E-03	1.096	0.003		
	69.4	2.77E-04	1.131	0.002		
	79.6	8.14E-05	1.165	0.002		
#2-31	29.6	1.00E+00	1.000		2.116E+05	0.9946
	39.1	1.58E-01	1.034	0.004		
	49.2	9.61E-03	1.065	0.002		
	59.2	8.60E-04	1.098	0.003		
	69.3	5.08E-05	1.128	0.002		
	79.5	1.14E-05	1.165	0.003		
#2-32	29.6	1.00E+00	1.000		1.496E+05	0.9916
	39.2	1.27E-01	1.031	0.003		
	49.3	1.99E-02	1.065	0.002		
	59.3	2.36E-03	1.094	0.003		
	69.4	8.51E-04	1.131	0.002		
	79.6	2.39E-04	1.165	0.003		
#2-33	29.6	1.00E+00	1.000		1.341E+05	0.9948
	39.1	1.42E-01	1.031	0.003		
	49.2	2.30E-02	1.065	0.004		
	59.2	5.69E-03	1.098	0.002		
	69.3	1.91E-03	1.131	0.002		
	79.5	4.55E-04	1.164	0.003		
Average					1.689E+05	0.991

Table 2.2 Standard deviation of regression between static creep tests and adjusted DMA predictions.

Sample #	R^2_a	R^2_b	Difference*
#2-12	0.657	0.812	9.84%
#2-13	0.575	0.748	16.89%
#2-14	0.919	0.905	2.39%
#2-15	0.731	0.853	4.52%
#2-17	0.525	0.880	2.29%
#2-20	0.910	0.724	3.47%
AVG	0.720	0.820	6.57%
STD	0.152	0.066	

Sample #	R^2_a	R^2_b	Difference*
#2-16	0.232	0.802	14.62%
#2-30	0.887	0.908	0.84%
#2-31	0.83	0.946	9.03%
#2-32	0.846	0.919	4.16%
#2-33	0.538	0.812	6.25%
AVG	0.667	0.877	6.98%
STD	0.250	0.059	

References

Bach, L. and R. E. Pentoney. 1968. Nonlinear mechanical behavior of wood. Forest Products Journal 18(3):60-66.

Bodig, J., and B. A. Jayne. 1982. Mechanics of Wood and Wood Composites. Van Nostrand Reinhold Co. New York.

Breese, M. C. and A. J. Bolton. 1993. The effect of temperature and moisture content on the time-dependent behavior of isolated earlywood specimens of Sitka Spruce (*Picea sitchensis*), loaded in compression in the radial direction. Holzforschung 47(6):523-528.

Davidson, R. W. 1962. The influence of temperature on creep in wood. Forest Products Journal 12(8):377-382.

Ferry, J. D. 1980. Viscoelastic Properties of Polymers. John Wiley and Sons, Inc., New York.

Gamalath, S. 1991. Long-term creep modeling of wood using time-temperature superposition principle. Ph.D. Dissertation. Wood Science and Forest Products, Virginia Polytechnic Institute & State University, Blacksburg, VA.

Holzer, S. M., J. R. Loferski, and D. A. Dillard. 1989. A review of creep in wood:concepts relevant to develop long-term behavior predictions for wood structures. Wood and Fiber Science 21(4):376-392.

Kelley, S. S., T. G. Rials, and W. G. Glasser. 1987. Relaxation behavior of the amorphous components of wood. Journal of Material Science 22:617-624.

McNatt, J. D. and M. O. Hunt. 1982. Creep of thick structural flakeboards in constant and cyclic humidity. Forest Products Journal 32(5):49-54.

Pearson, R. G. 1981. Time dependent properties. Pages 191-208 in John F.Oliver, ed. Adhesion in Cellulosic and Wood-based Composites. Plenum press, New York.

Salmén, Lennart. 1984. Viscoelastic properties of *in situ* lignin under vater-saturated conditions. Journal of Material Science 19:3090-3096.

Samarasinghe, Sandhya, J. R. Loferski, and S. M. Holzer. 1994. Creep modeling of wood using time-temperature superposition. Wood and Fiber Science 26(1): 122-130.

Schaffer, E. L. 1982. Influence of heat on the longitudinal creep of dry Douglas-fir. Pages 20-52 in R.W.Meyer and R.M.Kellog, ed. Structural Uses of Wood in Adverse Environments. Van Nostrand Reinhold Co., New York.

Schniewind, A. P. and J. D. Barrett. 1972. Wood as a linear orthotopic viscoelastic material. Wood Sci.and Tech. Vol.6:43-57.

Smulski, S. J. 1989. Creep functions for wood composite materials. Wood and Fiber Science, 21(1):45-54.

Tissaoui, J., J. R. Loferski, S. M. Holzer, D. A. Dillard, and B.H.Bond. 1992. Long-term creep law for wood in compression and tension parallel to grain. Proc.ASME, Mechanics of Cellulosic Materials, AMD-Vol.145/MD-Vol. 36:33-38.

Williams, M. L., R. F. Landel, and J. D. Ferry. 1955. The temperature dependence of relaxation mechanisms in amorphous polymers and other glass-forming liquids. J.Am.Chem.Soc. 77:3701-3707.

Wood Handbook. 1987. United States Department of Agriculture, U.S. Forest Products Lab. Agriculture Handbook No 72, U.S. Government Printing Office, Washington, D.C.

Yamada, T., T. Takemurea, and S. Kadita. 1961. On the rheology of wood. III. The creep and stress relaxation of buna. J. Japan Wood Res. Soc. 7(2):63-67.

CHAPTER 3
THERMAL AND DYNAMIC PROPERTIES OF WOOD-BASED COMPOSITES

Introduction

Wood-based composites are rapidly increasing in use for both nonstructural and structural applications. These composites have all the good characteristics of wood, plus the additional advantages of being able to engineer their end-use properties by judicious selection and combination of components. However, to be able to engineer these products, some knowledge must pre-exist on how the overall performance of the product is influenced by its components and production parameters. Dynamic mechanical analysis provides a means of accomplishing this goal.

Also of value is the ability to predict time-dependent properties, especially when considering the rapid introduction of new wood composites to the marketplace and the lack of long-term test data for these products. TTS is an empirical approach which is used in the study of polymers to extend the test frequency range. Given its success applications to other polymeric materials, time-temperature superposition (TTS) technique was applied to the study of particulate wood-based composites bonded with three types of adhesives.

Dynamic mechanical properties of wood-based composites are affected by properties of its adhesive and wood

components, as well as the numerous processing parameters. In order to improve the performance of wood-based composites, it is therefore necessary to develop a quantitative understanding of its viscoelastic characteristics. Since these composites consist of wood components in some form or shape bonded together by some types of adhesive, the relationship of the properties of its components to the composite need to be understood.

For this study, a particulate composite was selected to study this relationship. The composite consisted of relatively small particles bonded with one of three types of commonly used adhesives. It was felt that this composite, although not typical of commercial products because of the small size of its particles, did provide a uniform composite material with components proportional to the scale of the test sample. This composite would provide the same types of interaction and material behavior that is associated with commercial products.

The objective of this chapter is to determine the thermal and dynamic mechanical properties of three different types of adhesives and wood-based composites as affected by temperature and frequency. Included in the dynamic properties study was the suitability of using time-temperature superposition (TTS) to predict time-dependent properties of wood-based composites. Furthermore, the relationship between the static tensile strength

perpendicular to the panel (commonly referenced to as internal bond strength) and its dynamic property was investigated.

Literature Review

Wood-based composites consist of various types of wood elements bonded together with different adhesives in different combinations and configurations. Wood-based composites offer the potential, through control of process parameters, to be designed to match specific product end-use applications. The following variables have been found to influence the properties of wood-based composites: species, shape, and orientation of the wood component; type, formulation, and quantity of adhesives; and the process variables of temperature, pressure, time, as well as numerous others (Rice and Carey, 1978; Bodig and Jayne, 1982).

Adhesives for Wood-based Composites

The bonding of an adhesive to wood particles involves many material parameters. For particulate wood-based composites, the liquid adhesive is applied to the wood by either atomizing and spraying as droplets or through mechanical friction during blending to distribute as droplets. Adhesive properties such as wetting, viscosity, and molecular weight distribution have an effect on the bond strength of particleboard (Wilson *et al.*, 1979). The bond quality is affected also by time, temperature, pressure and

other processing parameters (Chow and Steiner, 1979b; Humphrey and Ren, 1989; Johnson and Kamke, 1994).

For all wood-based composites there are two basic forms in which adhesive coverage on the wood is obtained. First, adhesive can be applied as a continuous film form, such as is done for plywood, laminated veneer lumber, and laminated beams. Second, the adhesive can act as a network of droplets on wood fragments in a comminuted form such as in particleboard or orient strandboard. The comminuted form results in what is referred to as spot welding to provide a connected network of particulate wood components. Many articles have been published dealing with particulate wood-based composites in terms of its bonding process and the factors affecting bond formation (Allan and Neogi, 1971; Carroll and McVey, 1962; Chow, 1969; Chow and Steiner, 1979a; Freeman, 1959; Furuno, 1976; Maloney, 1970; Moore, 1975; Wilson *et al.*, 1976, 1978, 1979).

Yamada and Taki (1991) examined the relationship between the mechanical properties of adhesive and adhesion strength in composites. Takemura *et al.* (1986) investigated the molecular structure of resins and its impact on bonding. Bond strength was also found to be strongly dependent on rheological properties of adhesives (Motohashi *et al.*, 1984), i.e. the temperature dependence of bond strength was influenced by the glass transition of the adhesive.

Viscoelastic Properties of Wood-based Composites

When wood-based composites are subjected to sustained loads, after an initial elastic deformation they continue to deflect as time elapses -- this is referred to as creep. Creep of wood-based materials is a function of stress level, time, temperature, and relative humidity (Bodig and Jayne, 1982). Smulski (1989) showed that a nonlinear function could be used to model the creep of laminated timber and hardboard. Chow (1979) used a power law equation to describe the creep behavior of hardboard panels accurately with a correlation coefficient (R^2) for each regression model exceeding 0.90. A mechanical model with four-elements was used to characterize the creep behavior of manufactured hardboard (Moslemi, 1964). For particleboard, Bryan and Schniewind (1965) showed that the phenolic-bonded material displayed greater relative creep than the urea bonded material.

Wood-based composites are hygroscopic and their moisture content has a pronounced effect on many of their mechanical properties (Bodig and Jayne, 1982). The effect of moisture content (MC) on modulus of elasticity and long-term creep of different particulate composites has been well documented (Moslemi, 1964; Bryan and Schniewind, 1965; Steiner, 1984; Steiner and Warren, 1981). Relative creep due to humidity cycling was considerably higher than that at constant

humidity for wood-based composites (Dinwoodie *et al.*, 1981, 1991, 1992; McNatt and Hunt, 1982).

Dynamic Mechanical Analysis and Time-temperature Superposition

Dynamic mechanical analysis (DMA) of materials can be used to define the material's structure in terms of parameters such for polymers as molecular weight and crosslinking, or can be used to explain a material's response to environmental or external variables such as temperature, time or frequency, and relative humidity. DMA is widely used in research on the materials such as polymers and metals (Ferry, 1980; Nielsen, 1974), but applications of DMA on wood and wood-based composites have not been fully developed. Dynamic mechanical analysis (DMA) is a means of investigating mechanical response to periodic forces (or displacements). In the dynamic mechanical test, the storage modulus (E') measures the energy stored in the specimen and loss modulus (E") measures the dissipation of energy. The ratio between the loss modulus and the storage modulus is called internal friction (tanδ) (Ferry, 1980; Ludbrook and Whitwood, 1992).

As temperature varies, thermal induced transitions in material properties occur. Several inflections points can be noted in the internal friction (tanδ) versus temperature plot which coincide to those transitions. Each transition

corresponds to specific molecular motions significant to structure and property relationships of the material. The transition related to the motion of main backbone of material is named as glass transition temperature (T_g).

Time-dependent behavior is exhibited when materials are subjected to dynamic deformation at different frequencies. Characterization of the thermo-rheological of properties of composites has been reported using mechanical analysis (Murayama, 1978).

Time-temperature superposition technique (TTS) involves measurements of dynamic response at a number of different temperatures over a relatively small range of frequency and then shifting the results to a reference temperature to form a master curve. The process provides a larger frequency range than the experimental test covers. The relationship between storage modulus (E') at an arbitrarily selected reference temperature (T_0) and time (t), and its property at a different temperature (T), can be expressed as:

$$E'(T_0, t) = \frac{\rho(T_0)\ T_0}{\rho(T)\ T} E(T, t/a_T) \qquad \textbf{(3.1)}$$

where a_T is the shift factor, and ρ is the density (Ferry, 1980).

For highly crystalline polymers and temperature below glass transition (T_g), the temperature dependence of a_T follows an Arrhenius form:

$$\log a_T = \frac{E_a}{R} \left(\frac{1}{T} - \frac{1}{T_{ref}}\right) \qquad (3.2)$$

where:

R = gas constant,

E_a = activation energy.

The TTS technique has been successfully used in several polymer materials (Murayama, 1978). There are only a few reports documented in the literature on the application of TTS in forest products research (Kelley *et al.*, 1987; Gamalath, 1991; Tissaoui *et al.*, 1992; Samarasinghe *et al.*, 1994). The materials used in these studies were either solid or chemically-modified wood. There are no published data available in regard to applying TTS to wood-based composites.

Materials and Methods

Materials

Adhesives

Three types of the most commercially used adhesive (provided by Borden Chemical Co., Springfield, OR) were utilized in this study: urea-formaldehyde (UF) phenol-formaldehyde (PF) and resorcinol-formaldehyde (RF). Adhesive mixed with catalyst was cast in aluminum molds to provide test samples of pure adhesive (Table 3.1). Once cast at room temperature, the samples were allowed to completely cure in an oven at a temperature of 65°C for four hours. Cured resin was cut into 3mm x 12mm x 52mm for DMA test. There were six repetitions for each type of resin.

Composite Samples

Particulate composites were laboratory made from screened Douglas-fir particles of small size -- all particles could pass through a 0.9 mm mesh opening, of which 10% by weight could pass through a screen with a 0.3 mm mesh opening -- having a moisture content of 6% (ovendry weight basis).

Three different types of adhesive were used to make the boards at application levels of 10% and 15% as measured on an

ovendry solid weight basis. There were six boards made for each condition. The adhesives were applied gradually to the particles in a friction mixing blender. The blended particles, consisting of wood particles and adhesive, were distributed by hand evenly on an aluminum caul plate in a forming box. The boards were hot pressed at 4.8 MPa and 160°C (171°C for PF-bonded boards) for a duration of 5 minutes. Metal stops of 3mm thick were used to control the thickness of boards during pressing. The finished particulate composites had a specific gravity of 0.75 ± 0.07 with a moisture content of 3% (ovendry basis). Two samples of 3mm x 10mm x 53mm were cut from each board (total of 72 samples) for DMA test. One sample of 50.8mm x 50.8mm was cut from each board for static IB test.

Methods

Tensile Strength Test Perpendicular to Surface

The specimens for determining the tensile strength perpendicular to the surface, or also referred to as the internal bond strength, were 51 mm x 51 mm and the thickness of the finished boards, with a target thickness of 3mm. Aluminum blocks were bonded with hot melt adhesive to both faces of specimen. The samples were pulled by an applied force perpendicular to the surfaces, until failure. The

maximum loads at failure were recorded as the internal bond (IB) strength. Only the data of that the wood failure area is larger than half of total testing area is accepted. The IB values were adjusted according to the effective test area of each sample.

Thermal and Dynamic Mechanical Properties of Adhesives and Particulate Composites

The dynamic mechanical properties of cast adhesive beams were measured with a RSA II (Rheometrics®) at a fixed frequency mode of 100 rad/sec in the temperature range from 25° to 95°C. The temperature was increased in a stepwise manner at increments of 5°C with soaking time of 60 seconds and measurements repeated. Using stepwise temperature increases rather than a ramp increase, ensured that thermal equilibrium existed throughout the test sample during testing. After thermal equilibrium was achieved, the sample was tested in three-point bending by applying a sinusoidal strain maximum amplitude of 5×10^{-5} and measuring the resultant sinusoidal load for stress. The DMA properties measured were storage modulus (E'), loss modulus (E"), and internal friction ($\tan\delta$). There were six repetitions in each test group.

The glass transition temperature (T_g) was identified as the maximum point in a plot of the internal friction vs. temperature.

Similar test procedures were conducted on the particulate composites bonded with the different types and percentages of adhesive. The temperature range studied was from 25° to 225°C.

Application of DMA/TTS on Wood-based Composites

Both temperature and frequency effects on samples were measured by testing in the temperature-frequency sweep mode of the dynamic mechanical analyzer. Temperature ranged from 30° to 80°C and frequency was swept from 0.1 rad/sec to 100 rad/sec. It was conjectured that the correctness of the temperature range selected for the study would depend on the temperature properties of adhesive and wood.

Automatic TTS shift was done by using software and algorithm contained in RSA II (Rheometrics®). The reference temperature of 30°C was selected in this study. The shifting was completed by minimizing the difference between the reference and shifted moduli after it has been shifted. The most probable local residuals and the shift factors were calculated empirically. TTS shift resulted in a composite curve which is called a master curve. The shift factors were fitted into Arrhenius equations since the temperature range of TTS in this study was well below the glass transition temperature. From test obtained shifting factor, the

activation energy of such material was calculated according to Equation 3.2.

Results and Discussion

Correlation of IB and Internal Friction

It was postulated that during dynamic testing, energy would dissipate at the interface of the wood and adhesive based on the quality of adhesion. To examine this statement a plot was made of the statically obtained internal bond strength and the dynamically obtained internal friction for particulate composites (Fig. 3.1). The relationship was found to be linear with IB increasing as internal friction of the dynamic test decreased. The statistical linear regression for this relationship had a coefficient of determination of $R^2 = 0.76$. This correlation suggests that measurement of energy dissipation in the material does correspond to the quality of bonding. Thus, the poorer the bonding, the more energy dissipates. The result agrees with the findings of Murayama (1978). This result provides the feasibility of using dynamic mechanical analysis as a means of characterizing the degree of bonding in wood-based composites.

The reason for scattering of data points is due to the nature of samples. Particulate composite samples used in this study had a target thickness of 3mm which was relatively thin and had a uniform density through the thickness of the board. Therefore, out of 36 samples, there were only 18

samples in which the area of failure surface was larger than a half of total test area. The limited sample number used in this test affected the accuracy of the experiment. Further research using bigger sample number is highly recommended since the variability of particulate composites themselves is quite large.

Temperature Effect on the Dynamic Properties

The adhesive serves as a stress transfer element in the particulate network of the wood-based composite, therefore, the adhesive's properties are important in predicting its performance. Figure 3.2 shows the temperature effect on the dynamic properties of the three adhesives studied. The average storage moduli of cured adhesives at a temperature of 25°C were 1.3×10^{10} dyne/cm^2, 1.4×10^{10} dyne/cm^2, and 0.4×10^{10} dyne/cm^2 for UF, RF, and PF cured resins respectively. These results are consistent with those reported by Yamada and Taki (1991) for UF resin and RF resin. The storage modulus of a resin declined as temperature increased. By comparison, the storage modulus of RF and UF resins dropped faster than storage modulus of PF resin. The average glass transition temperatures (T_g)--as evidenced by the major peak in the internal friction curves of UF, PF, and RF resins--are 94°, 89° and 84°C, respectively. The glass transition temperature of UF resin is in the neighborhood of results of

Chow (1973) and Yamada and Taki (1991). The T_g of PF resin and RF resin is different among these findings since different hardening agents were used in three studies. This also indicated that resin cured in different condition would behave differently in dynamic testing. For example, an adhesive cured *in situ* may not be the same polymer network as when it cured in the presence of wood. This premise was confirmed by the difference between the storage moduli of cured resin and particulate composite.

Figure 3.3 shows the temperature effect on storage modulus of particulate composite bonded with UF resin (15%). Storage modulus of solid wood as well as storage modulus of resin were shown for comparison. The data showed that E' is about 1.3×10^{10} dyne/cm^2, 2.1×10^{10} dyne/cm^2 and 8.5×10^{10} dyne/cm^2 for cured resin, particulate composite, and solid wood at a temperature of 25°C, respectively. This plot only provided the qualitative description of three different materials since the portion of earlywood and latewood in the solid wood is not likely the same as in the composite.

During the process of making the composite, the adhesive system forms crosslinking bonds between the wood particles. Around a temperature of 90°C, the cured resin went through the glass transition while particulate composite only established the secondary transition (Fig.3.4.). The peaks of those secondary transitions were relatively small. The glass transition temperature of wood-based composite was

shifted to the range of higher than 200°C. In other words, at a certain temperature, the thermal energy was sufficient to initiate the micro-Brownian motion of the main chain in cured resin but was insufficient enough to induce main chain transition in the composite (Ferry, 1980; Murayama, 1978). As result, the height of the internal friction peaks decrease and the glass transition temperature of the composite shifted toward a higher temperature as the crosslinking increased. Therefore the internal friction is a sensitive indicator of the degree of crosslinking.

Figure 3.5 shows the internal friction of particulate composites bonded with various adhesives. The internal friction of boards bonded with RF resin (both 15% and 10%) increased at the lowest temperature. This agrees with the temperature dependence of the cured resin itself since cured RF resin had the lowest glass transition temperature. The lower the glass transition temperature of composites, the worse the heat resistance of adhesive strength is (Motohashi *et al.*, 1984; Yamada and Taki, 1991). But the result disagrees with saying that UF resin has less resistance to heat than PF resin and RF resin (Marra, 1983). The different curing process parameters could produce such disparity. The glass transition temperature of resin can be used to predict the heat resistance of wood-based composites. And the heat resistance of composites should be considered while the products are served in extreme conditions.

Storage moduli of the particulate composites bonded with different adhesives declined as the temperature increased (Figure 3.6). The boards bonded with PF resin (15%) had the highest storage modulus among those samples during the whole temperature ranges. In comparing the two levels of resin percentages for the same type of resin bonded composite, it was noted over the entire temperature range that those having 15% resin content had a higher storage modulus than those having 10% resin. At 25°C, the difference was about a factor of two. The results were expected since the larger resin amount provided more completed bonds among the wood particle network producing stiffer boards.

The curve represented samples bonded with RF resin (15%) has a small peak around 75°C corresponding the further crosslink during the DMA test

Time-temperature Superposition

The storage moduli of cured resin which were obtained at several temperatures, were shifted in their entirety along the frequency scale to obtain the master curve (Fig.3.7). It is evident from the figure that the master curves obtained for each resin provided smooth continuous curves. The scatter between the plot points and their deviation from the smoothed line in the figure appear well within experimental error. For the PF resin, the results showed that E' is about

1.3×10^9 dyne/cm^2 at 1×10^{-4} rad/sec and that it increased progressively with the frequency, giving 4.3×10^9 dyne/cm^2 at 100 rad/sec. Within the same frequency range, the storage modulus of RF resin increased from 5.0×10^9 dyne/cm^2 to 1.6×10^{10} dyne/cm^2 and UF resin increased from 3.9×10^9 dyne/cm^2 to 7.7×10^9 dyne/cm^2. The result agrees with the statement of PF bonded particleboard creep more than UF bonded board (Bryan and Schniewind, 1965).

When master curves of particulate composite (15% resin content) were generated, the superposition was less satisfactory in terms of smoothness of curves than the cured resin samples (Fig.3.8). Part of the discontinuity was created when master curves generated from three samples were averaged. The worst scatter was located in the region of low frequencies which indicated the temperature limit of the validity of TTS may be lower than 80°C. Since particulate composites have multiple viscoelastic components, there may be more than one set of relaxation mechanisms active in composites at a given temperature. The temperature range of TTS validity should depend on the temperature properties of adhesive, wood, and compatible deformation of adhesive and wood. From the present study's results, conclusion was drawn that the time-temperature superposition of the composite was applicable within experimental error in the temperature range of 30° to 70°C. Further research is recommended to investigate the relaxation mechanisms of composites at all

frequency scales and temperatures to determine the validity range of DMA/TTS.

The shift factors fit well in the Arrhenius equation, with an average correlation of coefficient (R) above 0.98. The apparent activation energy (E_a) calculated from experimental shifting factors was 183 kJ/mol, 200 kJ/mol and 218 kJ/mol for composites bonded with PF resin, RF resin and UF resin, respectively. Since the activation energy is related to the shifting factors of TTS, it can be used to predict the time-dependent property of material.

By completed DMA/TTS procedure, the dynamic test data was extended to four decades wider frequency range than test data. Since frequency domain in the dynamic test is associated with time scale in the static test, the dynamic properties at a low frequency would describe a long time performance of materials. The DMA/TTS technique predicts the same pattern of relationship between the time and mechanical properties that is associated with long-term creep.

Conclusions

The study shows that the dynamic properties of cured adhesives affect and can be used to predict the dynamic properties of particulate composites. Composite bonded with PF resin has highest storage modulus among those samples tested. The storage modulus of composite bonded with 15% of resin is about two times higher than those bonded with 10% resin.

The experimental data confirmed that crosslinks were formed between adhesive and wood particles during the composite bonding process which results in that the glass transition of particulate composite shifting to a higher temperature than cured resin.

Furthermore, the dynamic properties in terms of internal friction can be used to characterize the adhesive bonding.

The examination of the detailed dynamic behavior of wood-based composite shows that time-temperature superposition can be applied to wood-based composites within the temperature range of 30° to 70°C.

Regression Output:

Constant	0.05389
Std Err of Y Est	0.004723
R Squared	0.756832
No. of Observations	6
Degrees of Freedom	4
X Coefficient(s)	−1.1E−06
Std Err of Coef.	3.2E−07

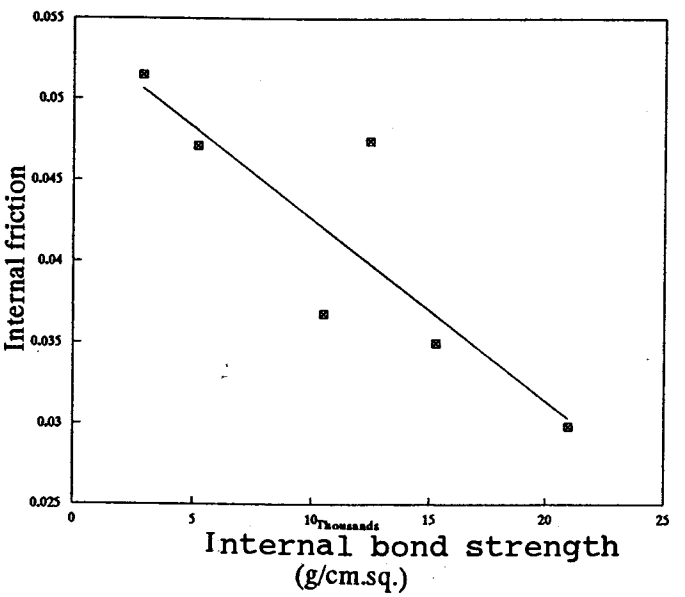

Figure 3.1 Relationship between internal bond strength and internal friction.

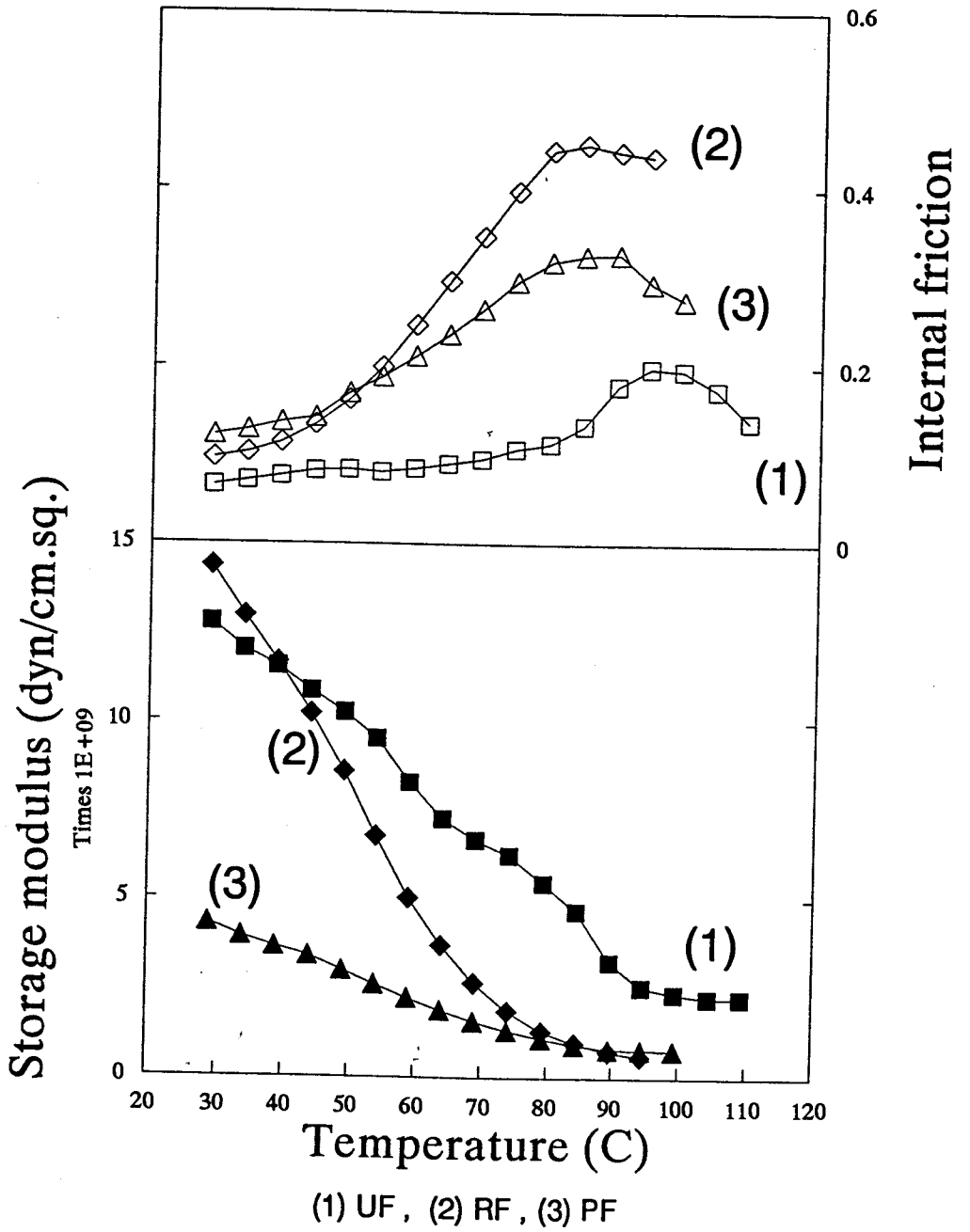

Figure 3.2 Temperature effect on the dynamic mechanical properties of different cured resins.

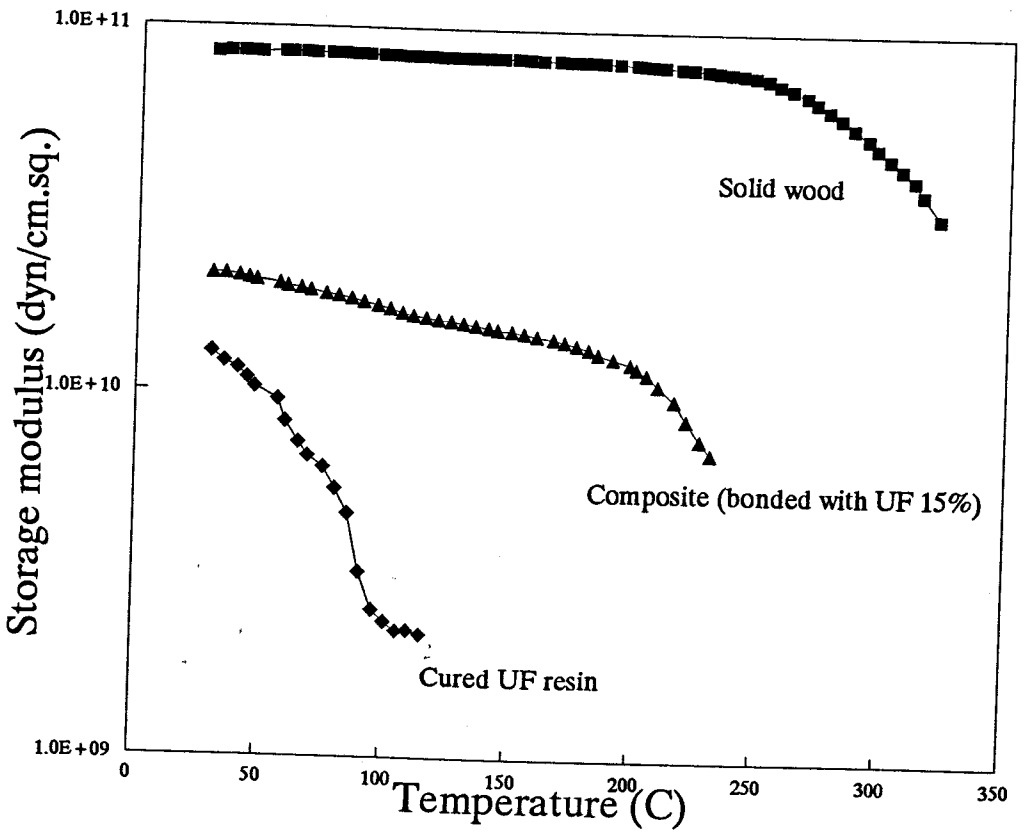

Figure 3.3 Comparison of storage modulus of solid wood, cured resin (UF), and particulate composite bonded with UF resin.

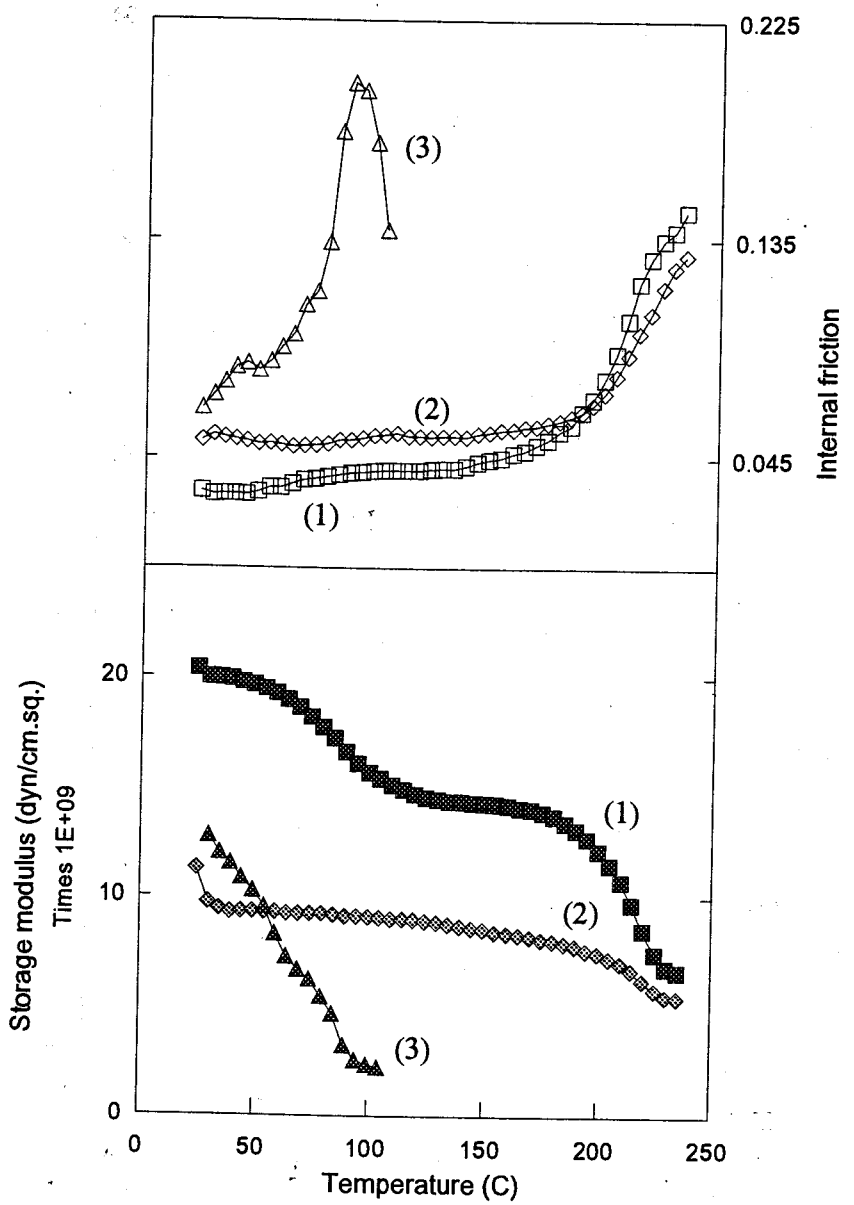

(1) composite (UF 15%)
(2) composite (UF 10%)
(3) cured UF rsin

Figure 3.4 Comparison of dynamic properties of cured resin, particulate composite bonded with UF resin (15% and 10%).

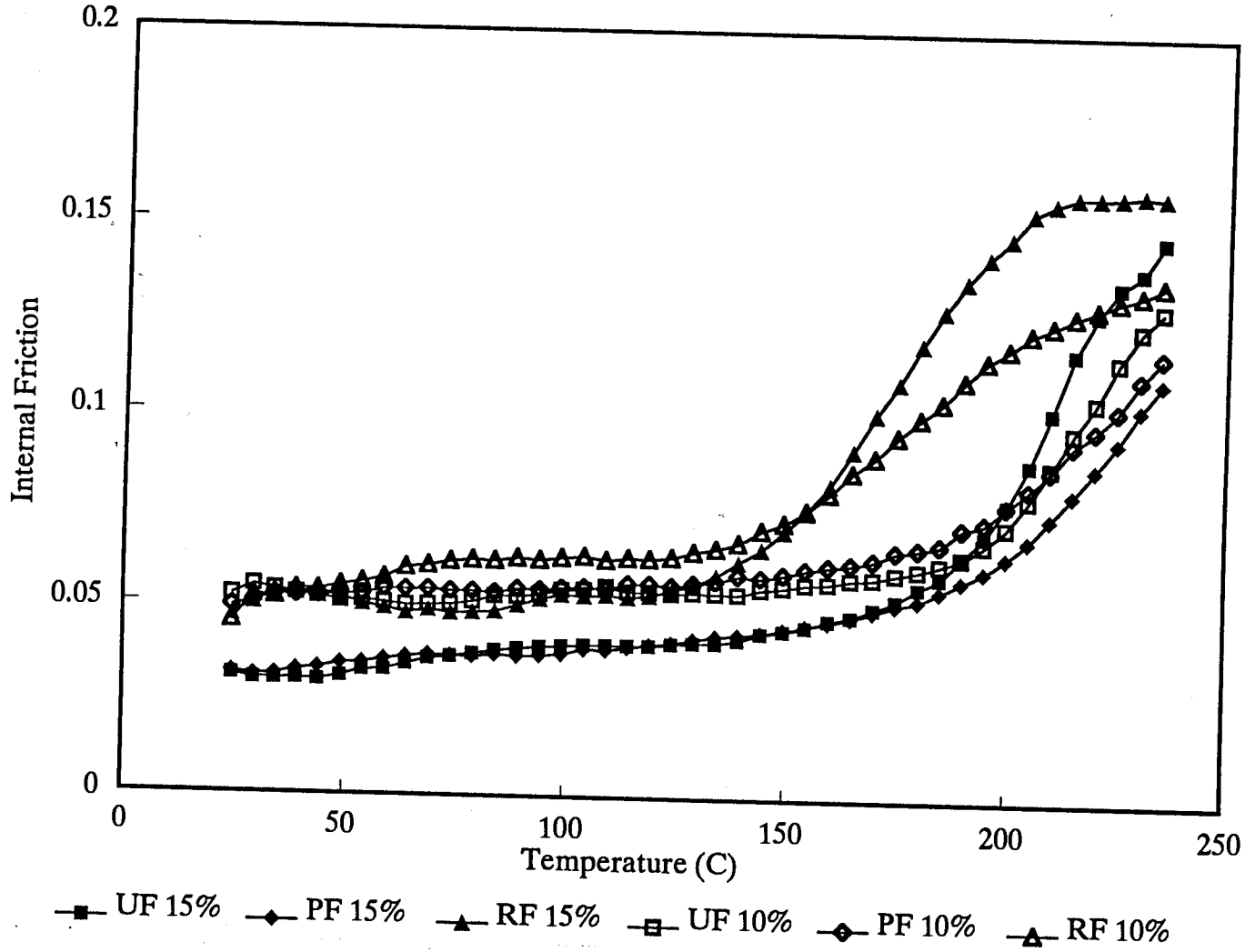

Figure 3.5 The internal friction of particulate composite bonded with different types and percentages of resin.

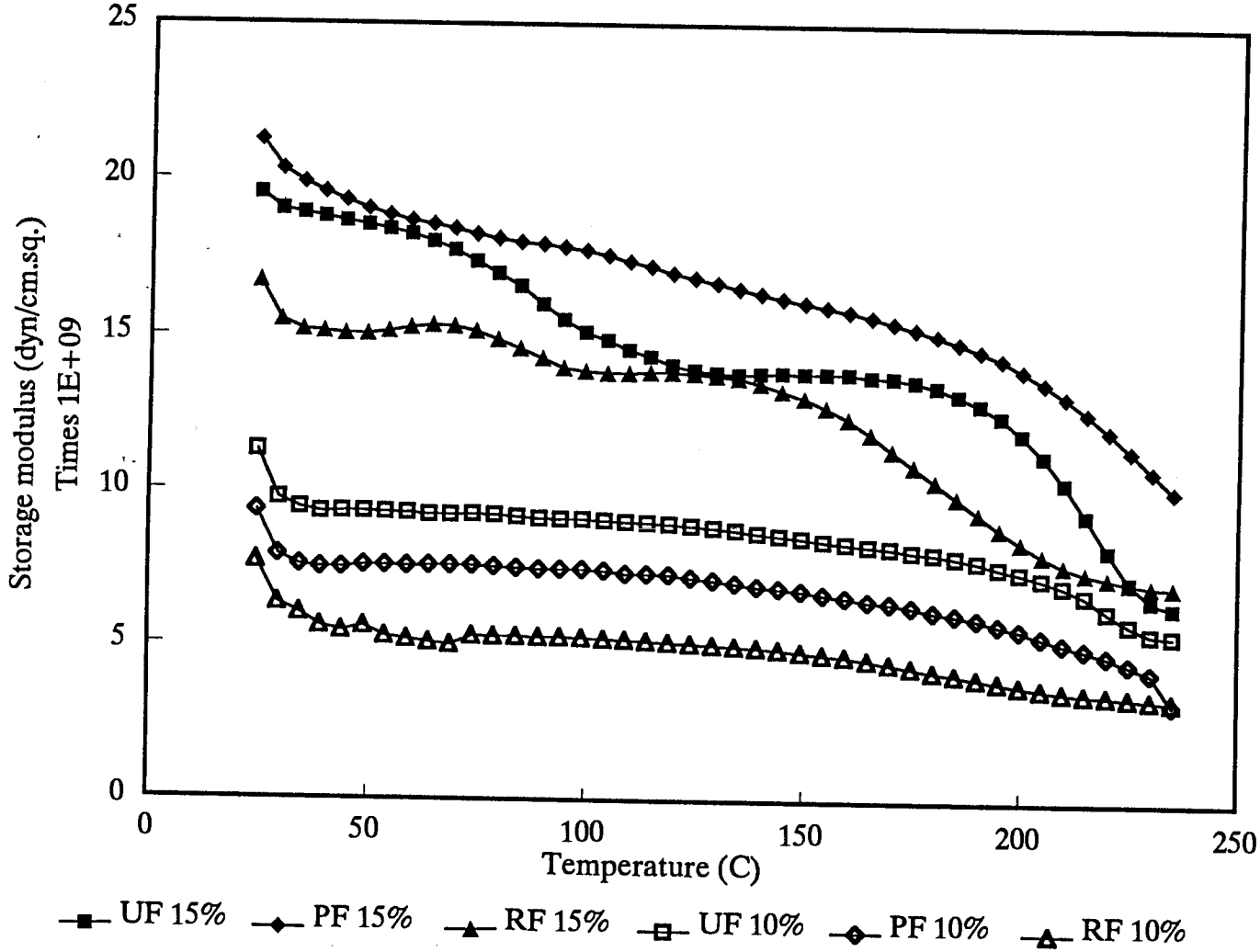

Figure 3.6 Storage modulus of particulate composite bonded with different types and percentages of resin.

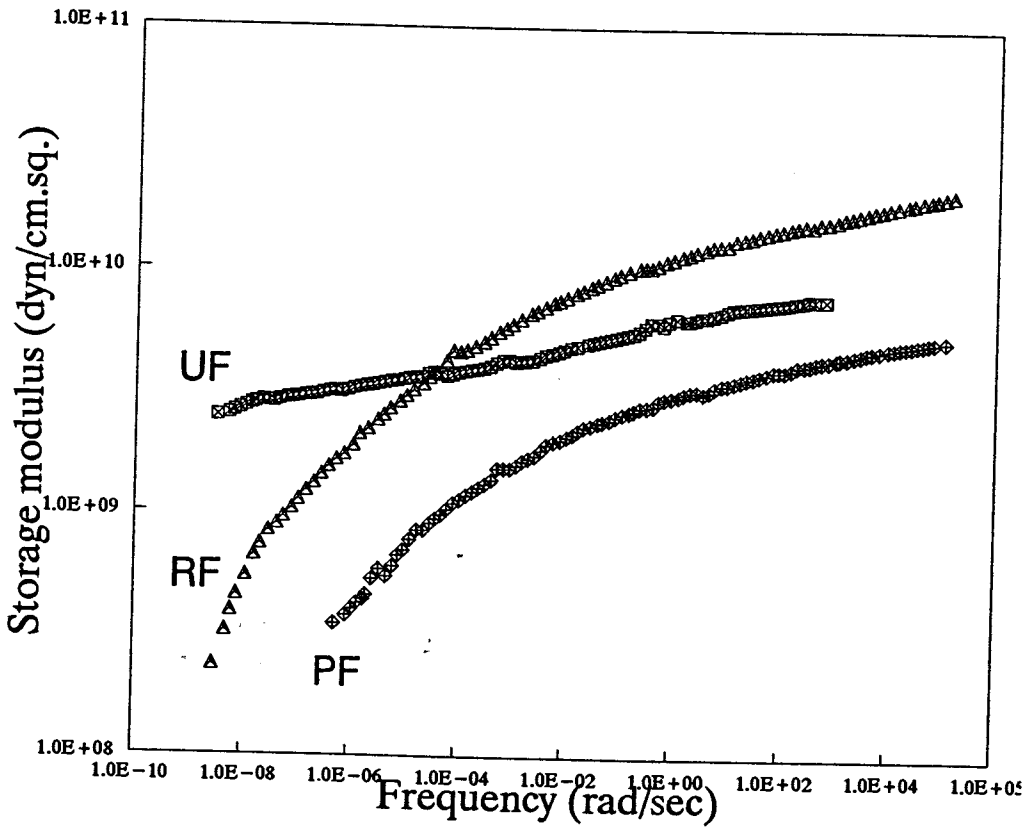

Figure 3.7 Master curves of different types of cured resin.

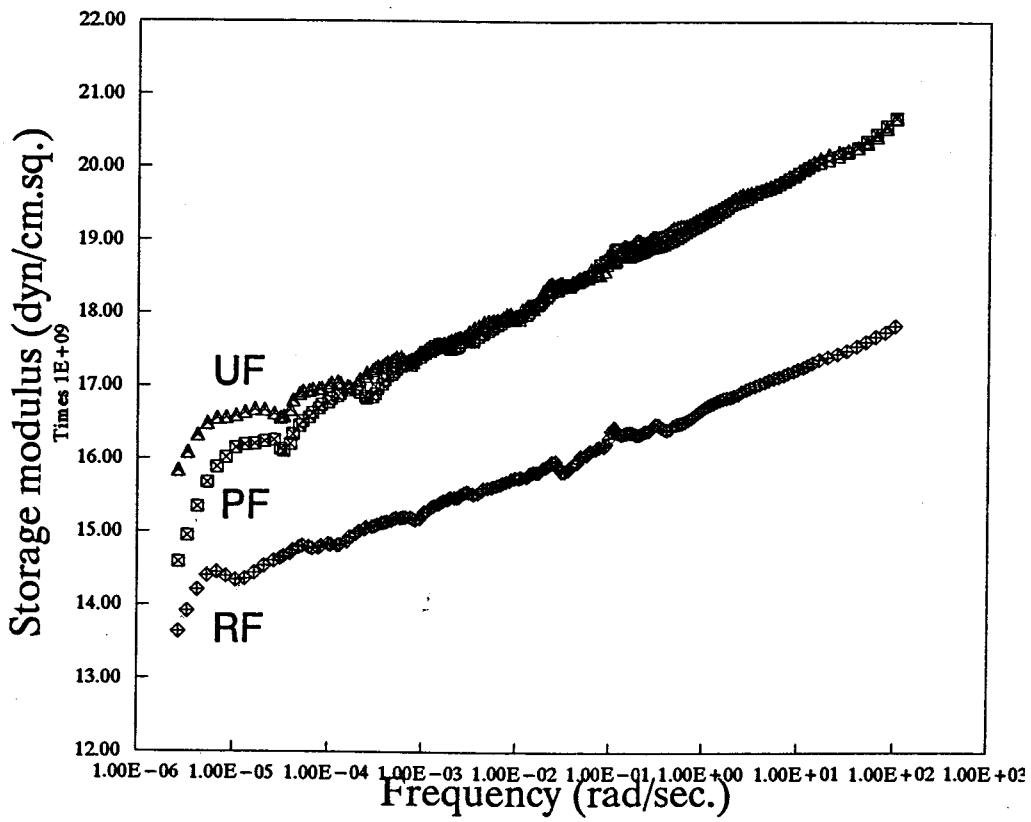

Figure 3.8 Master curves of particulate composite bonded with different resin types.

Table 3.1 Catalysts used for curing resins.

Adhesive	Solids content (%)	Catalyst	Catalyst % (wt. basis)	T_g (^oC)
Urea-formaldehyde	64	Ammonium chloride	1	94.3
Phenol formaldehyde	43	Propylene carbonate	18	89.3
Resorcinol formaldehyde	57	Paraform-aldehyde	8	84.5

References

Allan, G. G. and A. N. Neogi. 1971. Mechanism of adhesion of phenol-formaldehyde resins to cellulosic and lignocellulosic substrates. J.Adhes. 3(1):13-18.

Bodig, J., and B. A. Jayne. 1982. Mechanics of Wood and Wood Composites. Van Nostrand Reinhold Co. New York.

Bryan, E. L. and A. P. Schniewind. 1965. Strength and rheological properties of particleboard. Forest Products Journal: 143-149.

Carroll, M. N. and D. T. McVey. 1962. An analysis of resin efficiency in particleboard. For.Prod. J.:305-310.

Chow, P. 1979. Effects of load level, core density, and shelling ratio on creep behavior of hardboard composites. Wood and Fiber 11(1):57-65.

Chow, S. 1969. A kinetic study of the polymerization of phenol-formaldehyde resin in the presence of cellulosic materials. Wood Sci. 1(4):215-221.

Chow, S. 1973. Softening temperatures and durability of wood adhesives. Holzforschung 27(2):64-68.

Chow, S, and P. R. Steiner. 1979a. Comparison of the cure of phenol-formaldehyde novalac and resol systems by differential scanning calorimetry. J.Appl. Polym. Sci. 23:1973-1985.

Chow, S, and P. R. Steiner. 1979b. Comparison of curing and bonding properties of particleboard- and waferboard-type phenolic resins. Forest Products Journal 29(11):49-55.

Dinwoodie, J. M., J. Higgins, B. H. Paxton and D. J. Robson. 1992. Creep in chipboard. Part 11: The effect of cyclic changes in moisture content and temperature on the creep behavior of a range of boards at different levels of stressing. Wood Science and Technology 26:429-448.

Dinwoodie, J. M., B. H. Paxton, J. S. Higgins and D. J. Robson. 1991. Creep in chipboard. Part 10: the effect of variables climate on the creep behavior of a range of chipboards and one waferboard. Wood Sci.Technol. 26:39-51.

Dinwoodie, J. M., B. H. Paxton, and C. B. Pierce. 1981. Creep in chipboard. Part 3: Initial assessment of the

influence of moisture content and level of stressing on rate of creep and time to failure. Wood Sci.Technol. 15:125-144.

Ferry, J. D. 1980. Viscoelastic Properties of Polymers. John Wiley & Sons, Inc. New York.

Freeman, H. A. 1959. Relation between physical and chemical properties of wood and adhesion. Forest Products Journal 19(12):451-458.

Furuno, T. 1976. Structure of the interface between wood and synthetic polymer. Mokuzai Gakkaishi 22(8):473-478.

Gamalath, S. 1991. Long-term creep modeling of wood using time-temperature superposition principle. Ph.D. Dissertation. Wood Science and Forest Products, Virginia Polytechnic Institute & State University, Blacksburg, VA.

Humphrey, P. and S. Ren. 1989. Bonding kinetics of thermosetting adhesive systems used in wood-based composites: the combined effect of temperature and moisture content. J. Adhesion Sci. Technol. 3(5):397-413.

Johnson, S. E. and F. A. Kamke. 1994. Characteristics of phenol-formaldehyde adhesive bonds in steam injection pressed flakeboard. Wood and Fiber Science 26(2):259-269.

Kelley, S. S., T. G. Rials, and W. G. Glasser. 1987. Relaxation behavior of the amorphous components of wood. Journal of Material Science 22:617-624.

Ludbrook, B. D. and R. J. Whitwood. 1992. The use of thermal analysis to investigate the cure of reactive adhesives. Int.J.Adhesion and Adhesives 12(3):138-144.

Maloney, T. M. 1970. Resin distribution in layered particleboard. Forest Products Journal 20(1):43-52.

Marra, A. A. 1983. Applications of wood bonding. Pages 365-418 in R. F. Blomquist, A. W. Christiansen, R. H. Gillespie, and G. E. Myers, ed. Adhesive Bonding of Wood and other Structural Materials. Pennsylvania State University, University Park, Pa

McNatt, J. D. and M. O. Hunt. 1982. Creep of thick structural flakeboards in constant and cyclic humidity. Forest Products Journal 32(5):49-54.

Moore, W. E. 1975. Problems in the determination of cured phenol-formaldehyde resins in paper and wood. Forest Products Journal 25(4):39-41.

Moslemi, A. A. 1964. Some aspects of viscoelastic behavior of hardboard. Forest Products Journal 14(8):337-342.

Motohashi, Kenji, B. Tomita, H. Mizumachi, and H. Sakaguchi. 1984. Temperature dependency of bond strength of polyvinyl acetate emulsion adhesives for wood. Wood and Fiber Science 16(1):72-85.

Murayama, Takayuki. 1978. Dynamic Mechanical Analysis of Polymeric Material. Materials Science Monographs, Vol.1. Elsevier Scientific Publishing Co. New York.

Nielsen, L. E. 1974. Mechanical Properties of Polymers and Composites. Dekker, New York.

Pearson, R. G. 1981. Time dependent properties. in Oliver, J. F. ed. Adhesion in Cellulosic and Wood-based Composites:191-209. Plenum Press. New York.

Rice, J. T. and R. H. Carey. 1978. Wood density and board composition effects on phenolic resin-bonded flakeboard. Forest Products Journal 28(4):21-27.

Samarasinghe, Sandhya, J. R. Loferski, and S. M. Holzer. 1994. Creep modeling of wood using time-temperature superposition. Wood and Fiber Science 26(1): 122-130.

Smulski, S. J. 1989. Creep functions for wood composite materials. Wood and Fiber Science, 21(1):45-54.

Steiner, Paul R. 1984. Predicting creep behavior of wood adhesives by torsional braid analysis. J. Adhesion Vol 16:279-294.

Steiner P.R., and S. R. Warren. 1981. Rheology of wood-adhesive cure by torsional braid analysis. Holzforschung 35:273-278.

Takemura, A., H. Kuriyama, T. Moriguchi, B. Tomita, and H. Mizumachi. 1986. Dynamic mechanical properties and adhesive strength of polyacrylates I. Mokuzai Gakkaishi 32(10):813-819.

Takemura, A., B. Tomita, and H. Mizumachi. 1986. Dynamic mechanical properties and adhesive strength of polyacrylates II. Mokuzai Gakkaishi 32(11):883-887.

Tissaoui, J., J. R. Loferski, S. M. Holzer, D. A. Dillard, and B. H. Bond. 1992. Long-term creep law for wood in compression and tension parallel to grain. Proc. ASME,

Mechanics of Cellulosic Materials, AMD-Vol.145/MD-Vol. 36:33-38.

Wilson, J. B., and M. D. Hill. 1978. Resin efficiency of commercial blenders for particleboard manufacture. Forest Products Journal 28(2):49-54.

Wilson, J. B., G. L. Jay, and R. L. Krahmer. 1979. Using resin properties to predict bond strength of oak particleboard. Adhesives Age 22(6):26-30.

Wilson, J. B. and R. L. Krahmer. 1976. Particleboard: microscopic observations of resin distribution and wood fracture. Forest Products Journal 26(11):42-45.

Yamada, Masaaki, and K. Taki. 1991. Viscoelastic properties of thermosetting resin adhesives and their adhesive strength over a wide temperature range. Mokuzai Gakkaishi 37(6):529-534.

SUMMARY

Temperature, frequency and humidity dependence of solid wood and particulate composites were investigated by applying dynamic mechanical analysis. The dynamic properties of wood and composites were affected by the wood components, adhesives used in composites, and processing parameters to produce the composites. Higher moisture contents of solid wood resulted in lower storage moduli.

The glass transition temperature was about 294°C, 288°C, 273°C for the whole wood, earlywood and latewood respectively (at frequency of 100 rad/sec). As the test frequency decreased, the glass transition temperature decreased. The glass transition temperature was 94°C, 89°C and 84°C for UF resin, PF resin, and RF resin, respectively. The temperature dependence of the composite was strongly influenced by the type of the adhesive used for bonding.

Time-temperature superposition technique was successfully applied to predict the time-dependent properties of dry solid wood and particulate composite. Comparable static creep tests showed reasonably good agreement with the results obtained by time-temperature superposition. The resulting master curve extends the DMA data range to seven decades from the test data which covered only three decades. The TTS principle was found to be valid within the

temperature range of 30° to 80°C for dry Douglas-fir and 30° to 70°C for particulate composites.

BIBLIOGRAPHY

Allan, G. G. and A. N. Neogi. 1971. Mechanism of adhesion of phenol-formaldehyde resins to cellulosic and lignocellulosic substrates. J.Adhes. 3(1):13-18.

Bach, L. and R. E. Pentoney. 1968. Nonlinear mechanical behavior of wood. Forest Products Journal 18(3):60-66.

Back, E. L., and E. I. Didriksson. 1969. Four secondary and the glass transition temperature of cellulose, evaluated by sonic pulse technique. Svensk Papperstidning, 72(21):687-694.

Back, E. L., and N. L. Salmén. 1982. Glass transitions of wood components hold implications for molding and pulping processes. Tappi, 65(7):107-110.

Becker, H., H. Höglund, and G. Tistad. 1977. Frequency and temperature in chip refining. Paperi ja Puu, 59(3):123-130.

Blankenhorn, P. R. 1972. Dynamic mechanical behavior of black cherry. Ph.D. thesis. The Pennsylvania State University, University Park, Pa.

Blankenhorn, P. R., D. E. Kline, and F. C. Beall. 1973. Dynamic mechanical behavior of black cherry. Wood and Fiber Science, 4(4):298-308.

Bodig, J., and B. A. Jayne. 1982. Mechanics of Wood and Wood Composites. Van Nostrand Reinhold Co. New York.

Breese, M. C. and A. J. Bolton. 1993. The effect of temperature and moisture content on the time-dependent behavior of isolated earlywood specimens of Sitka Spruce (*Picea sitchensis*), loaded in compression in the radial direction. Holzforschung 47(6):523-528.

Bryan, E. L. and A. P. Schniewind. 1965. Strength and rheological properties of particleboard. Forest Products Journal 15(4):143-149.

Carroll, M. N. and D. T. McVey. 1962. An analysis of resin efficiency in particleboard. For.Prod. J.:305-310.

Chow, P. 1979. Effects of load level, core density, and shelling ratio on creep behavior of hardboard composites. Wood and Fiber 11(1):57-65.

Chow, S. 1969. A kinetic study of the polymerization of phenol-formaldehyde resin in the presence of cellulosic materials. Wood Sci. 1(4):215-221.

Chow, S. 1973. Softing temperatures and durability of wood adhesives. Holzforschung, 27(2):64-68.

Chow, S., and P. R. Steiner. 1979a. Comparison of the cure of phenol-formaldehyde novalac and resol systems by differential scanning calorimetry. J.Appl. Polym.Sci. 23:1973-1985.

Chow, S., and P. R. Steiner. 1979b. Comparison of curing and bonding properties of particleboard- and waferboard-type phenolic resins. Forest Products Journal, 29(11):49-55.

Davidson, R. W. 1962. The influence of temperature on creep in wood. Forest Products Journal 12(8):377-382.

Dinwoodie, J. M., J. Higgins, B. H. Paxton and D. J. Robson. 1992. Creep in chipboard. Part 11: The effect of cyclic changes in moisture content and temperature on the creep behavior of a range of boards ar different levels of stressing. Wood Sci.Technol. 26:429-448.

Dinwoodie, J. M., B. H. Paxton, J. S. Higgins and D. J. Robson. 1991. Creep in chipboard. Part 10: the effect of variables climate on the creep behavior of a range of chipboards and one waferboard. Wood Sci.Technol. 26:39-51.

Dinwoodie, J. M., B. H. Paxton, and C. B. Pierce. 1981. Creep in chipboard. Part 3: Initial assessment of the influence of moisture content and level of stressing on rate of creep and time to failure. Wood Science Technology 15:125-144.

Ferry, J. D. 1980. Viscoelastic Properties of Polymers. John Wiley and Sons, Inc.

Freeman, H. A. 1959. Relation between physical and chemical properties of wood and adhesion. Forest Products Journal, 19(12):451-458.

Fujimura, Taira, M. Inoue, and I. Uemura. 1990. Durability of wood with acyl-high-polymer II. Dimensional stability with crosslinked acyl copolymer in wood. Mokuzai Gakkaishi, Vol.36, No.10: 851-859.

Furuno, T. 1976. Structure of the interface between wood and synthetic polymer. Mokuzai Gakkaishi, 22(8):473-478.

Gamalath, S. 1991. Long-term creep modeling of wood using time-temperature superposition principle. Ph.D. Dissertation. Wood Science and Forest Products, Virginia Polytechnic Institute & State University, Blacksburg, VA.

Goldsmith, Valerie, and P. U. A. Grossman. 1967. The effect of frequency of vibration on the viscoelastic properties of wood. Journal Inst. Wood Sci., 18:44-53.

Handbook of Chemistry and Physics. 1983. Ed by Weast, Robert C, Melvin J. Astle, and Willian H. Beyer. CRC Press,Inc. Boca Raton, Florida.

Höglund, H., U. Sohlin, and G. Tistad. 1976. Physical properties of wood in relation to chip refining. Tappi 59(6):144-147.

Holzer, S. M., J. R. Loferski, and D. A. Dillard. 1989. A review of creep in wood:concepts relevant to develop long-term behavior predictions for wood structures. Wood and Fiber Science 21(4):376-392.

Humphrey, P. and S. Ren. 1989. Bonding kinetics of thermosetting adhesive systems used in wood-based composites: the combined effect of temperature and moisture content. J.Adhesion Sci.Technol. 3(5):397-413.

Ifju, G., R. W. Wellwood, and J. W. Wilson. 1965. Relationship between certain intra-increment physical measurements on Douglas Fir. Pulp Paper Mag. Can., 66: T475-T483.

Irvine, G. M. 1984. The glass transitions of lignin and hemicellulose and their measurement by differential thermal analysis. Tappi 67(5):118-121.

Johnson, S. E. and F. A. Kamke. 1994. Characteristics of phenol-formaldehyde adhesive bonds in steam injection pressed flakeboard. Wood and Fiber Science 26(2):259-269.

Kelley, S. S., T. G. Rials, and W. G. Glasser. 1987. Relaxation behavior of the amorphous components of wood. Journal of Material Science 22:617-624.

Klason, Carl, and Joesf Kubát. 1976. Thermal transitions in cellulose. Svensk Papperstidning, (15):494-500.

Koponen, S., T. Toratti, and P. Kanerva. 1989. Modeling longitudinal elastic and shrinkage properties of wood. Wood Sci. Technol. 23:55-63.

Koponen, S., T. Toratti, and P. Kanerva. 1991. Modeling elastic and shrinkage properties of wood based on cell structure. Wood Sci.Technol. 25:25-32.

Ludbrook, B. D. and R. J. Whitwood. 1992. The use of thermal analysis to investigate the cure of reactive adhesives. Int.J.Adhesion and Adhesives 12(3):138-144.

Maloney, T. M. 1970. Resin distribution in layered particleboard. Forest Products Journal 20(1):43-52.

Marra, A. A. 1983. Applications of wood bonding. Pages 365-418 in R.F.Blomquist, A.W.Christiansen, R. H. Gillespie, and G. E. Myers, ed. Adhesive Bonding of Wood and other Structural Materials. Pennsylvania State University, University Park, PA.

Marsoem, S. N., P. Bordonne and T. Okuyama. 1987. Mechanical responses of wood to repeated loading II. Effect of wave form on tensile fatigue. Mokuzai Gakkaishi, Vol.33(5):354-360.

McNatt, J. D. and M. O. Hunt. 1982. Creep of thick structural flakeboards in constant and cyclic humidity. Forest Products Journal 32(5):49-54.

Moore, W. E. 1975. Problems in the determination of cured phenol-formaldehyde resins in paper and wood. Forest Products Journal 25(4):39-41.

Moslemi, A. A. 1964. Some aspects of viscoelastic behavior of hardboard. Forest Products Journal 14(8):337-342.

Moslemi, A. A. 1967. Dynamic viscoelasticity in hardboard. Forest Products Journal. Vol 17(1):25-33.

Motohashi, Kenji, B. Tomita, H. Mizumachi, and H. Sakaguchi. 1984. Temperature dependency of bond strength of polyvinyl acetate emulsion adhesives for wood. Wood and Fiber Sci. 16(1):72-85.

Murakami, Koichi, and Hideaki Matsuda. 1989. Oligoesterified wood based on anhydride and epoxide VII. Dynamic mechanical properties of oligoesterified wood. Mokuzai Gakkaishi, Vol.36(1):49-56.

Murayama, Takayuki. 1978. Dynamic Mechanical Analysis of Polymeric Material. Materials Science Monographs, Vol.1. Elsevier Scientific Publishing Co. New York.

Nakano, T., S. Honma, and A. Matsumoto. 1990a. Physical properties of chemically-modified wood containing metal I. Mokuzai Gakkaishi, 36(12):1063-1068.

Nakano, T., S. Honma, and A. Matsumoto. 1990b. Physical properties of chemically-modified wood containing metal II. Mokuzai Gakkaishi, 37(10):924-929.

Nielsen, L. E. 1974. Mechanical Properties of Polymers and Composites. Dekker, New York.

Panshin, A. J., and C. de Zeeuw. 1980. Textbook of Wood Technology. McGraw-Hill Book Company, New York.

Pearson, R. G. 1981. Time dependent properties. Pages 191-208 in Johm F.Oliver, ed. Adhesion in Cellulosic and Wood-based Composites. Plenum press, New York.

Rasband, Wayne. 1992. Menu of NIH *Image* 1.47.

Rheometrics Solids Analyzer, Owner's Manual. 1991. Rheometrics,Inc. Piscataway, NJ.

Rials, T. G., and W. G. Glasser. 1984. Characterizing wood components as network polymer dynamic mechanical analysis. Wood and Fiber Science, 16(4):537-542.

Rials, T. G., and W. G. Glasser. 1989. Multiphase materials with lignin. VI. Effect of cellulose derivative structure on blend morphology with lignin. Wood and Fiber Science, 2(1):80-90.

Rice, J. T. and R. H. Carey. 1978. Wood density and board composition effects on phenolic resin-bonded flakeboard. Forest Products Journal 28(4):21-27.

Sadoh, T. 1981. Viscoelastic properties of wood in swelling systems. Wood Sci.Technol., 15:57-66.

Salmén, L. 1984. Viscoelastic properties of *in situ* lignin under water-saturated conditions. J. Mater. Sci., 19:3090-3096.

Samarasinghe, Sandhya, J. R. Loferski, and S. M. Holzer. 1994. Creep modeling of wood using time-temperature superposition. Wood and Fiber Science 26(1): 122-130.

Schaffer, E. L. 1982. Influence of heat on the longitudinal creep of dry Douglas-fir. Pages 20-52 in R. W. Meyer and R. M. Kellog, ed. Structural Uses of Wood in Adverse Environments. Van Nostrand Reinhold Co., New York.

Schniewind, A. P. and J. D. Barrett. 1972. Wood as a linear orthotopic viscoelastic material. Wood Sci. and Tech. Vol. 6:43-57.

Sellevold, E. J., F. Radjy, P. Hoffmeyer, and L. Bach. 1975. Low temperature internal friction and dynamic modulus for beach wood. Wood and Fiber, 7(3):162-169.

Smulski, S. J. 1989. Creep functions for wood composite materials. Wood and Fiber Science, 21(1):45-54.

Takemura, A., H. Kuriyama, T. Moriguchi, B. Tomita, and H. Mizumachi. 1986. Dynamic mechanical properties and adhesive strength of polyacrylates I. Mokuzai Gakkaishi 32(10):813-819.

Takemura, A., B. Tomita, and H. Mizumachi. 1986. Dynamic mechanical properties and adhesive strength of polyacrylates II. Mokuzai Gakkaishi 32(11):883-887.

Tissaoui, J., J. R. Loferski, S. M. Holzer, D. A. Dillard, and B. H. Bond. 1992. Long-term creep law for wood in compression and tension parallel to grain. Proc. ASME, Mechanics of Cellulosic Materials, AMD-Vol.145/MD-Vol. 36:33-38.

Wang, Yage, and P. Cheng. 1988. With the dynamic method to examine the glass's transition of Populus lignin. Journal of Nanjing Forestry University, 2:81-85. (in Chinese).

Williams, M. L., R. F. Landel, and J. D. Ferry. 1955. The temperature dependence of relaxation mechanisms in amorphous polymers and other glass-forming liquids. J. Am. Chem. Soc. 77:3701-3707.

Wilson, J. B., G. L. Jay, and R. L. Krahmer. 1979. Using resin properties to predict bond strength of oak particleboard. Adhesives Age 22(6):26-30.

Wilson, J. B., and M. D. Hill. 1978. Resin efficiency of commercial blenders for particleboard manufacture. Forest Products Journal 28(2):49-54.

Wilson, J. B., and R. L. Krahmer. 1976. Particleboard: microscopic observations of resin distribution and wood fracture. Forest Products Journal 26(11):42-45.

Winter, R. 1986. Compression of wood with superimposed small sinusoidal oscillations. Part II: High temperature. Wood and Fiber Science 18(1):11-22.

Winter, R., and P. J. Mjöberg. 1985. Compression of wood with superimposed small sinusoidal oscillations. Part I. Room temperature. Wood and Fiber Science 17(4):444-463.

Wood Handbook. 1987. United States Department of Agriculture, U.S. Forest Products Lab. Agriculture Handbook No 72, U.S. Government Printing Office, Washington, D.C.

Yamada, Masaaki, and K. Taki. 1991. Viscoelastic properties of thermosetting resin adhesives and their adhesive strength over a wide temperature range. Mokuzai Gakkaishi 37(6):529-534.

Yamada, T., T. Takemurea, and S. Kadita. 1961. On the rheology of wood. III. The creep and stress relaxation of buna. J. Japan Wood Res. Soc. 7(2):63-67.

Young, R. A. 1978. Thermal transitions of wood polymers by torsional pendulum analysis. Wood Science Vol. 11(2): 97-101.

APPENDICES

Appendix 1A. Rheometrics Solid Analyzer.

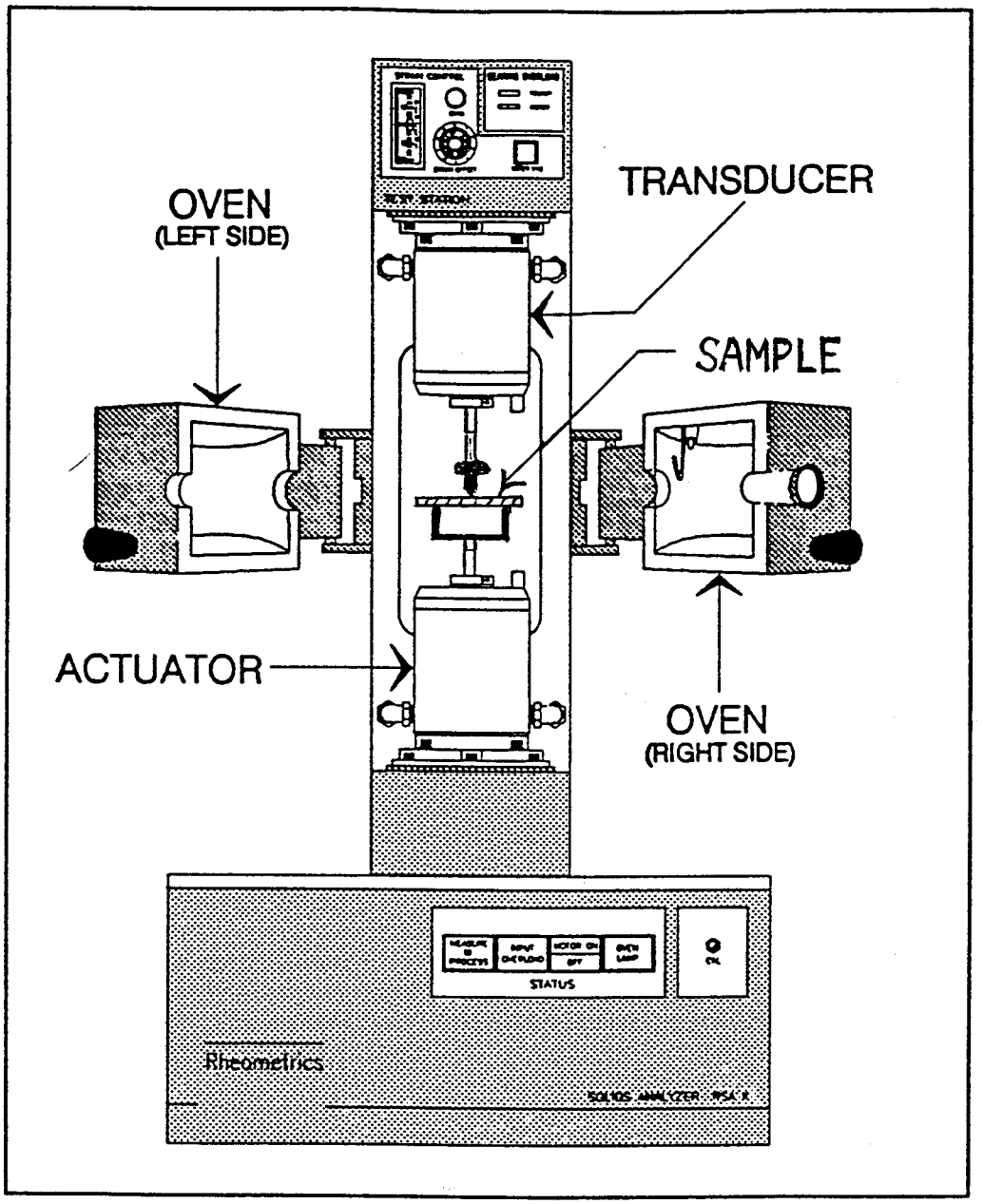

Figure A.1 Rheometrics Solid Analyzer, RSA II.

Appendix 1B. Physical properties of samples.

Table A.1 Physical properties of samples used in frequency effect test.

Sample #	Dimension Length(mm)	Width(mm)	Thick. (mm)	Weight (gram)	Specific Gravity	# of GRs
1–7	52.07	11.98	1.97	0.550	0.447	8
1–15	52.12	12.04	1.99	0.533	0.427	9
1–21	52.12	11.94	1.91	0.555	0.467	10

Table A.2 Physical properties of samples used in studying of temperature effect.

Sample #	Dimension (mm) Length	Width	Thickness	Weight (gram)	Specific Gravity	# of GRs
1–2	52.09	12.18	1.92	0.58	0.476	8
1–4	52.03	11.88	1.94	0.55	0.457	8
1–12	52.10	11.83	1.85	0.50	0.441	7
1–11	52.05	11.96	1.78	0.55	0.496	8
1–10	52.17	12.00	1.89	0.56	0.473	10
1–5	52.07	11.93	1.95	0.54	0.446	6
1–8	52.09	11.93	2.01	0.55	0.438	9
1–6	52.06	11.86	1.89	0.55	0.469	11
1–9	52.15	11.96	1.91	0.55	0.462	11
Average					0.462	8.67
STD					0.018	1.63
C.V.					3.86%	18.84%

Table A.3 Data table for variation of late-wood percentages among the samples.

Sample (Group)	Number of growth rings (per sample)	Late-wood portion (%)
1-13(A)	6	32.45
1-17(A)	9	25.98
1-14(A)	7	27.85
1-18(A)	5	19.10
1-4(A)	6	31.57
1-6(A)	12	19.40
1-c-1(B)	1	17.11
1-c-2(B)	1	13.32
1-c-3(B)	1	13.17
1-c-4(B)	1	17.65
1-c-5(B)	1	13.39
1-c-6(B)	1	13.38

Summary of results

	Portion of Latewood		No. of growth ring		No. of rings/mm	
	Average	Stand. Dev.	Average	Stand. Dev.	Average	Stand. Dev.
A	26.05965	5.277126	7.5	2.362908	0.740544	0.20208
B	14.6694	1.921735	1	0	0.108915	0.001565

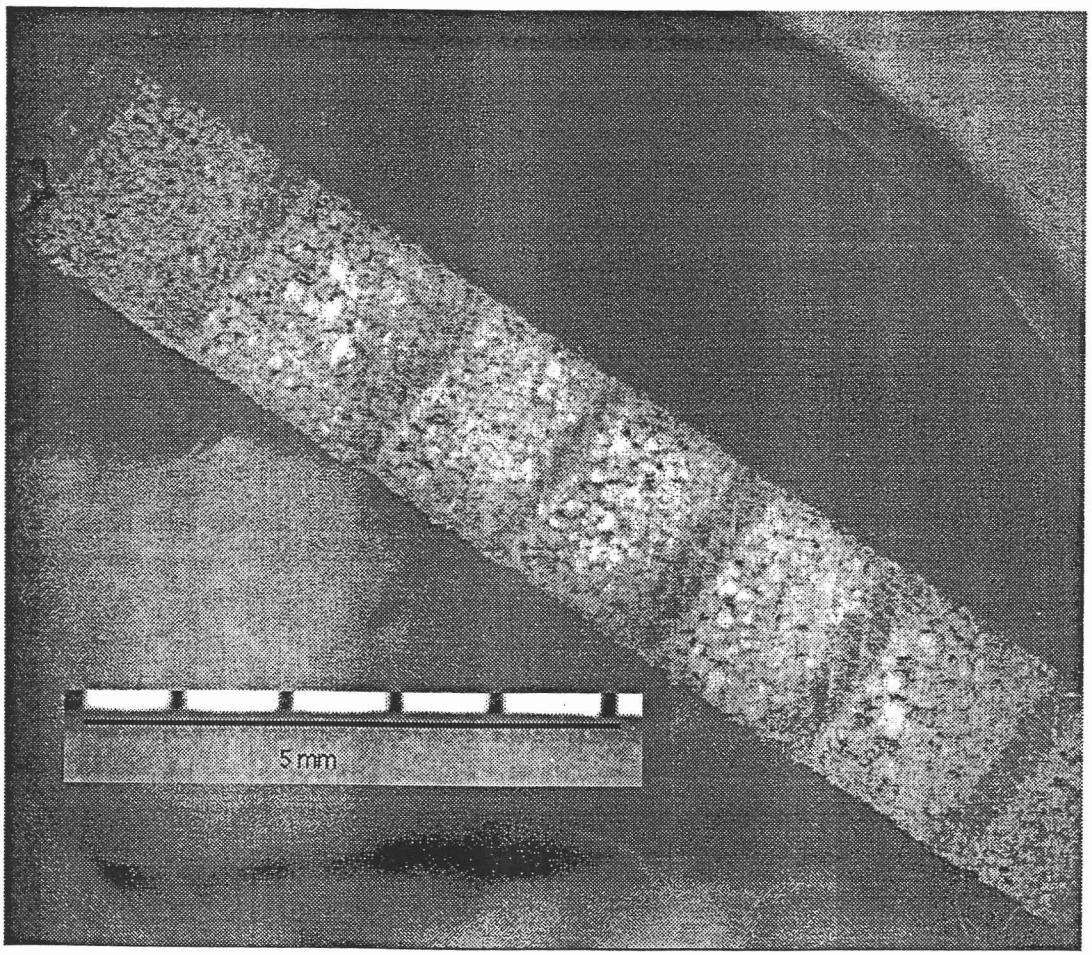

Figure A.2 The image of cross-section of a sample, included a scale.

Table A.4 Physical properties of earlywood and latewood samples.

earlywood		latewood		early–and latewood	
Sample #	Specific Gravity	Sample #	Specific Gravity	Sample #	Specific Gravity
1–A–1	0.235	1–B–1	0.775	1–C–1	0.485
1–A–2	0.238	1–B–2	0.806	1–C–2	0.495
1–A–3	0.253	1–B–3	0.897	1–C–3	0.501
1–A–4	0.255	1–B–4	0.705	1–C–4	0.517
1–A–5	0.254	1–B–5	0.865	1–C–5	0.501
1–A–6	0.238	1–B–6	0.951	1–C–6	0.531
Average	0.245	Average	0.833	Average	0.505
STD	0.009	STD	0.081	STD	0.015

Appendix 1C. Actual moisture contents and dynamic properties of samples

Table A.5 Actual moisture contents of samples.

Temp. (°C)	MC before test	MC after test	MC change
8.2	59.41%	43.34%	16.07%
8.7	57.30%	52.77%	4.52%
9.3	55.88%	40.17%	15.71%
10.2	60.81%	52.03%	8.78%
8.4	57.17%	52.41%	4.76%
8.9	55.19%	50.48%	4.71%
23.5	50.64%	47.07%	3.58%
23.3	55.05%	52.34%	2.71%
23.3	48.33%	45.61%	2.73%
23.2	58.73%	56.04%	2.68%
23.2	57.75%	55.26%	2.49%
23.2	53.65%	51.32%	2.33%
36.9	69.78%	62.50%	7.28%
36.9	71.58%	64.01%	7.57%
36.8	67.62%	61.26%	6.36%
36.8	80.46%	72.96%	7.50%
37.1	76.52%	69.71%	6.81%
36.8	72.30%	66.31%	5.99%
49.1	76.73%	68.00%	8.73%
50.8	78.42%	71.11%	7.31%
50.5	77.95%	70.33%	7.62%
50.5	89.98%	82.01%	7.97%
50.6	83.11%	75.15%	7.96%
51	82.52%	74.96%	7.57%
9.4	13.84%	11.01%	2.83%
8.6	13.04%	12.52%	0.52%
10.6	19.86%	18.06%	1.80%
8.9	15.27%	13.68%	1.59%
9.4	16.79%	15.39%	1.40%
11.7	19.90%	16.83%	3.07%
23.9	15.52%	14.53%	0.99%
23.9	15.35%	14.49%	0.85%
23.8	19.24%	17.75%	1.49%
23.9	16.13%	15.04%	1.09%
23.9	14.88%	13.85%	1.04%
23.9	16.69%	15.18%	1.51%
37.5	14.66%	13.98%	0.67%
37.3	14.49%	13.32%	1.17%
37.2	16.48%	14.79%	1.70%
37.3	14.51%	13.30%	1.21%
37.3	13.45%	12.20%	1.25%
37.2	14.69%	13.24%	1.45%
51.6	12.62%	12.49%	0.13%
52	13.25%	11.64%	1.61%
52.2	12.83%	11.54%	1.28%
51.8	11.62%	10.80%	0.81%
51.9	11.96%	11.89%	0.07%
51.8	11.48%	10.61%	0.87%

Table A.5 Actual moisture contents of samples (Continued).

Temp. (°C)	MC before test	MC after test	MC change
8.6	19.50%	17.13%	2.38%
9.1	13.18%	11.80%	1.38%
9.8	12.19%	11.60%	0.59%
8.4	11.72%	11.12%	0.60%
7.1	11.98%	11.44%	0.54%
9.8	11.94%	11.28%	0.67%
21.8	9.91%	9.75%	0.16%
22.2	7.88%	7.75%	0.13%
22.5	7.40%	7.29%	0.12%
22.6	7.25%	7.20%	0.05%
22.7	7.57%	7.49%	0.09%
22.9	7.47%	7.18%	0.29%
37.3	6.58%	6.55%	0.03%
37.3	5.13%	5.11%	0.01%
37.6	5.03%	4.88%	0.14%
37.4	5.43%	5.27%	0.16%
37.6	5.42%	5.33%	0.08%
37.3	6.12%	5.87%	0.25%
51	4.40%	4.24%	0.16%
51.8	3.31%	3.20%	0.11%
51.5	3.66%	3.60%	0.06%
51.9	3.03%	2.97%	0.07%
51.6	3.16%	3.13%	0.03%
51.6	3.67%	3.50%	0.17%
10.3	3.92%	4.03%	0.11%
10.8	4.10%	4.18%	0.08%
9.4	4.21%	4.19%	0.02%
10.1	4.46%	4.55%	0.09%
9	4.01%	4.11%	0.11%
9.3	4.00%	4.06%	0.05%
25.8	0.77%	0.99%	0.22%
25.4	1.04%	1.19%	0.15%
25.4	1.06%	1.16%	0.10%
25.2	1.31%	1.44%	0.13%
25	0.90%	1.00%	0.09%
25	0.92%	1.03%	0.10%
38.1	0.31%	0.33%	0.02%
36.9	0.56%	0.60%	0.05%
37.1	0.41%	0.41%	0.01%
37	0.70%	0.81%	0.11%
37.3	0.33%	0.37%	0.04%
37.1	0.37%	0.35%	0.02%
51.1	0.04%	0.16%	0.12%
51.1	0.21%	0.28%	0.07%
51.6	0.21%	0.25%	0.05%
53.5	0.37%	0.42%	0.06%
51.5	0.17%	0.22%	0.05%
51.2	0.00%	0.11%	0.11%

Table A.5 Actual moisture contents of samples (Continued).

Temp. (°C)	MC before test	MC after test	MC change
9.1	9.69%	9.16%	0.53%
10.7	9.67%	9.30%	0.37%
8.9	9.80%	9.29%	0.51%
9.9	10.08%	9.53%	0.55%
8.9	9.95%	9.58%	0.38%
12.5	9.59%	9.15%	0.44%
23.9	9.98%	9.58%	0.41%
23.8	10.07%	9.72%	0.34%
23.9	9.93%	9.62%	0.31%
23.9	10.01%	9.66%	0.35%
23.8	10.18%	9.85%	0.34%
23.8	9.74%	9.43%	0.31%
37.3	9.64%	9.10%	0.53%
37.3	9.64%	9.09%	0.55%
37.5	9.32%	8.97%	0.36%
37.4	9.38%	9.14%	0.24%
37.2	9.57%	9.10%	0.48%
37.6	9.10%	8.67%	0.43%
51.6	8.20%	7.68%	0.52%
51.7	8.11%	7.68%	0.43%
51.4	7.92%	7.44%	0.48%
51.8	7.71%	7.30%	0.41%
51.8	7.95%	7.53%	0.41%
51.8	7.48%	7.13%	0.34%
9	11.20%	10.52%	0.68%
10.8	10.84%	10.35%	0.49%
10.5	11.30%	10.37%	0.93%
9.6	12.17%	11.61%	0.56%
12.3	11.43%	10.84%	0.59%
9.7	11.95%	11.41%	0.54%
23.3	12.74%	12.02%	0.72%
23.6	12.41%	11.85%	0.56%
23.6	12.17%	11.65%	0.52%
23.8	12.78%	12.13%	0.65%
23.8	11.62%	11.10%	0.53%
23.9	12.25%	11.65%	0.60%
37.4	10.01%	9.49%	0.52%
37.3	9.71%	9.30%	0.41%
37.4	9.96%	9.43%	0.53%
37.4	9.91%	9.43%	0.48%
37.2	9.18%	8.75%	0.44%
37.5	9.63%	9.08%	0.55%
51.6	6.73%	6.44%	0.29%
51.8	6.40%	6.12%	0.28%
52.4	6.54%	6.27%	0.27%
51.7	6.43%	6.17%	0.26%
51.7	5.92%	5.65%	0.27%
52	6.00%	5.69%	0.31%

Table A.6 Dynamic properties at different temperatures and moisture contents.

temperature (C)	MC (%)	E' (average) E' (STD) (dyn/cm^2)	E" (average) E" (STD) (dyn/cm^2)	temperature (C)	MC (%)	E' (average) E' (STD) (dyn/cm^2)	E" (average) E" (STD) (dyn/cm^2)
8.95	53.08%	2.146E+10 1.163E+10	3.664E+09 6.491E+08	10.32	11.16%	2.526E+10 3.464E+09	1.834E+09 3.902E+08
23.28	52.65%	1.288E+10 2.918E+09	2.805E+09 4.088E+08	23.67	12.03%	2.726E+10 6.447E+09	2.140E+09 1.610E+08
36.88	69.58%	1.268E+10 1.607E+09	2.843E+09 1.327E+08	37.37	9.49%	1.860E+10 6.440E+09	1.693E+09 3.004E+08
50.42	77.52%	1.156E+10 3.715E+09	2.526E+09 7.693E+08	51.87	6.20%	2.045E+10 4.382E+09	1.349E+09 5.300E+08
9.82	4.15%	3.403E+10 5.847E+09	1.770E+09 2.696E+08	10.00	9.57%	3.592E+10 1.504E+10	2.172E+09 5.177E+08
25.30	1.07%	2.660E+10 8.330E+09	2.006E+09 1.587E+08	23.85	9.81%	2.926E+10 5.980E+09	1.827E+09 2.790E+08
37.25	0.46%	3.077E+10 7.138E+09	1.600E+09 3.521E+08	37.38	9.23%	2.414E+10 6.677E+09	1.437E+09 2.625E+08
51.67	0.20%	3.010E+10 7.339E+09	1.694E+09 3.745E+08	51.68	7.68%	2.108E+10 1.052E+10	1.480E+09 2.857E+08
8.80	12.91%	2.451E+10 9.203E+09	2.484E+09 4.114E+08	9.77	15.52%	2.560E+10 8.289E+09	2.175E+09 7.355E+08
22.45	7.85%	2.775E+10 5.407E+09	2.556E+09 3.439E+08	23.88	15.72%	2.075E+10 6.863E+09	2.000E+09 3.144E+08
37.42	5.56%	2.342E+10 5.739E+09	1.798E+09 5.835E+08	37.30	14.09%	1.849E+10 4.394E+09	1.516E+09 1.489E+08
51.57	3.49%	2.104E+10 5.402E+09	1.863E+09 3.475E+08	51.88	11.89%	1.798E+10 3.180E+09	1.437E+09 1.948E+08

STD: Standard deviation

Appendix 1D. Summary of statistical analysis.

Table A.7 Statistical analysis of temperature effect in each moisture content conditions

Data: MC1.E_ (Group 1)
Level codes: MC1.Temp
Average moisture content: 1.47%

Analysis of variance

Source of variation	Sum of Squares	d.f.	Mean square	F-ratio	Sig. level
Between groups	1.674049	3	.5580165	.893	.4621
Within groups	12.503500	20	.6251750		
Total (corrected)	14.177550	23			

Data: MC2.E_ (Group 2)
Level codes: MC2.Temp
Average moisture content: 7.45%

Analysis of variance

Source of variation	Sum of Squares	d.f.	Mean square	F-ratio	Sig. level
Between groups	1.395901	3	.4653002	.881	.4677
Within groups	10.563643	20	.5281821		
Total (corrected)	11.959543	23			

Table A.7 Statistical analysis of temperature effect in each moisture content conditions (Continued).

Data: MC3.E_ (Group 3)
Level codes: MC3.Temp
Average moisture content: 14.31%

Analysis of variance

Source of variation	Sum of Squares	d.f.	Mean square	F-ratio	Sig. level
Between groups	2.1773538	3	.7257846	1.666	.2063
Within groups	8.7137462	20	.4356873		
Total (corrected)	10.891100	23			

Data: MC4.E_ (Group 4)
Level codes: MC4.Temp
Average moisture content: 63.21%

Analysis of variance

Source of variation	Sum of Squares	d.f.	Mean square	F-ratio	Sig. level
Between groups	3.7805942	3	1.2601981	2.624	.0787
Within groups	9.6056216	20	.4802811		
Total (corrected)	13.386216	23			

Appendix 1E. Investigation of Sources of Error

Variability of the material

In spite of the careful attention given to the preparation of specimens, there were differences among the samples used in this study. For example, Table A.2 shows the physical properties of the samples. The average specific gravity is 0.46 with standard deviation of 0.02, compared to the published value for coast type Douglas-fir being 0.48 (Wood Handbook, 1987).

Linearity of material

Marsoem *et al.* (1987) concluded that wood behaves like a linear viscoelastic material up to about 25% of static strength. In their study, samples which had about twelve percent moisture content were subjected to repeated loading with six different wave-forms. The damage occurred whenever stress exceeds 25% and wood acts nonlinearly. Salmen (1984) believed that the amplitude varies within the linear viscoelastic range if deformation is kept less than 0.1%.

Linear viscoelastic behavior can be defined in terms of response to loading. One strain ramp test has been done to provide the relationship between strain and responding stress (Fig. A.3). After initial alignment, there was linearity between stress and strain to which Hooke's law applied. The coefficient of determination (R^2) equals 0.999 in the linear

regression analysis. When the required strain was smaller than 1.0×10^{-4}, the average of storage moduli equals 1.2×10^{11} dyn/cm^2 with standard deviation of 5.7×10^{9} dyn/cm^2. When the strain is larger than 1.0×10^{-4}, the nonlinearity appeared, and the storage moduli is not independent with strain anymore. In the dynamic mechanical analysis of this study, the maximum strain was only half of this value, assuring linear behavior which is far less than the values mentioned above.

Regression Output:

Constant	−8059556
Std Err of Y Est	76727.44
R Squared	0.999452
No. of Observations	160
Degrees of Freedom	158
X Coefficient(s)	2.3E+10
Std Err of Coef.	42951601

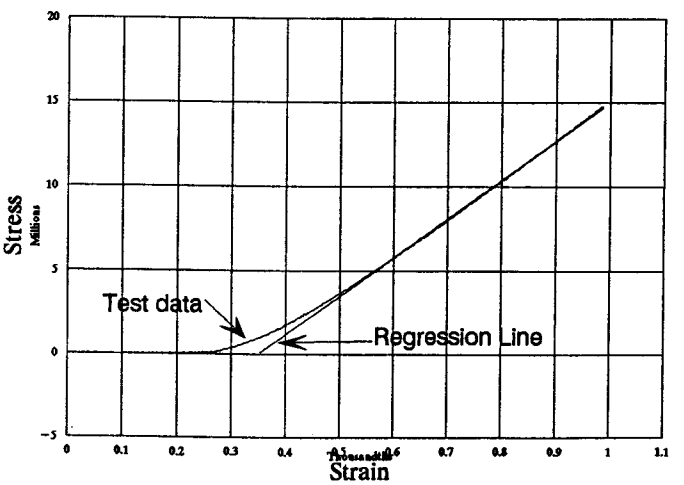

Figure A.3 Stress-strain diagram of Douglas-fir and result of regression analysis.

Appendix 1F. Investigation of Effect of Grain Orientation on Dynamic Properties of Earlywood and Latewood

In order to investigate the effect of grain orientation on dynamic properties, the tests were done by loaded force radially and tangentially. For the earlywood, the difference between the dynamic properties of samples loaded in different grain orientations was not significant with p=0.07 (Ostle and Malone, 1988). The average storage modulus was about two times larger loaded tangentially than radially for latewood. The effect of grain orientation on storage modulus was significant at the 0.71 percent level.

Table A.8 The effect of grain aeration on the dynamic properties of earlywood and latewood.

	Latewood samples		Earlywood samples	
	E' (dyn/cm²)	E" (dyn/cm²)	E' (dyn/cm²)	E" (dyn/cm²)
Load tangentially				
#1	9.94E+10	7.00E+09	2.33E+10	7.70E+08
#2	2.09E+11	7.12E+09	2.29E+10	9.05E+08
#3	2.41E+11	9.79E+09	3.42E+10	1.14E+09
#4	1.89E+11	6.40E+09	2.18E+10	9.53E+08
#5	2.17E+11	5.31E+09	3.38E+10	1.12E+09
#6	2.79E+11	5.28E+09	2.18E+10	8.82E+08
Average	2.06E+11	6.82E+09	2.63E+10	9.62E+08
STD	5.54E+10	1.52E+09	5.48E+09	1.32E+08
Load radially				
#1	1.50E+11	4.38E+09	1.64E+10	5.01E+08
#2	7.53E+10	4.43E+09	1.81E+10	8.77E+08
#3	1.14E+11	2.86E+09	2.48E+10	1.13E+09
#4	6.92E+10	4.00E+09	1.54E+10	7.06E+08
#5	1.56E+11	7.47E+09	2.65E+10	6.80E+08
#6	6.06E+10	2.17E+09	1.90E+10	8.38E+08
Average	1.04E+11	4.22E+09	2.00E+10	7.89E+08
STD	3.85E+10	1.67E+09	4.16E+09	1.95E+08

Appendix 2A. Creep Test Condition and Test Data.

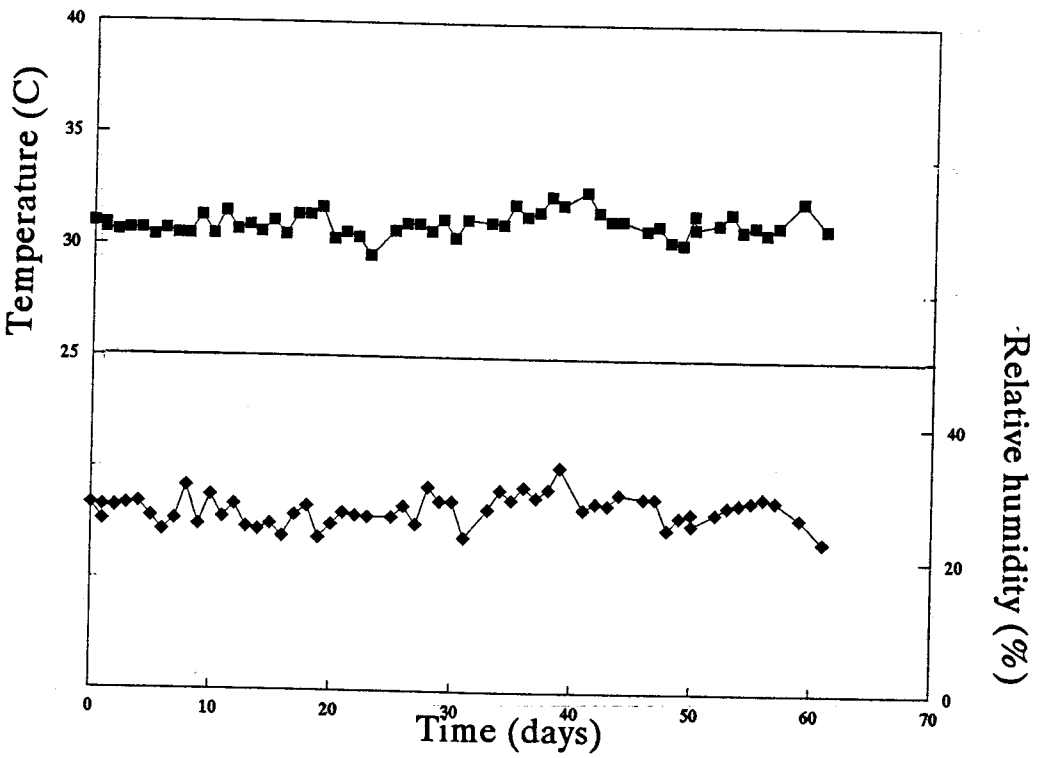

Figure A.4 The environmental condition of long-term creep test.

Table A.9 Parameters of empirical curve fitting of creep compliance.

Sample #	n	m	D0	R^2
2	0.271	8.8E−14	3.0E−11	0.97
3	0.209	3.2E−13	2.7E−11	0.97
4	0.251	1.2E−13	2.5E−11	0.97
5	0.255	1.4E−13	2.9E−11	0.98
6	0.237	1.7E−13	2.7E−11	0.97
7	0.246	1.4E−13	2.9E−11	0.97
11	0.168	6.2E−13	2.7E−11	0.97
12	0.123	1.5E−12	2.6E−11	0.96
13	0.238	1.7E−13	2.7E−11	0.98
Avg	0.211	3.6E−13	2.7E−11	0.97
STD	0.049	4.3E−13	1.5E−12	

8	0.212	6.4E−13	4.5E−11	0.96
9	0.264	2.8E−13	3.9E−11	0.97
10	0.225	3.7E−13	3.5E−11	0.97
14	0.262	2.0E−13	3.4E−11	0.98
Avg	0.241	3.7E−13	3.8E−11	0.97
STD	0.023	1.7E−13	4.3E−12	

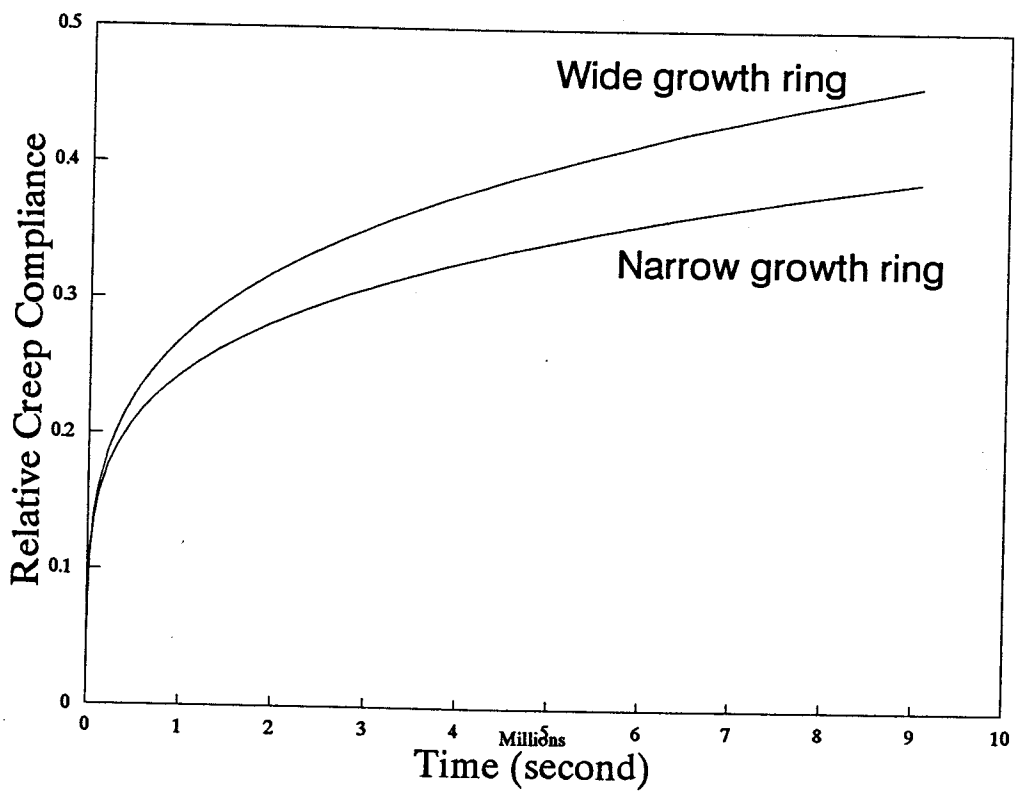

Figure A.5 Average creep compliance obtained from static creep tests.

Appendix 2B. Relaxation spectrum of wood.

Table A.10 Statistical analysis of difference between the values of H at different temperatures.

Sample #2-17						
Temperature (C)	29.485	39.133	49.255	59.262	69.358	79.573
Difference in H (dyne/cm.sq.)	1.8700E+08	-5.4000E+07	-1.0600E+08	-3.5000E+07	-6.7000E+07	2.6000E+07
	8.3000E+07	-1.8400E+07	-5.7900E+07	-2.0600E+07	-3.8600E+07	4.3000E+06
	3.6600E+07	-4.0000E+05	-4.0100E+07	-1.3600E+07	-2.8500E+07	-8.6000E+06
	1.6000E+07	5.6000E+06	-3.3500E+07	-1.2100E+07	-2.4300E+07	-1.5000E+07
	1.4900E+07	4.4000E+06	-3.3000E+07	-1.4400E+07	-2.1800E+07	-1.6300E+07
	2.2500E+07	2.9000E+06	-3.7000E+07	-1.7700E+07	-2.0000E+07	-1.5300E+07
	2.4800E+07	7.1000E+06	-4.3200E+07	-2.0500E+07	-1.9100E+07	-1.4600E+07
	2.3200E+07	1.4800E+07	-5.0200E+07	-2.2800E+07	-1.8700E+07	-1.4300E+07
	2.6200E+07	1.9800E+07	-5.7100E+07	-5.4600E+07	1.0800E+07	-1.3900E+07
	3.2400E+07	2.0900E+07	-6.3500E+07	-2.4300E+07	-2.1800E+07	-1.2700E+07
	4.0300E+07	1.8200E+07	-6.8400E+07	-2.1400E+07	-2.5900E+07	-1.0300E+07
	4.8900E+07	1.2000E+07	-6.7100E+07	-1.9000E+07	-2.8900E+07	-8.5000E+06
Average		2.7417E+06	-5.4750E+07	-2.3000E+07	-2.5317E+07	-8.2667E+06
Stand. deviation		1.9994E+07	1.9718E+07	1.1121E+07	1.6778E+07	1.1632E+07

Sample #2-16					
Temperature (C)	29.655	39.144	49.282	59.277	69.382
Difference in H (dyne/cm.sq.)	2.0900E+08	7.9000E+07	1.8600E+08	2.3690E+08	3.1100E+07
	1.2480E+08	4.5500E+07	1.2150E+08	1.4850E+08	3.6500E+07
	9.2300E+07	3.3900E+07	1.0050E+08	1.1900E+08	4.2800E+07
	7.9200E+07	2.9800E+07	9.4000E+07	1.0980E+08	4.8300E+07
	3.2143E+08	2.9000E+07	9.4300E+07	1.0780E+08	5.2800E+07
	7.3600E+07	3.0800E+07	9.7900E+07	1.0920E+08	5.6400E+07
	7.4700E+07	3.5000E+07	1.0250E+08	1.1250E+08	5.9500E+07
	7.6100E+07	3.9500E+07	1.0720E+08	1.1760E+08	6.2500E+07
	7.7000E+07	4.4100E+07	1.1180E+08	1.2410E+08	6.5200E+07
	7.9300E+07	4.7800E+07	1.1630E+08	1.3090E+08	6.7600E+07
	8.2400E+07	4.9400E+07	1.1880E+08	1.3700E+08	6.8800E+07
	8.4700E+07	4.7600E+07	1.1850E+08	1.4050E+08	6.9400E+07
Average		4.2617E+07	1.1411E+08	1.3282E+08	5.5075E+07
Stand. deviation		1.3118E+07	2.3632E+07	3.3892E+07	1.2420E+07

Appendix 2C. Time-temperature Superposition Master Curves

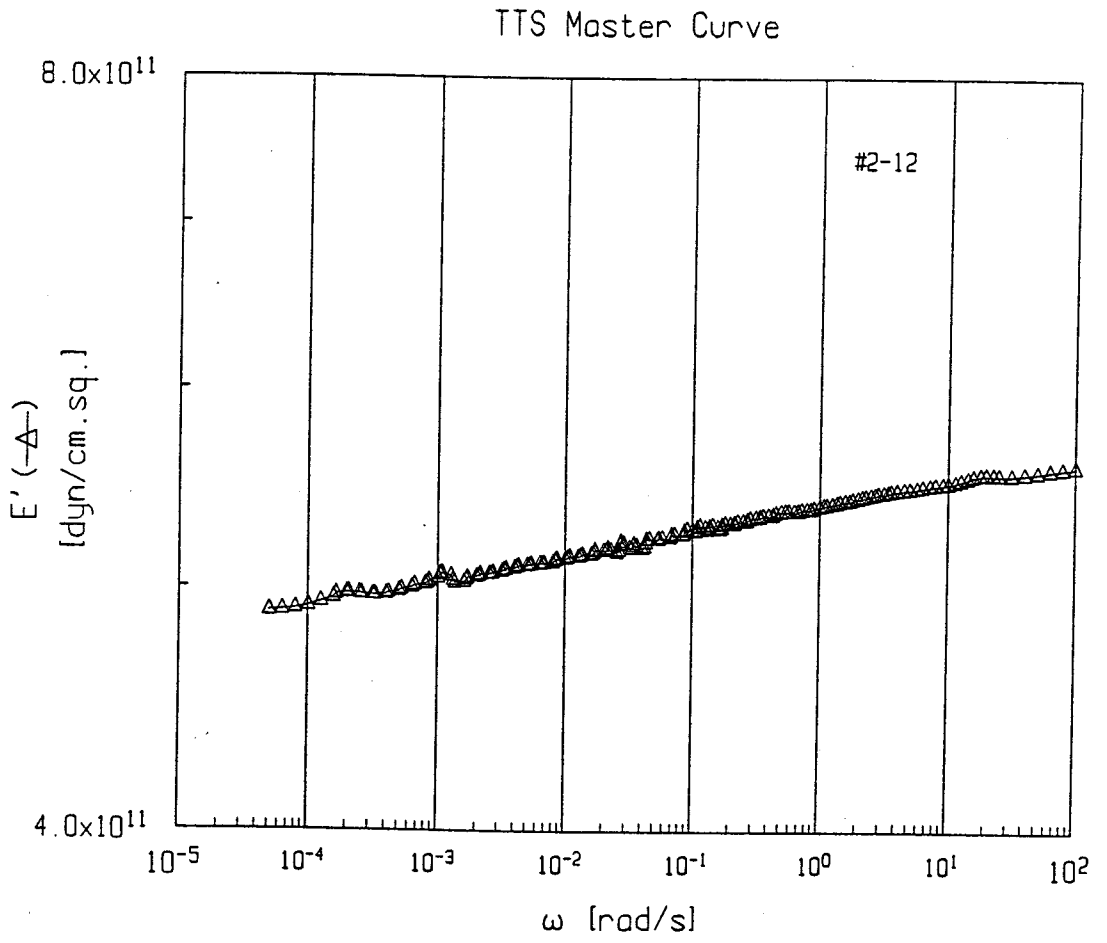

Figure A.6 TTS master curve (sample #2-12).

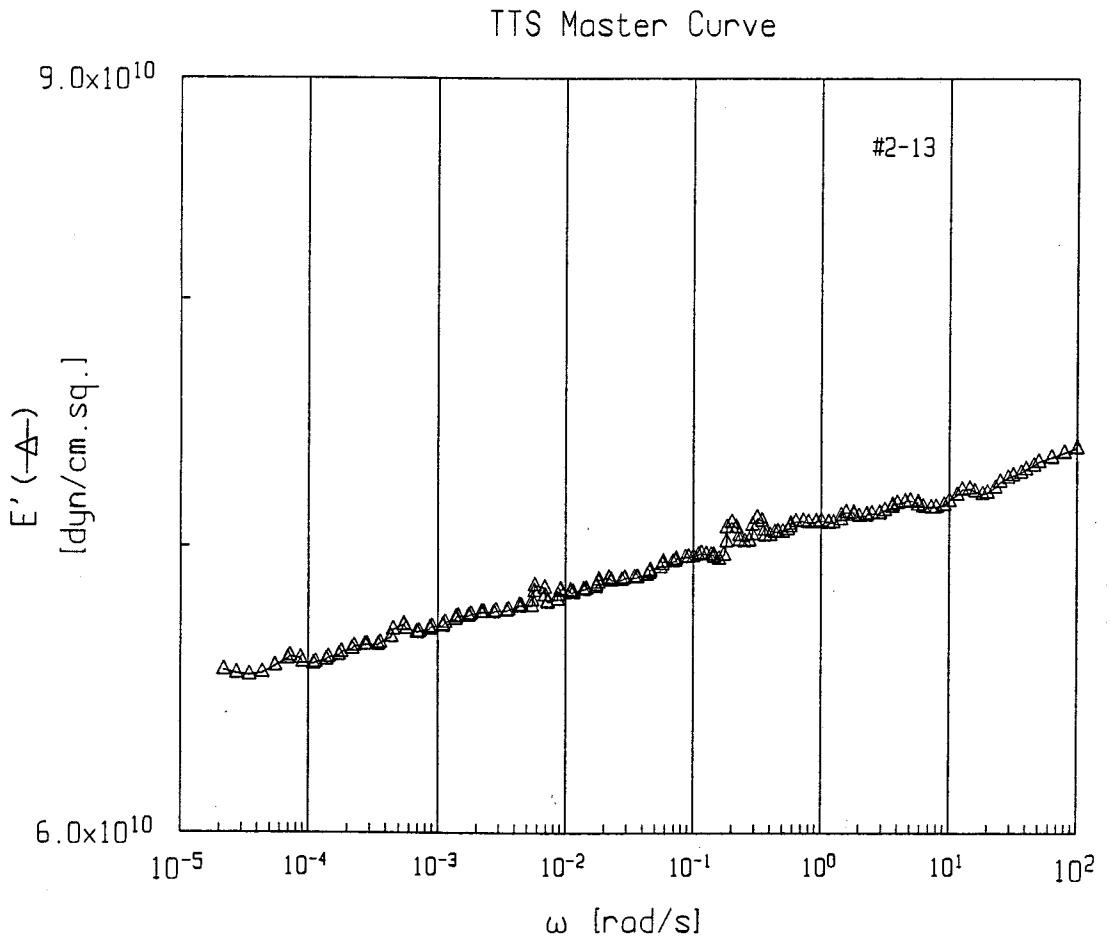

Figure A.7 TTS master curve (sample #2-13).

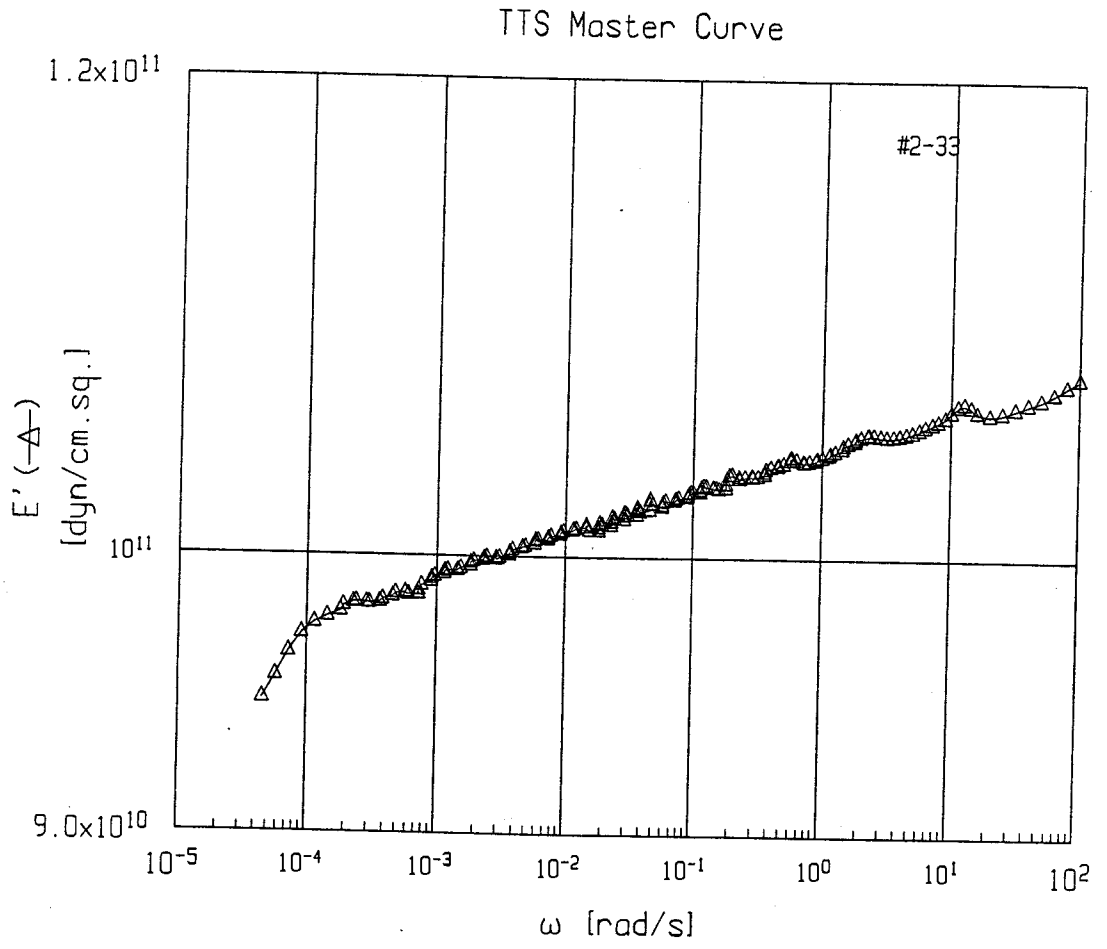

Figure A.8 TTS master curve (sample #2-33).

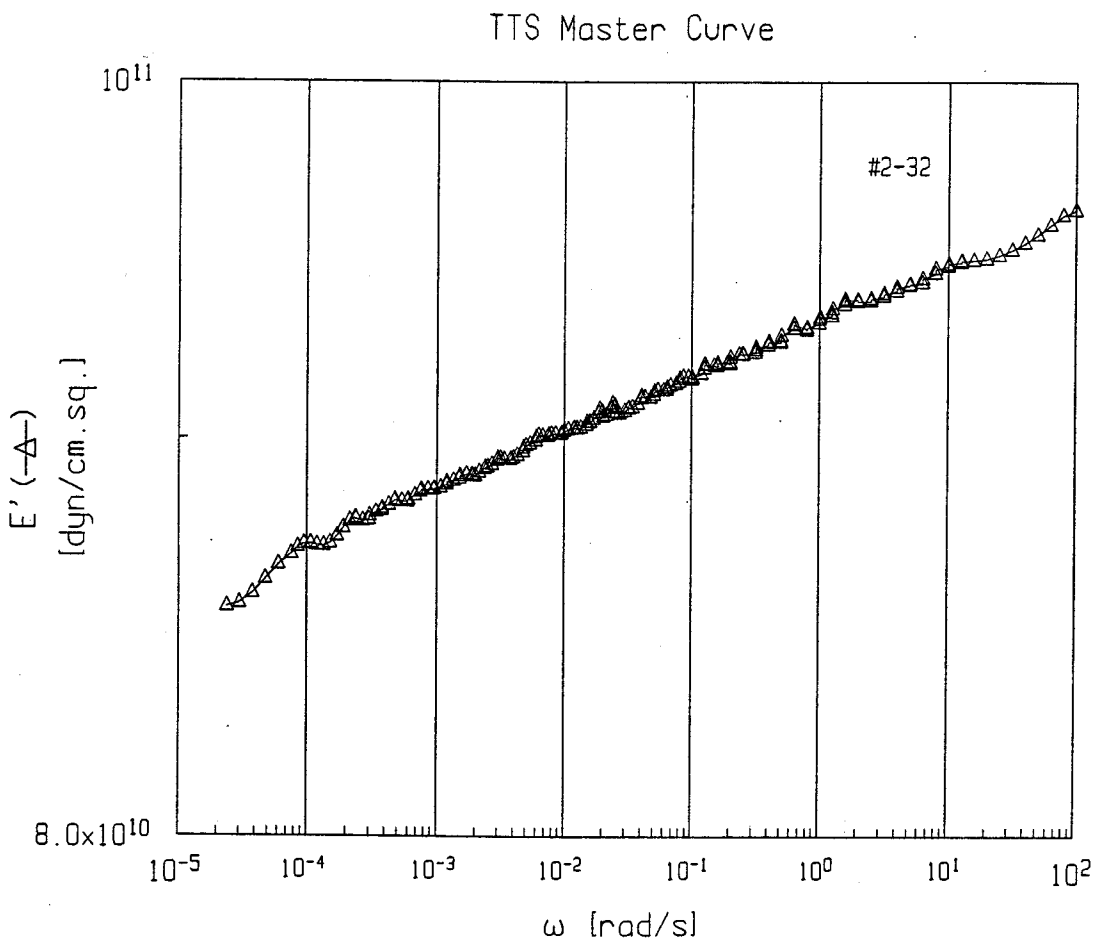

Figure A.9 TTS master curve (sample #2-32).

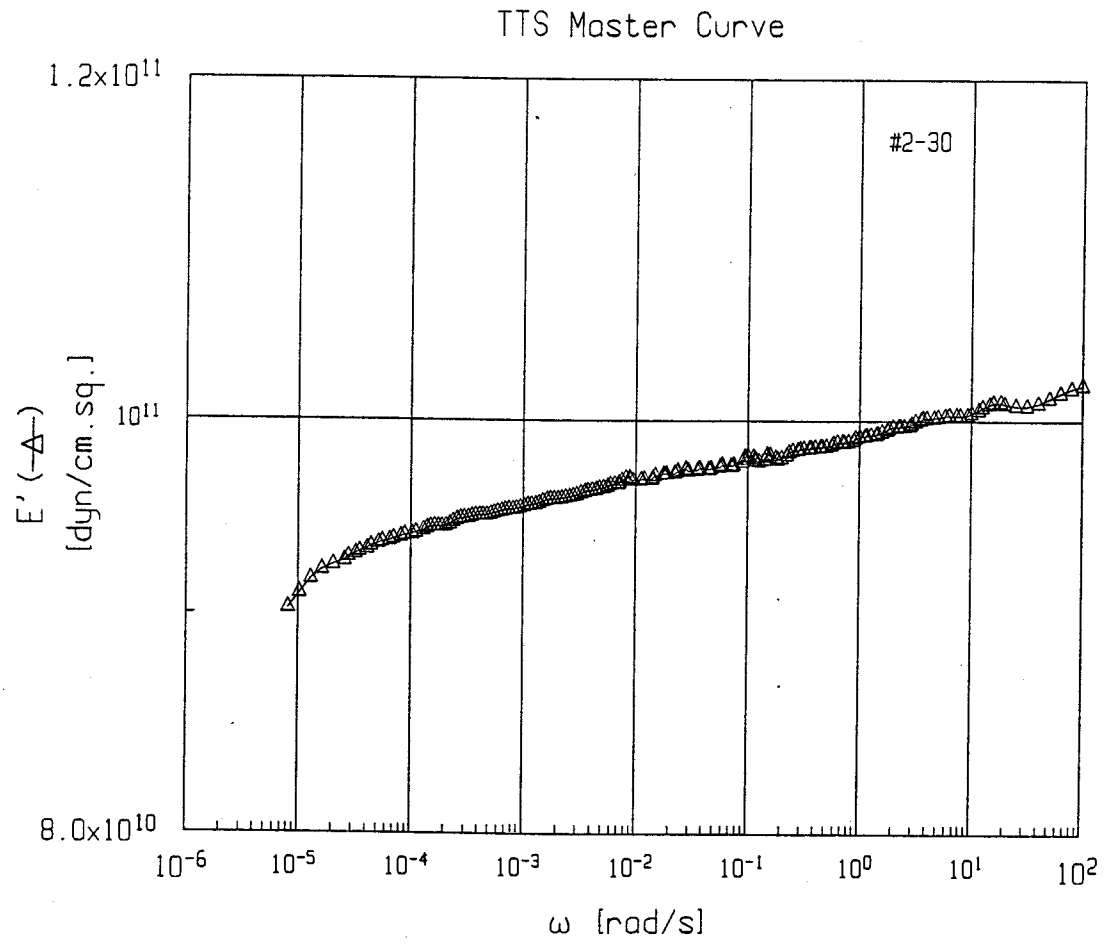

Figure A.10 TTS master curve (sample #2-30).

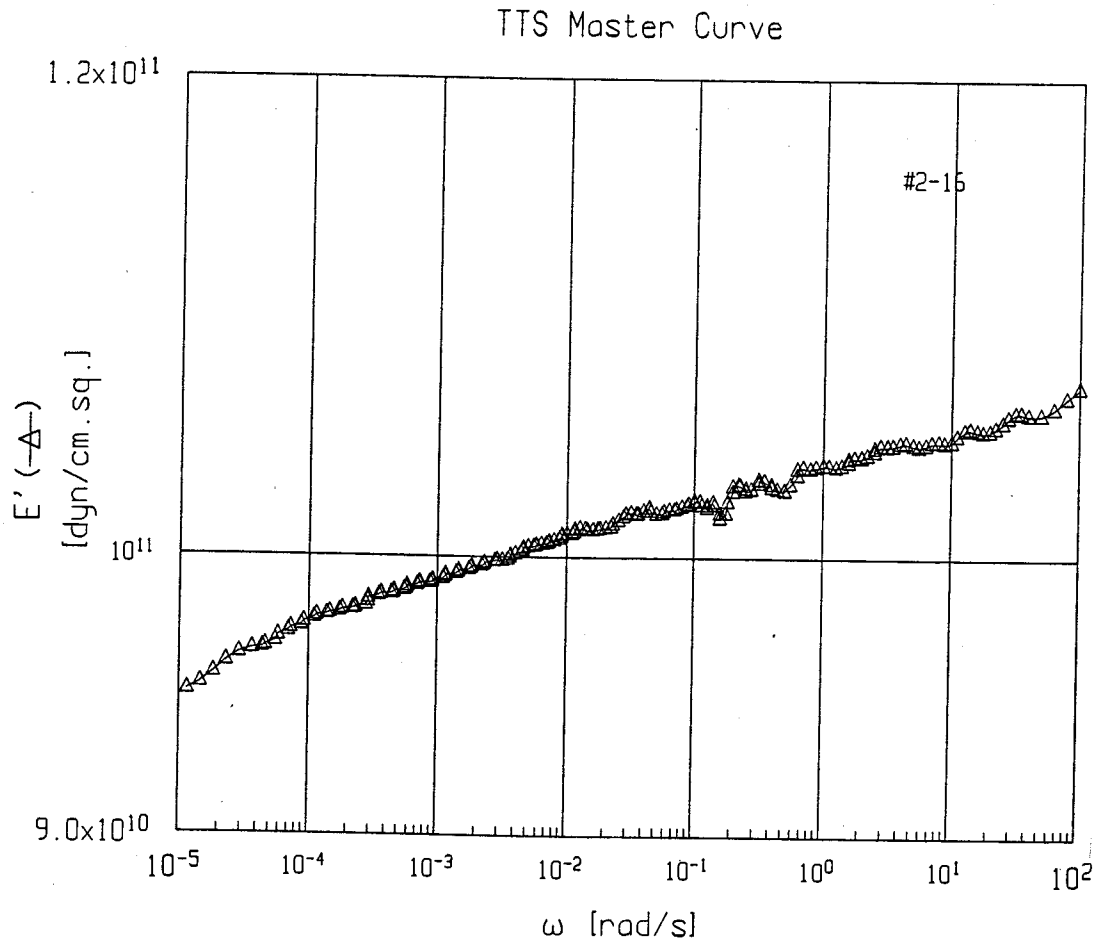

Figure A.11 TTS master curve (sample #2-16).

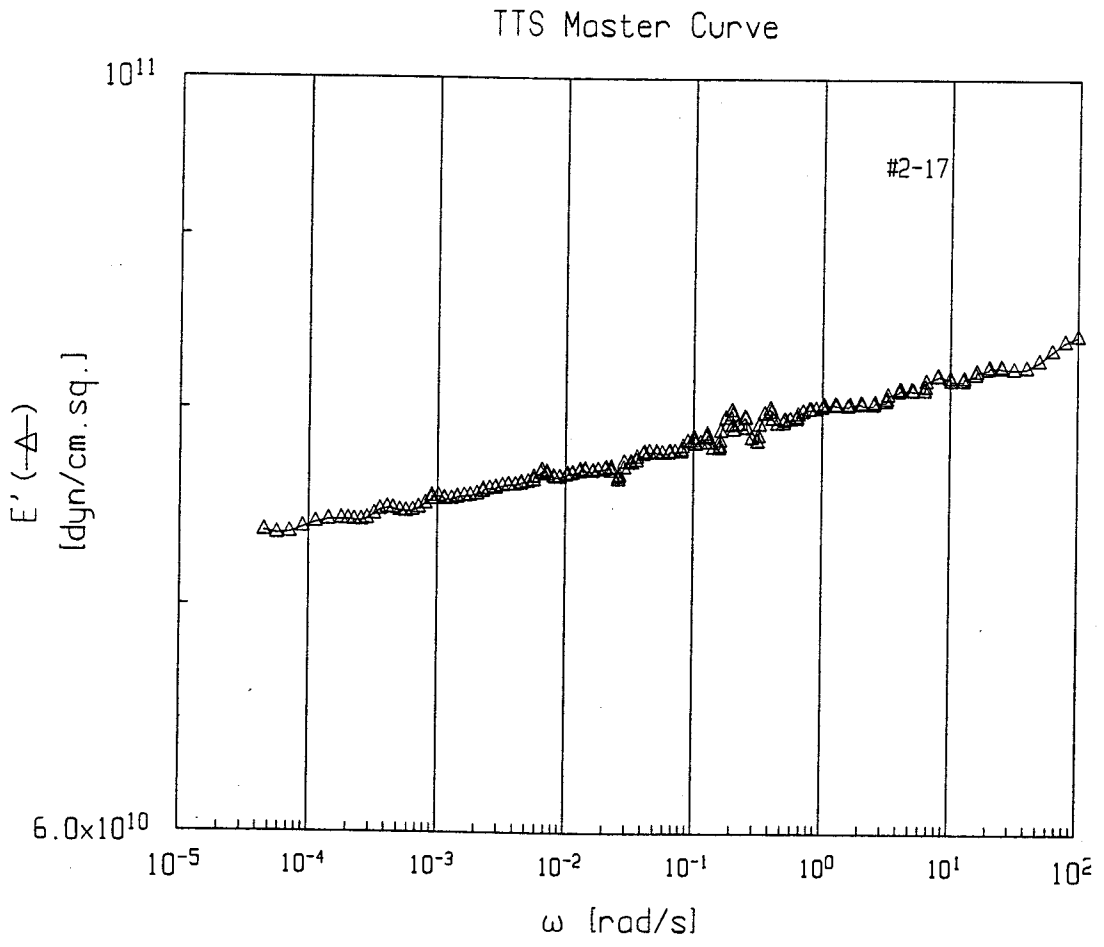

Figure A.12 TTS master curve (sample #2-17).

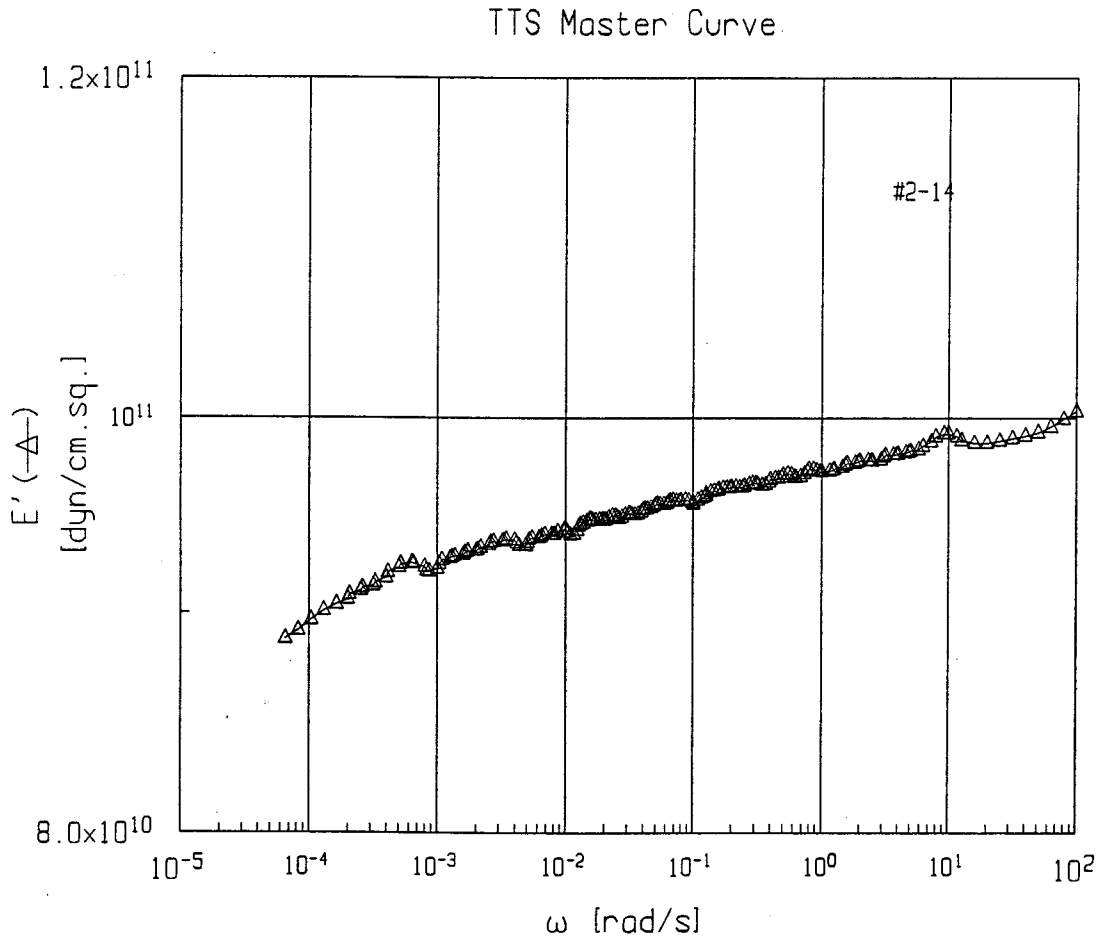

Figure A.13 TTS master curve (sample #2-14).

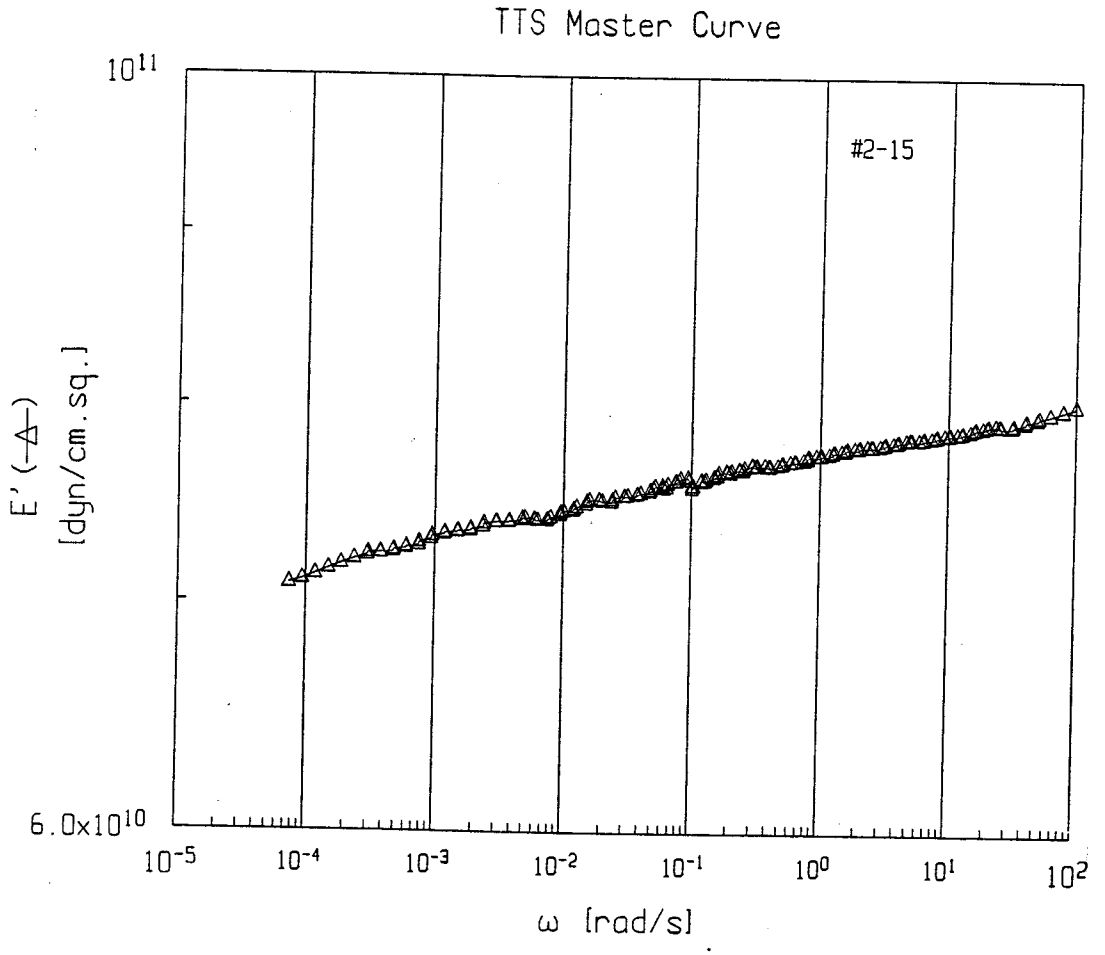

Figure A.14 TTS master curve (sample #2-15).

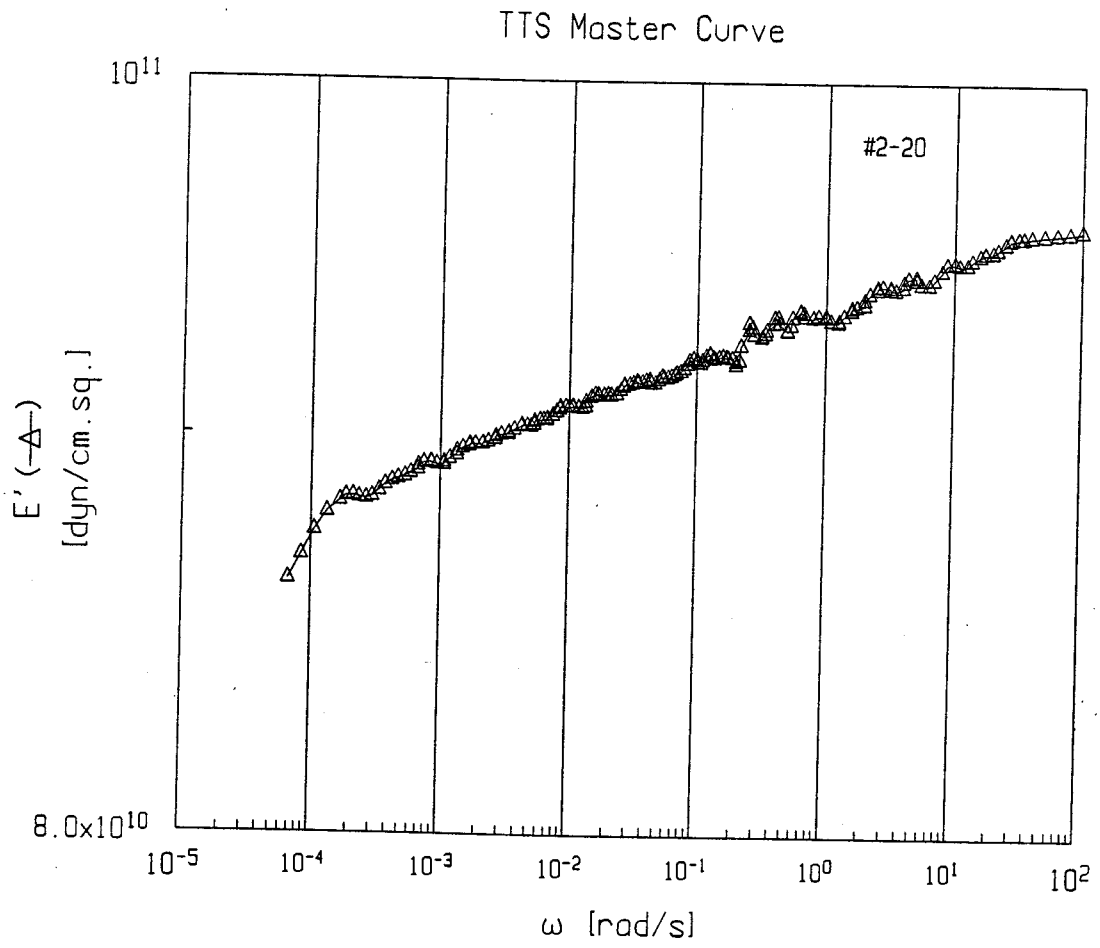

Figure A.15 TTS master curve (sample #2-20).

Appendix 3A. Material Properties of Particleboard Specimens

Table A.11 Average properties of particleboard.

Resin type	Resin content (%)	Specific gravity	E'* (dyn/cm^2)
UF	15	0.763	2.0×10^{10}
UF	10	0.698	1.1×10^{10}
PF	15	0.821	2.1×10^{10}
PF	10	0.701	9.5×10^{9}
RF	15	0.795	1.7×10^{10}
RF	10	0.718	7.7×10^{9}

*: E' was tested at temperature of 25°C and frequency of 100 rad/sec.

Appendix 3B. TTS Master Curves and Shift Factors

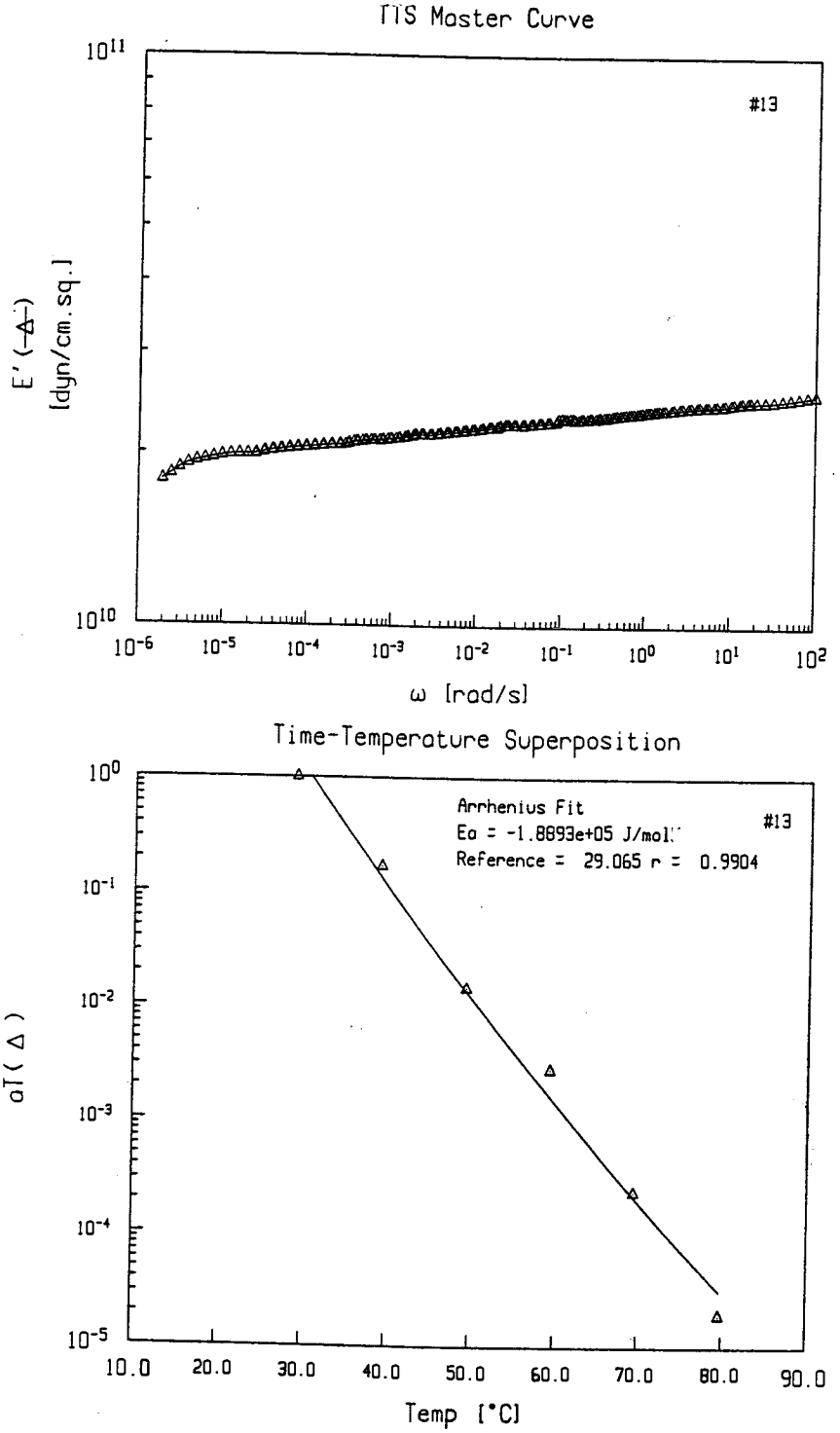

Figure A.16 TTS master curve and shift factor of particleboard bonded with PF resin (15%).

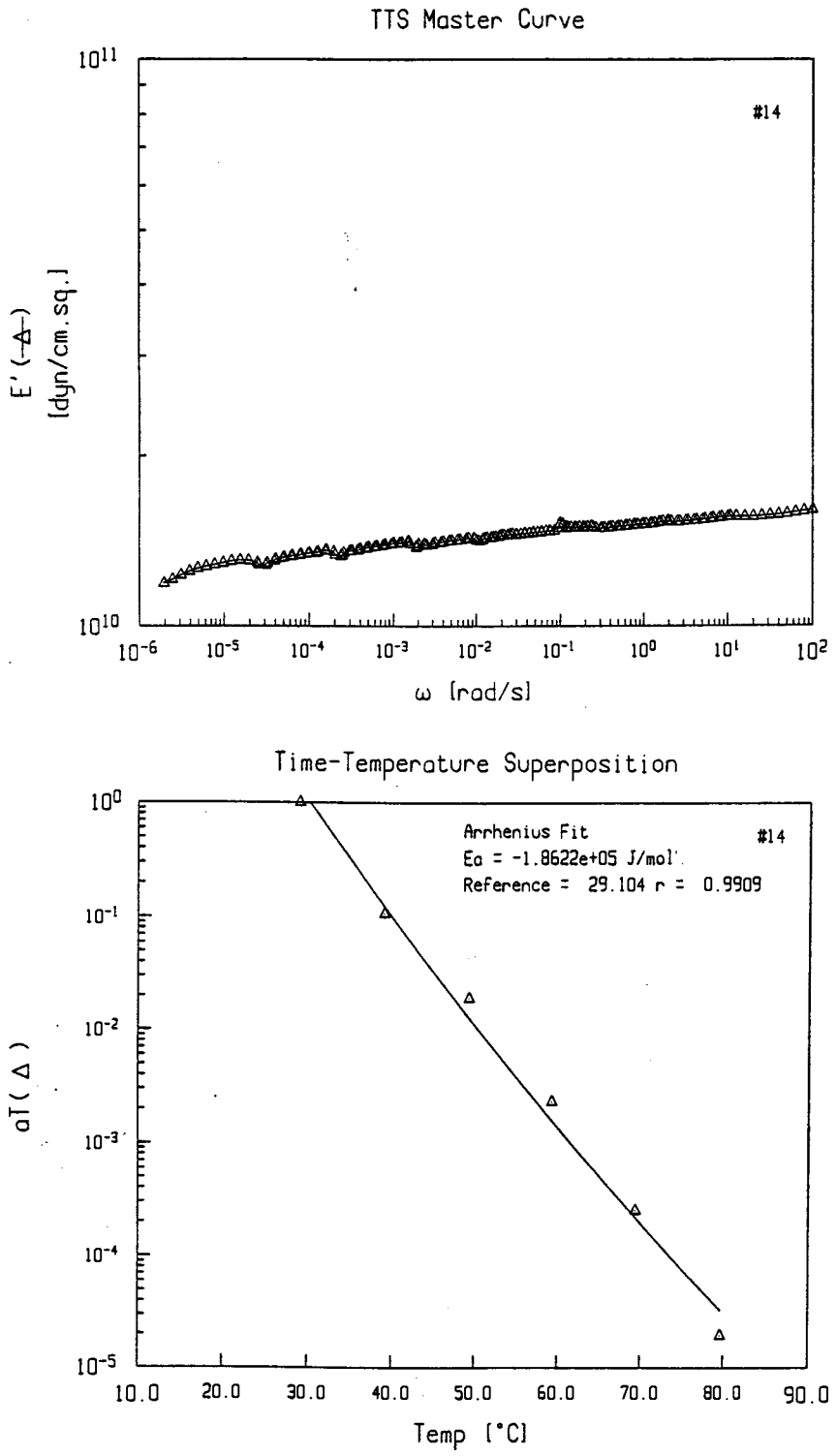

Figure A.17 TTS master curve and shift factor of particleboard bonded with PF resin (15%).

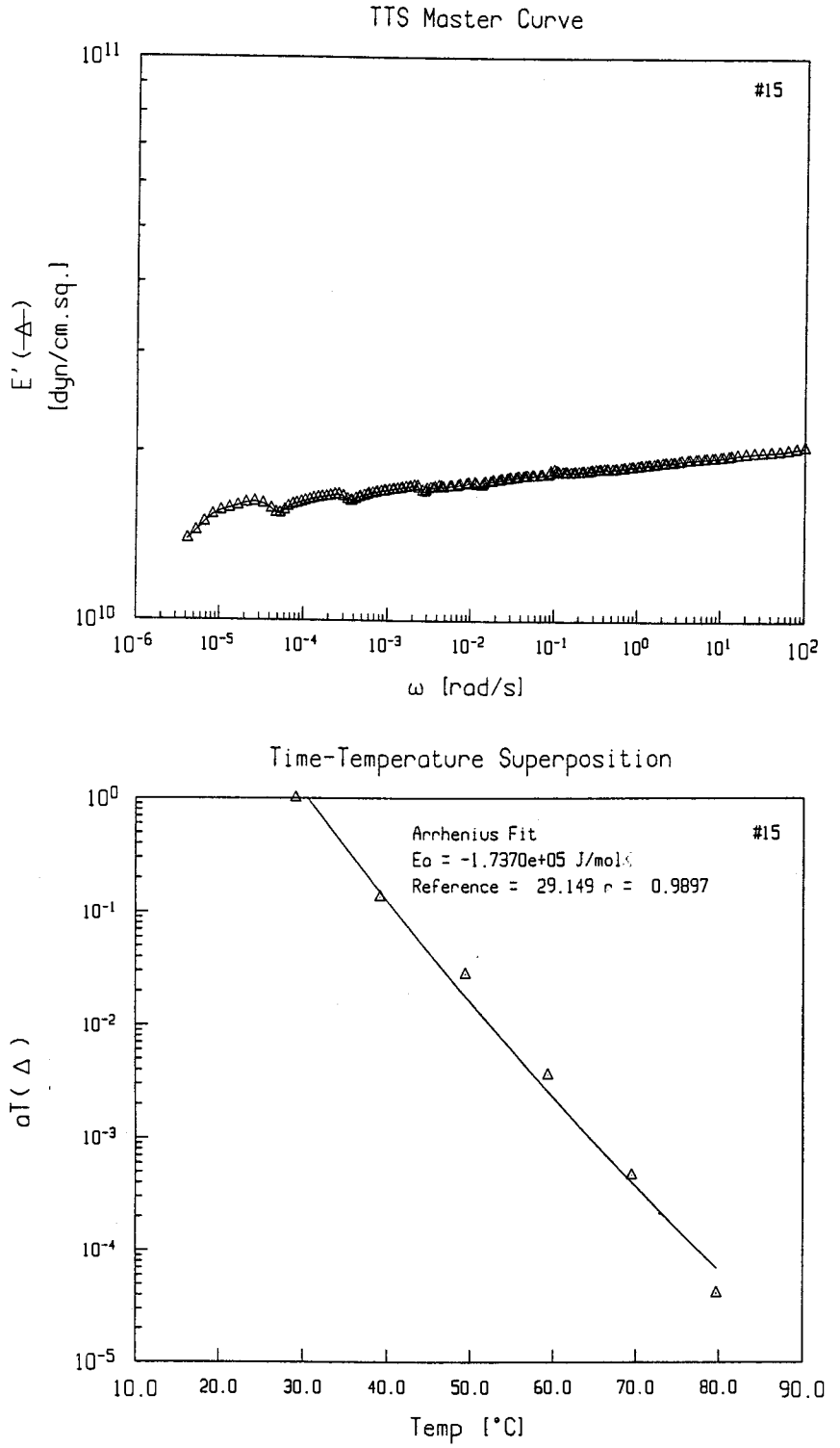

Figure A.18 TTS master curve and shift factor of particleboard bonded with PF resin (15%).

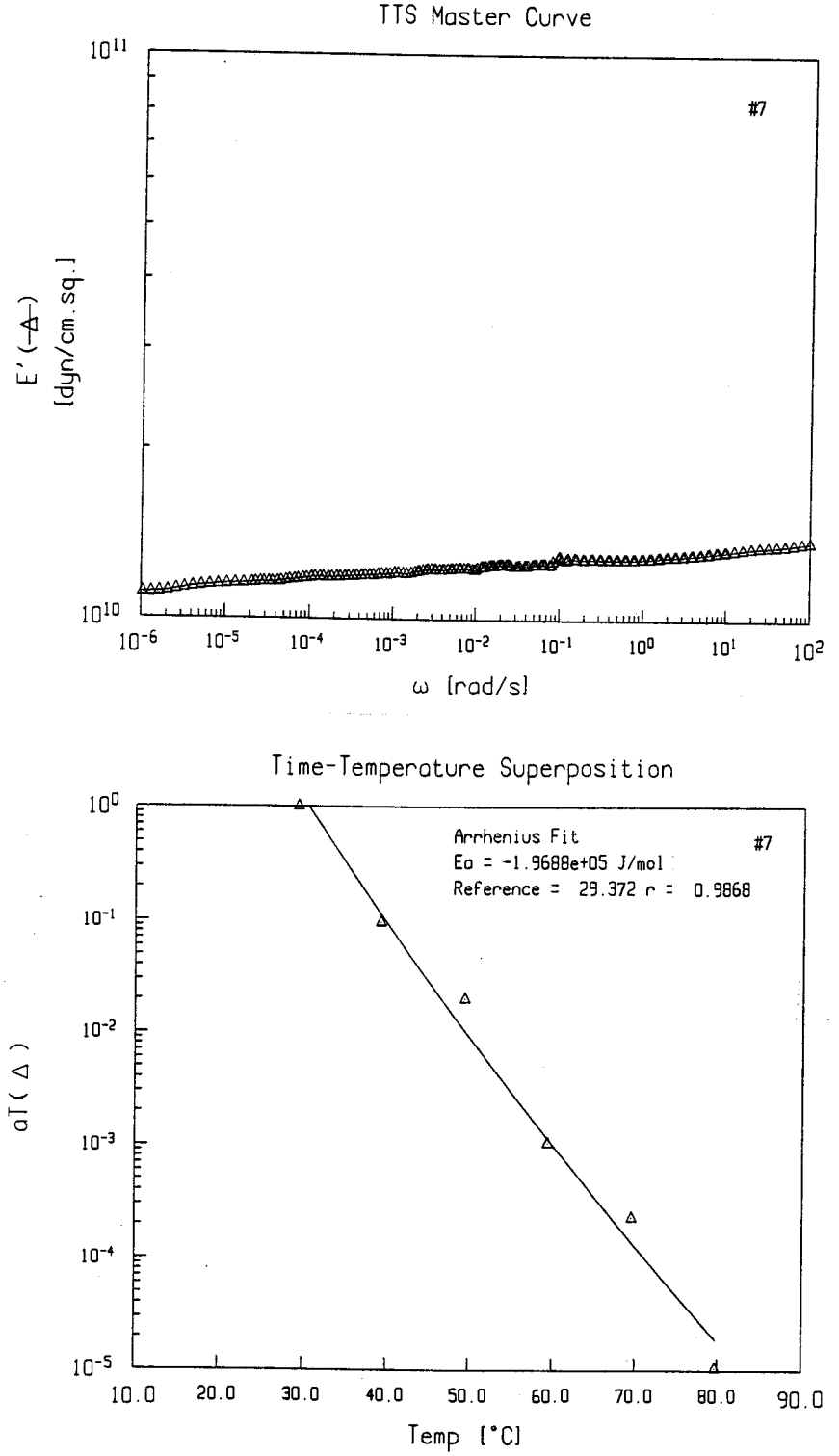

Figure A.19 TTS master curve and shift factor of particleboard bonded with UF resin (15%).

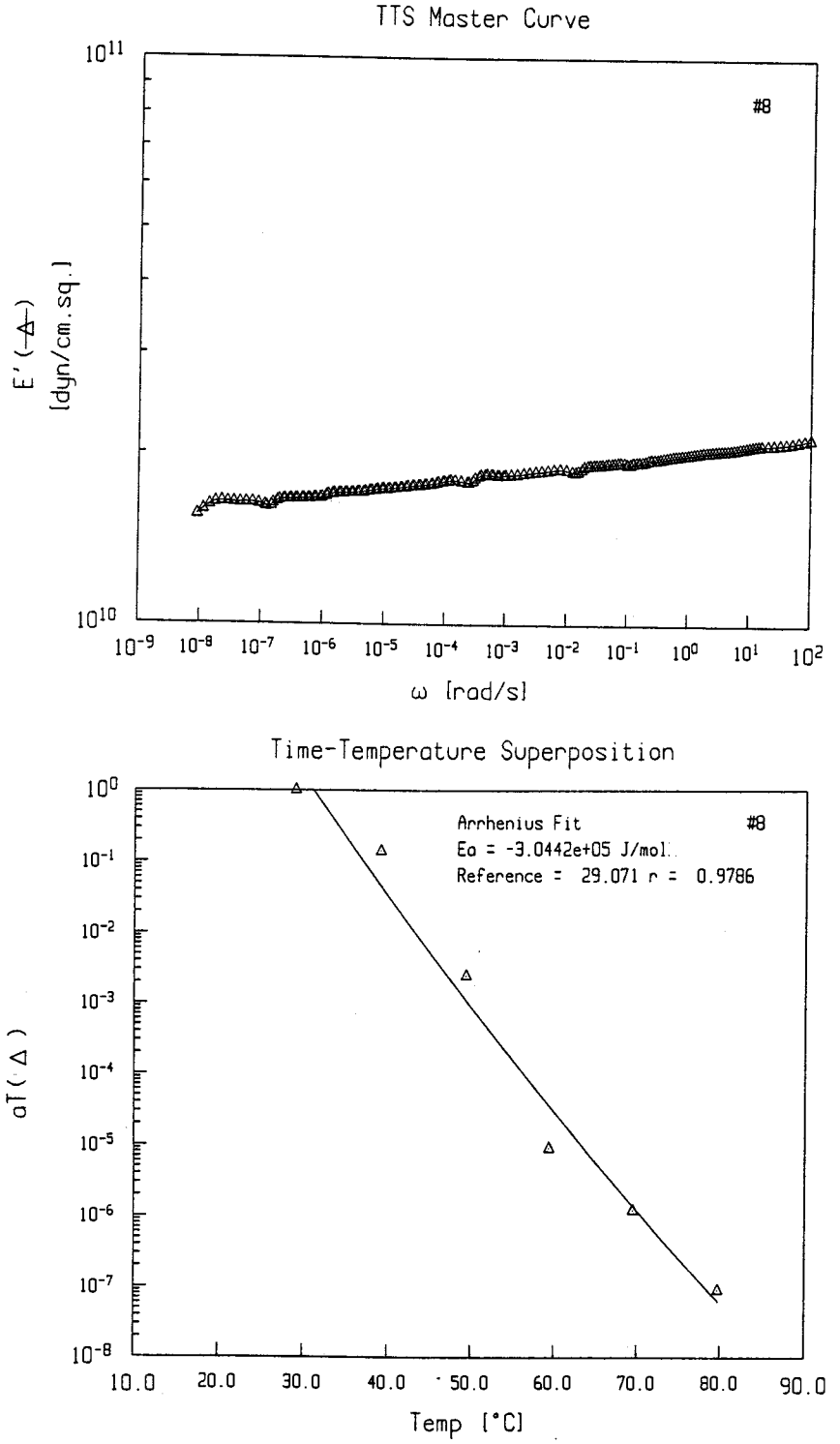

Figure A.20 TTS master curve and shift factor of particleboard bonded with UF resin (15%).

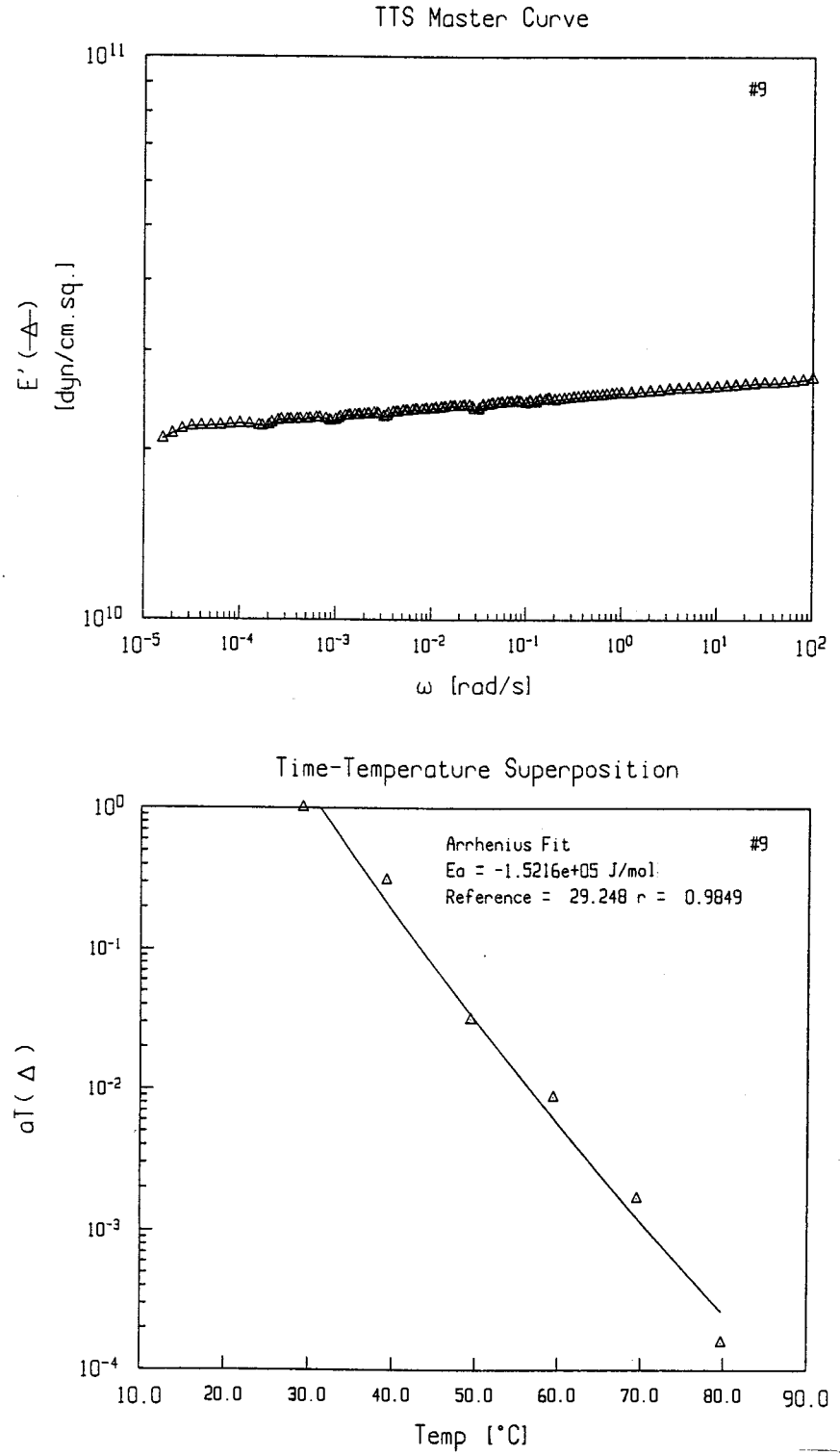

Figure A.21 TTS master curve and shift factor of particleboard bonded with UF resin (15%).

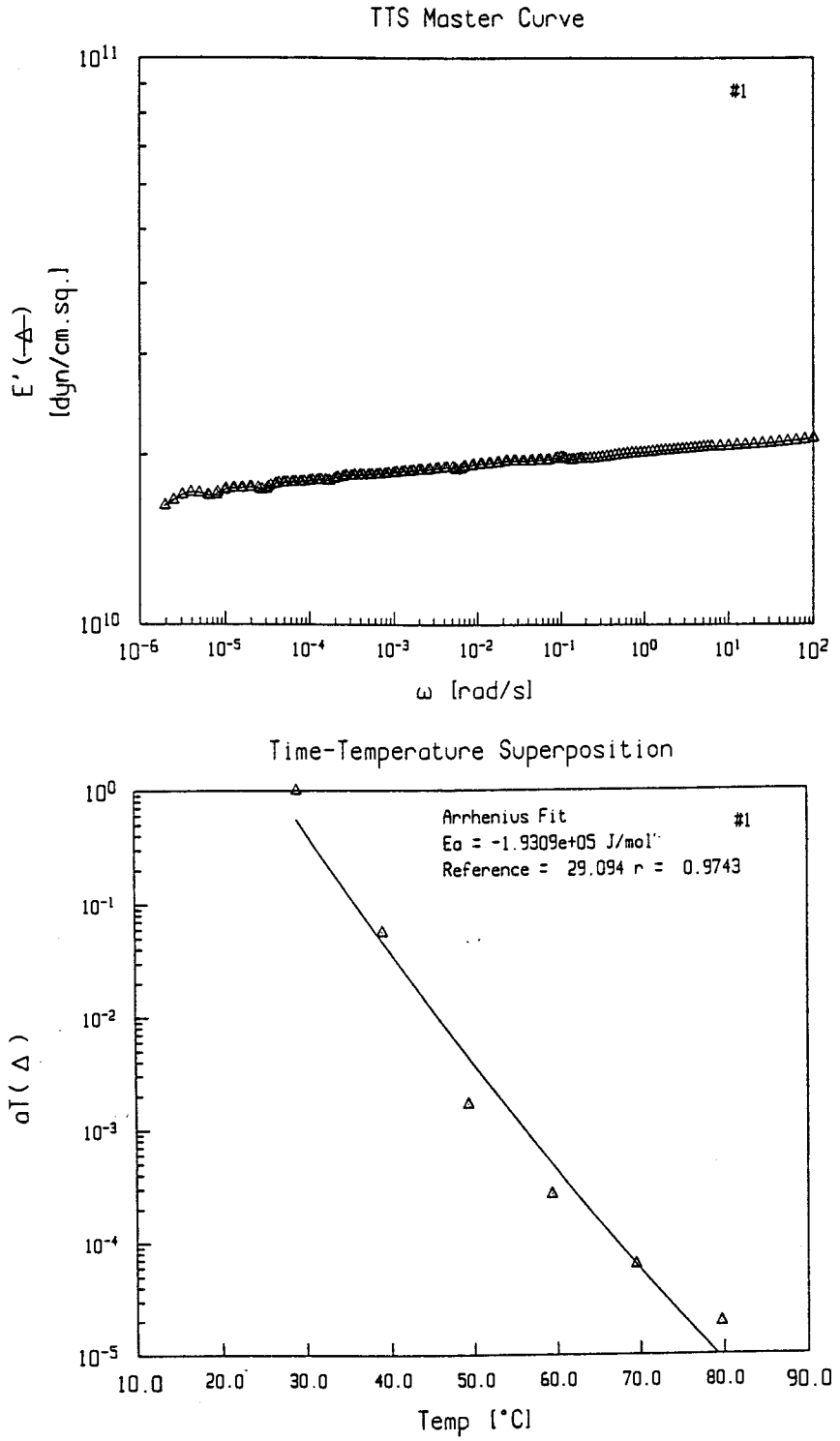

Figure A.22 TTS master curve and shift factor of particleboard bonded with RF resin (15%).

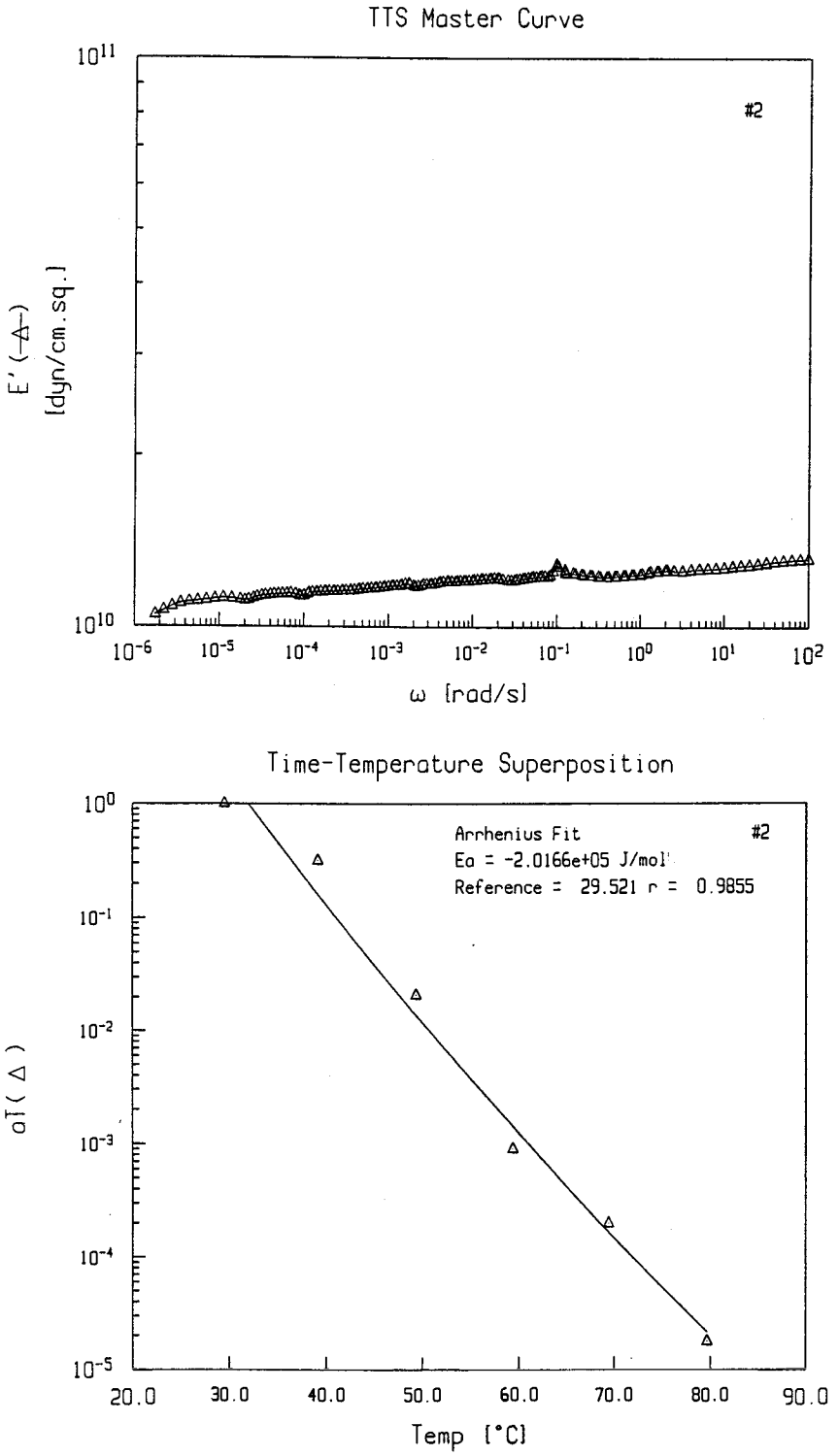

Figure A.23 TTS master curve and shift factor of particleboard bonded with RF resin (15%).

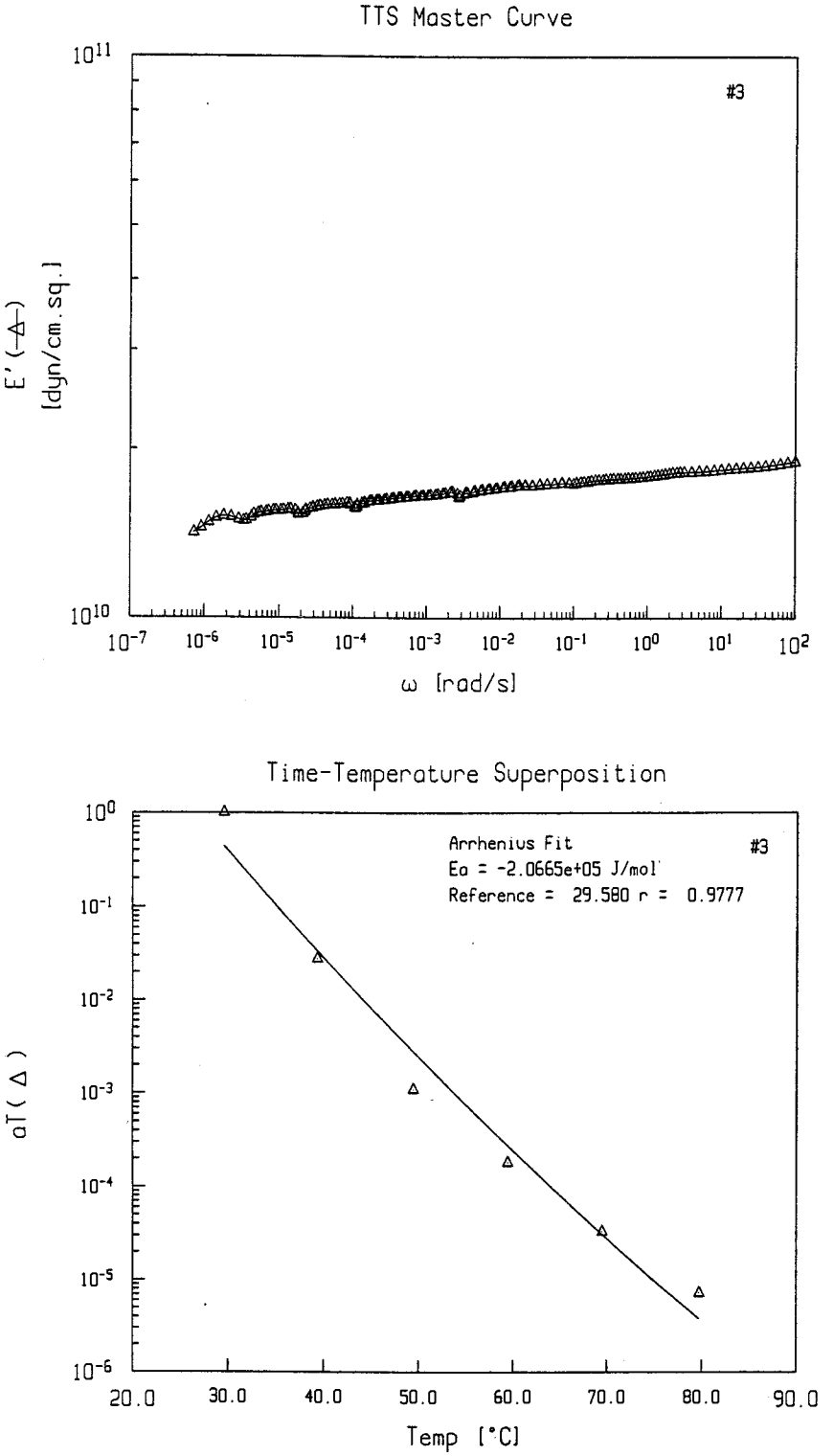

Figure A.24 TTS master curve and shift factor of particleboard bonded with RF resin (15%).